Multiscale modeling and computation of flow through porous media

Yalchin Efendiev

Department of Mathematics

Texas A& M University

College Station, TX

Collaborators: T. Hou, V. Ginting, A. Pankov, J. Aarnes, L. Durlofsky, S. Lee, L. Jiang, T. Strinopoulos

Introduction

- Multiple spatial and temporal scales are present in many physical processes.
- Because of wide range of scales direct numerical simulations are not affordable.
- One of the typical approaches is empirical or semi-empirical modeling of the effects of small scale
- The main goal of multiscale computation is to bypass empirical modeling that is often used for multiscale processes.

Outline

- Porous media and heterogeneity
- Multiscale finite element methods (MsFEM) on coarse-grid
- Applications of multiscale finite element methods to porous media flows
- Multiscale finite element methods using limited global information
- Upscaling of transport equations
- Generalizations of MsFEM to nonlinear problems. Homogenization of nonlinear parabolic equation with random fluxes.
  $D_t u_\epsilon = div(a_\epsilon(x,t,u_\epsilon,D_x u_\epsilon)) + a_{0,\epsilon}(x,t,u_\epsilon,D_x u_\epsilon)$.
- Upscaling of two-phase flow in flow-based coordinate system.
- Uncertainty quantification using upscaled models
- Flow in deformable inelastic media
- Conclusion and future work

Darcy's law and permeability

Darcy's empirical law, 1856: The volumetric flux $u(x,t)$ (Darcy velocity) is proportional to the pressure gradient

$$u = -\frac{k}{\mu}\nabla p = -K\nabla p,$$

where $k(x)$ is the measured permeability of the rock, μ is the fluid viscosity, $p(x,t)$ is the fluid pressure, $u(x,t)$ is the Darcy velocity.
We obtain the second order elliptic system

$$u = -K\nabla p \quad \text{in } Q \quad \text{Darcy's Law}$$

$$div(u) = f \quad \text{in } Q \quad \text{conservation}$$

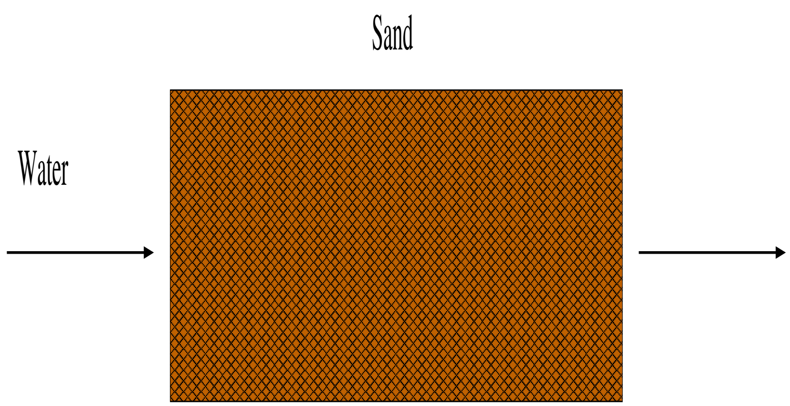

Heterogeneities

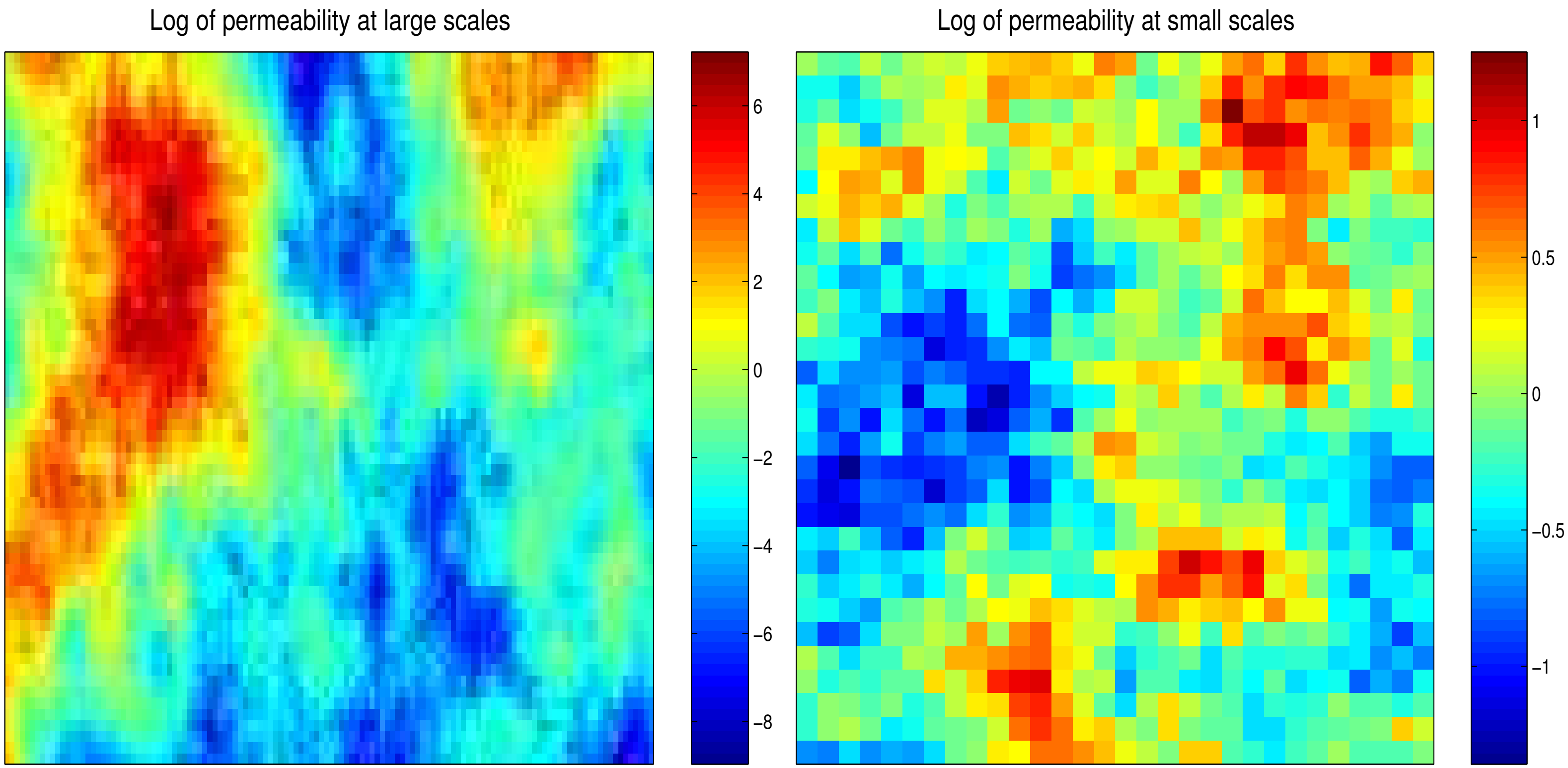

Upscaling: The system must be represented on a larger scale by incorporating the fine details in an average sense.

Multiscale finite element

A simple example

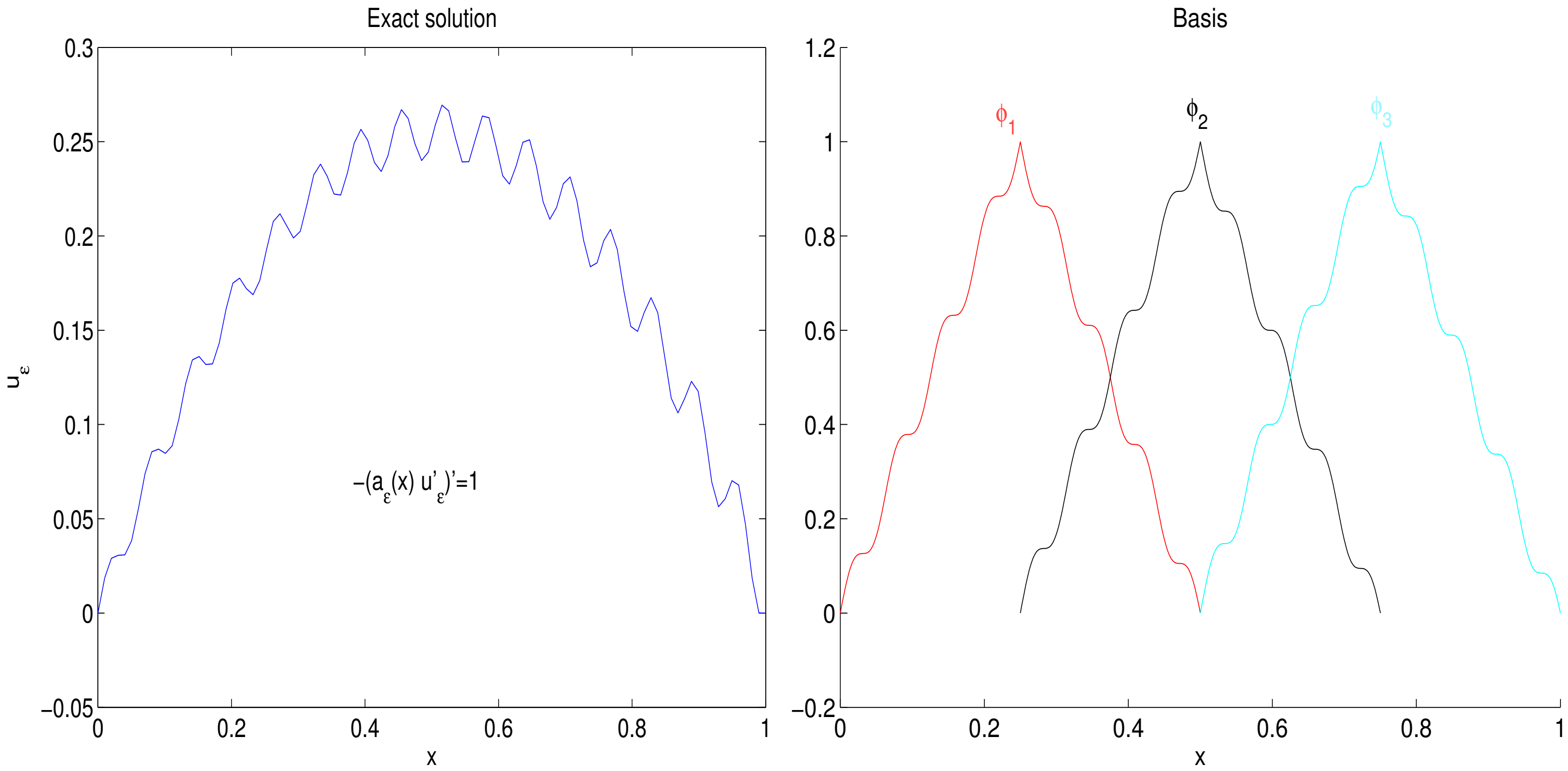

$$a_\epsilon(x) = 1/(2 + 1.99\cos(x/\epsilon)),\ \epsilon = 0.01.$$

Multiscale Finite Element Methods

Hou and Wu (1997) used this idea and defined multiscale finite elements. Consider

$$div(k_\epsilon(x)\nabla p_\epsilon) = f,$$

where ϵ is a small parameter.

- The central idea is to incorporate the small scale information into the finite element bases
- Basis functions are constructed by solving the leading order homogeneous equation in an element K

$$div(k_\epsilon(x)\nabla \phi^i) = 0 \quad \text{in} \quad K$$

- It is through the basis functions that we capture the local small scale information of the differential operator.

Multiscale Finite Element Methods

- Boundary conditions?

$$\phi^i = \text{linear function on } \partial K, \quad \phi^i(x_j) = \delta^{ij}$$

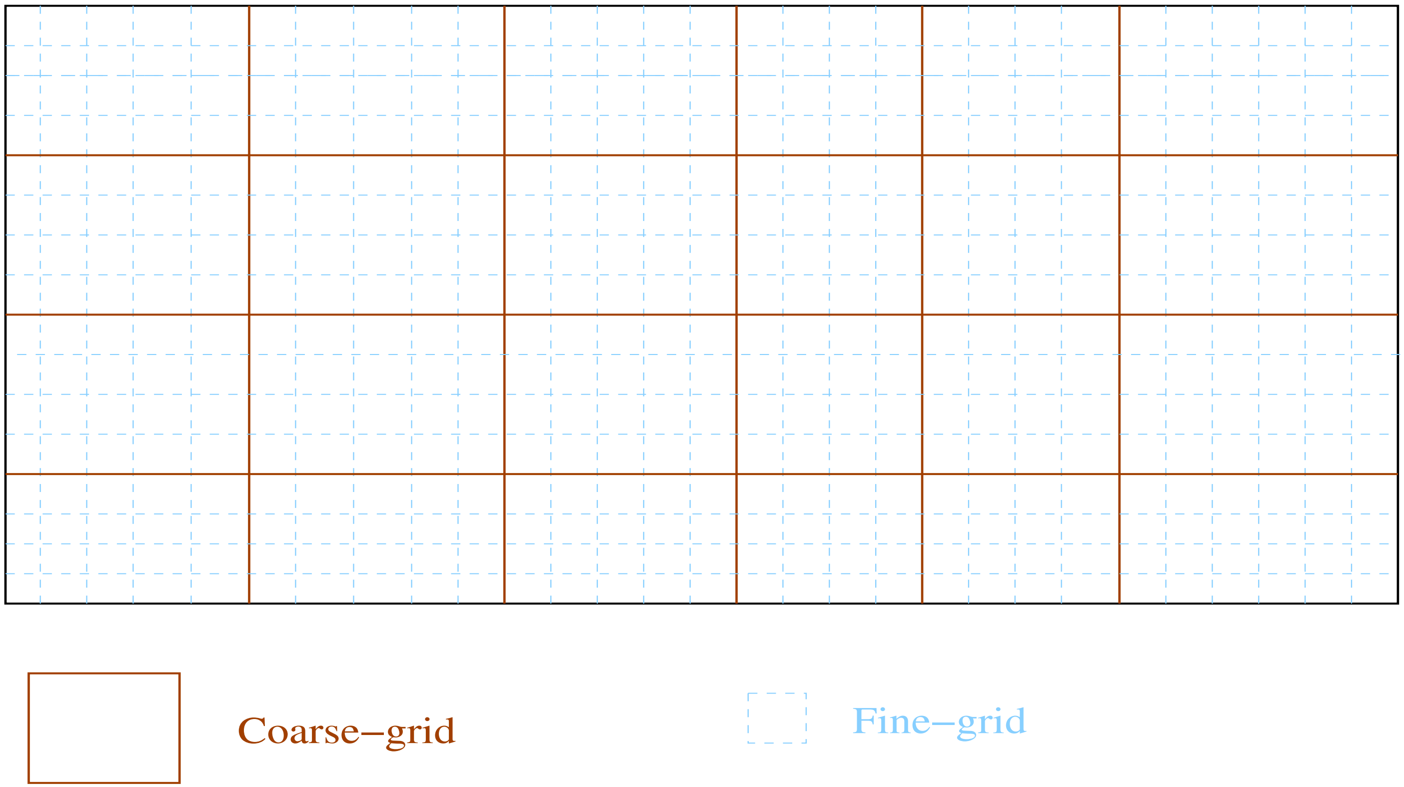

Multiscale Finite Element Methods

- Except for the multiscale basis functions, MsFEM is the same as the traditional FEM (finite element method). Find $p_\epsilon^h \in V^h = \{\phi^i\}$ such that

$$k(p_\epsilon^h, v^h) = f(v^h) \quad \forall v^h \in V^h,$$

where

$$k(u,v) = \int_Q k_{ij}^\epsilon(x) \frac{\partial u}{\partial x_i} \frac{\partial v}{\partial x_j} dx, \quad f(v) = \int_Q f v dx$$

- The coupling of the small scales is through the variational formulation
- Similar ideas have been used for:
Subgrid modeling (by T. Arbogast, I. Babuska, T. Hughes and others)
Subgrid stabilization (by F. Brezzi, L Franco, J.L. Guermond, T. Hughes, A. Russo, and others).
- Computational advantages: 1) The method is adaptive; 2)The method is well suited for parallel computation

Brief introduction to homogenization

$p_\epsilon \in H_0^1(Q)$

$$div(k(x, \frac{x}{\epsilon})\nabla p_\epsilon) = f,$$

where $k(x,y)$ is a periodic function with respect to y. Consider formal expansion

$$p_\epsilon = p_0(x,y) + \epsilon p_1(x,y) + \epsilon^2 p_2(x,y) + ...$$

Taking into account

$$\nabla A(x, \frac{x}{\epsilon}) = \nabla_x A + \frac{1}{\epsilon}\nabla_y A$$

we have

$$(div_x + \frac{1}{\epsilon} div_y)[k(x,y)(\nabla_x + \frac{1}{\epsilon}\nabla_y)(p_0(x,y) + \epsilon p_1(x,y) + \epsilon^2 p_2(x,y) + ...) = f.$$

$$\epsilon^{-2}: \ div_y(k(x,y)\nabla_y p_0(x,y)) = 0.$$

From here, $p_0(x,y) = p_0(x)$.

Brief introduction to homogenization

$$\epsilon^{-1}: \; div_y(k(x,y)\nabla_y p_1(x,y)) = -div_y(k(x,y))\nabla_x p_0.$$

From here, $p_1(x,y) = N_l(x,y)\frac{\partial}{\partial x_l}p_0$, where

$$div_y(k(x,y)\nabla_y N_k) = -\nabla_{x_i} k_{il}(x,y).$$

$$\epsilon^0: \; div_y(k(x,y)\nabla_y p_2) + div_y(k(x,y)\nabla_x p_1) + div_x(k(x,y)\nabla_y p_1) + div_x(k(x,y)\nabla_x p_0) = f.$$

Taking the average and noting that

$$\langle div_y A(x,y)\rangle = \int_Y div_y A(x,y)dy = 0,$$

we get

$$div_x\langle k(x,y)\nabla_y p_1\rangle + div_x(\langle k(x,y)\rangle\nabla_x p_0) = f.$$

From here, we conclude that

$$div_x(k^*(x)\nabla_x p_0) = f,$$

where $k^*(x) = \langle k(x,y) + k(x,y)\nabla_y N\rangle$.

Basic convergence in homogenization

$$p_\epsilon \longrightarrow p_0 \text{ weakly in } H^1,$$

$$u_\epsilon = k\nabla p_\epsilon \longrightarrow k^*\nabla p_0 \text{ weakly in } L_2$$

For bounded domains, we have $p_\epsilon = p_0(x) + \epsilon N(x,y)\cdot\nabla p_0 + \theta + \epsilon^2 p_2(x,y) + ...$, where

$$div(k\nabla\theta) = 0$$

$$\theta = -\epsilon N(x,y)\cdot\nabla p_0.$$

It can be shown that (e.g., JKO 94) $\|\theta\|_{H^1(Q)} \leq C\sqrt{\epsilon}$.

Convergence property of MsFEM

Consider $k_\epsilon(x) = k(x/\epsilon)$, where $k(y)$ is periodic in y.
h - computational mesh size.
Theorem (by T. Hou, X. Wu, Z. Cai) Denote p_ϵ^h the numerical solution obtained by MsFEM, and p_ϵ the solution of the original problem. Then,
If $h >> \epsilon$,

$$\|p_\epsilon - p_\epsilon^h\|_{1,Q} \le C(h + \sqrt{\frac{\epsilon}{h}})$$

- This theorem shows that MsFEM converges to the correct solution as $\epsilon \longrightarrow 0$
- The ratio ϵ/h reflects two intrinsic scales. We call ϵ/h the resonance error
- The theorem shows that there is a scale resonance when $h \approx \epsilon$. Numerical experiments confirm the scale resonance.

Resonance errors

- For problems with scale separation, we can choose $h \gg \epsilon$ in order to avoid the resonance, but for problems with continuous spectrum of scales, we cannot avoid this resonance.
- To demonstrate the influence of the boundary condition of the basis function on the overall accuracy of the method we perform multiscale expansion of ϕ^i
- Multiscale expansion of ϕ^i

$$\phi^i = \phi_0(x) + \epsilon\phi_1(x, x/\epsilon) + \epsilon\theta + \dots,$$

- $\phi_1(x, x/\epsilon) = N^k(x/\epsilon)\frac{\partial}{\partial x_k}\phi_0$, where $N^k(x/\epsilon)$ is a periodic function which depends on $k(x/\epsilon)$.
- θ satisfies

$$div(k_\epsilon \nabla\theta) = 0 \text{ in } K, \quad \theta^i = -\phi_1(x, x/\epsilon) + (\phi^i - \phi_0)/\epsilon \text{ on } \partial K$$

- Oscillations near the boundaries (in ϵ vicinity) of θ^i lead to the resonance error

Illustration of θ

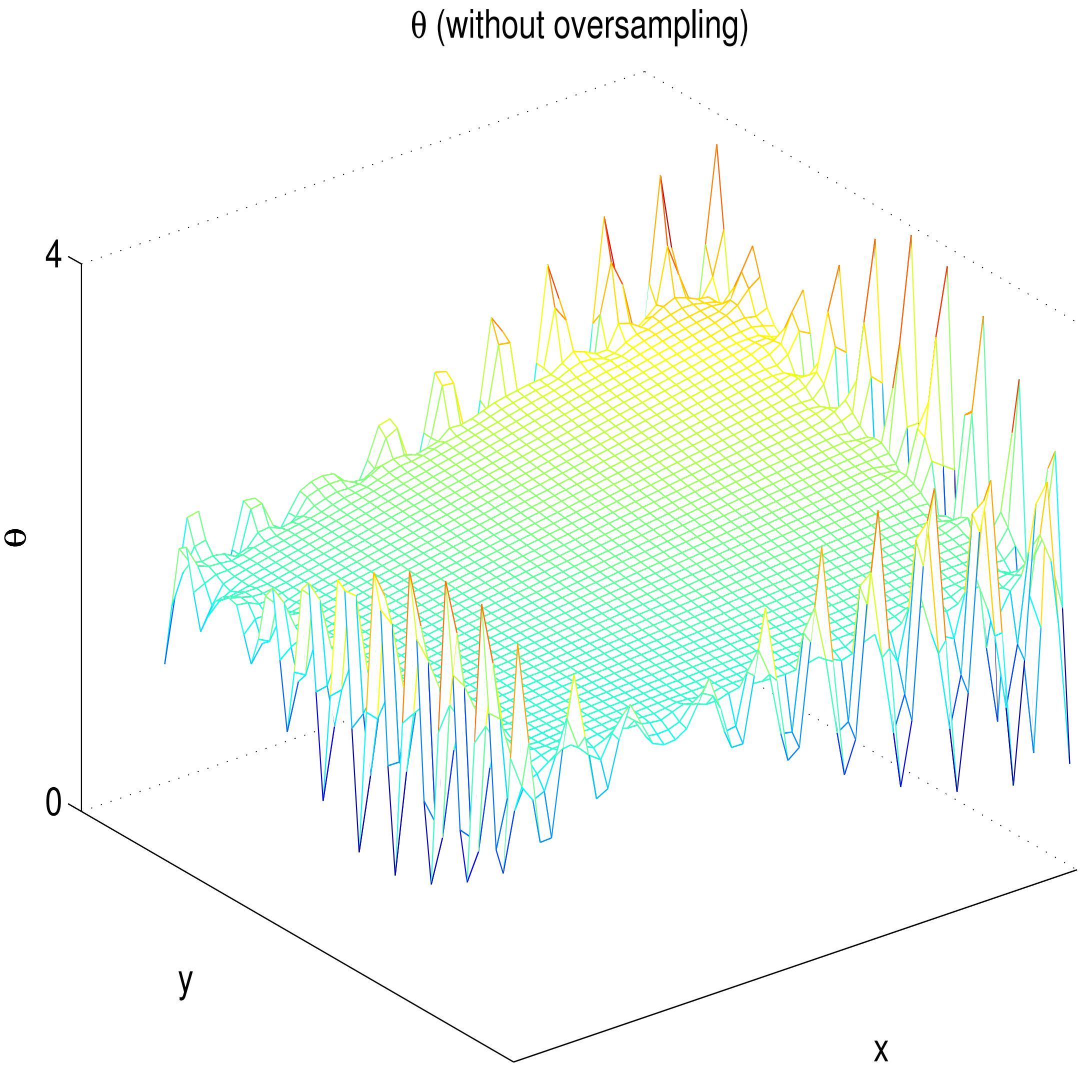

Oversampling technique

- To capture more accurately the small scale information of the problem, the effect of θ needs to be moderated
- Since the boundary layer of θ is thin $(O(\epsilon))$ we can sample in a domain with size larger than $h+\epsilon$ and use only interior sampled information to construct the basis functions.
- Let ψ^k be the functions in the domain S,

$$div(k_\epsilon(x)\nabla\psi^k)=0 \text{ in } S, \quad \psi^k = \text{linear function on } \partial S, \ \psi^k(s_i)=\delta_{ik}.$$

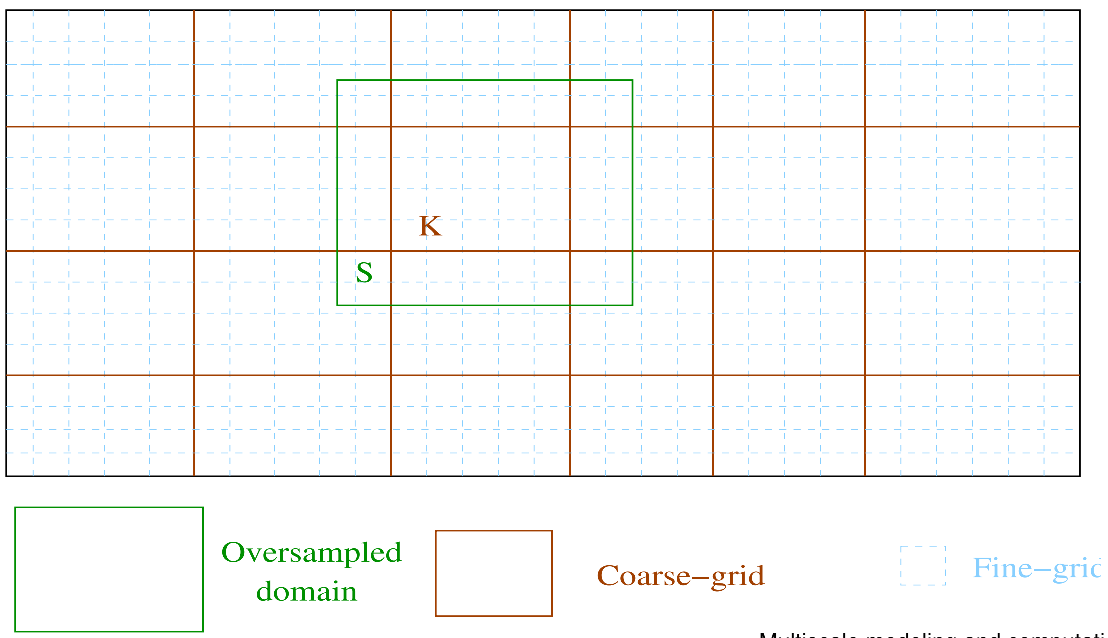

Oversampling technique

- The base functions in a domain $K \subset S$ constructed as

$$\phi^i|_K = \sum c_{ij} \psi^j|_K, \quad \phi^i(x_k) = \delta^{ik}$$

- The method is non-conforming.
- The derivation of the convergence rate uses the homogenization method combined with the techniques of non-conforming finite element method (Efendiev et al., SIAM Num. Anal. 1999)
- By a correct choice of the boundary condition of the base functions we eliminate the boundary layer in θ. We show that this leads to cancellation of the main resonance error.

Illustration of θ with oversampling

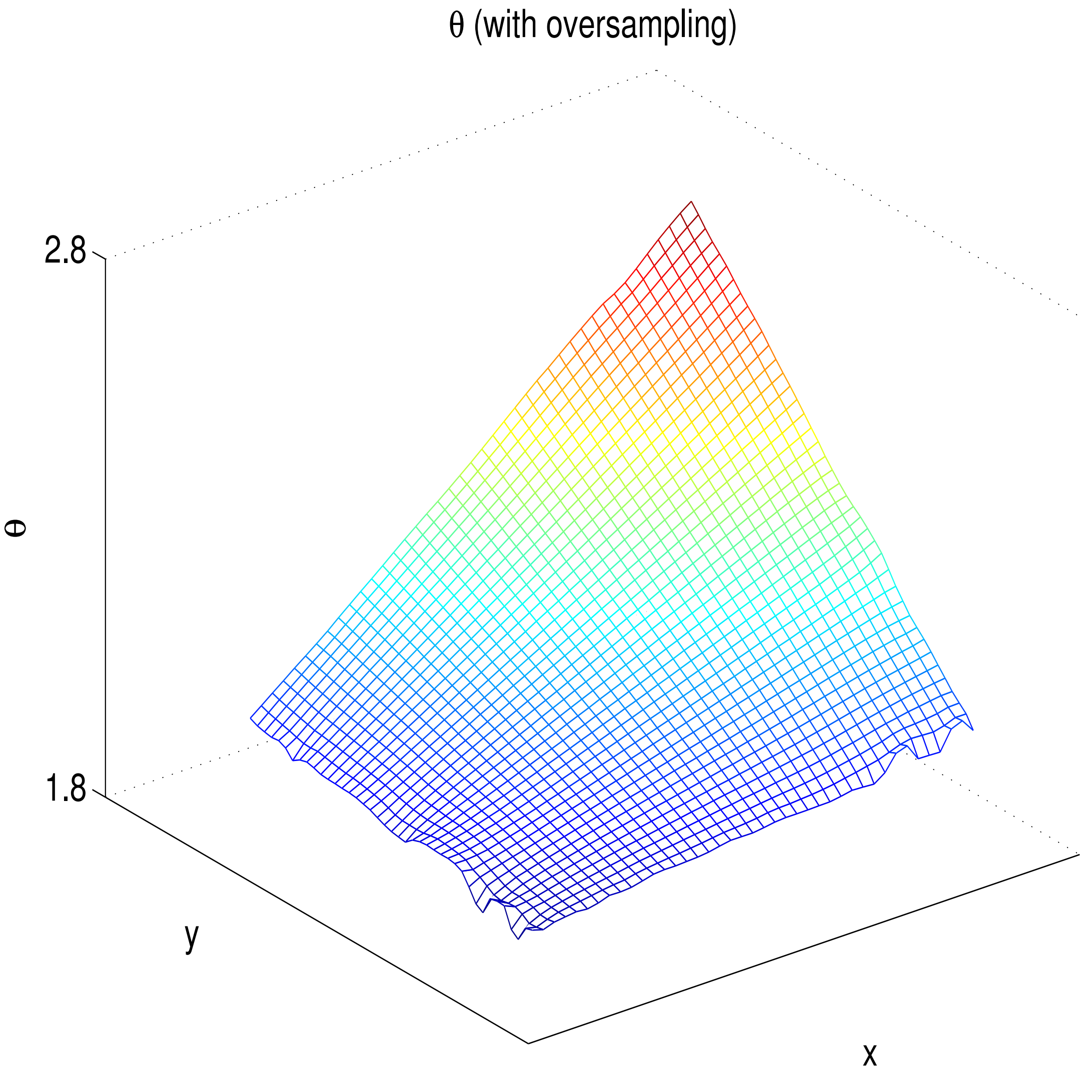

Numerical Results

Table 1: $\|U_\epsilon^h - U_0^h\|_{l_2}$, $\epsilon/h = 0.64$

h	MsFEM		MsFEM-os		Resolved FEM	
	l_2	rate	l_2	rate	h_{fine}	l_2
1/16	3.54e-4		7.78e-5		1/256	1.34e-4
1/32	3.90e-4	-0.14	3.38e-5	1.02	1/512	1.34e-4
1/64	4.00e-4	-0.05	1.97e-5	0.96	1/1024	1.34e-4
1/128	4.10e-4	-0.02	1.03e-5	0.95	1/2048	1.34e-4

The convergence of MsFEM

- The MsFEM for elliptic equation with discontinuous coefficients The convergence rate of MsFEM does not deteriorate in this case. The base functions capture the singularities of the solution.
- The convergence of MsFEM for problems with multiple scales $\epsilon_1 \ll \epsilon_2 \ll ... \ll \epsilon_n$.
- The convergence of MsFEM for random coefficients (continuous ϵ-spectrum).
- The expansion of the base function, $\phi_\epsilon^i(\mathbf{x}, \omega) = \phi_0(\mathbf{x}) + \epsilon\phi_1(\mathbf{x}, \mathbf{x}/\epsilon, \omega) + \epsilon\theta$, where $\phi_1(\mathbf{x}, \mathbf{x}/\epsilon, \omega) = N^k(\mathbf{x}/\epsilon, \omega)\nabla_k\phi_0(\mathbf{x})$.
- The estimates for stationary fields approximating $N(\mathbf{x}/\epsilon, \omega)$ have been derived under the strong mixing condition for the coefficients (Yurinskii, 86) (power decay of two point correlation).
- The convergence rate of MsFEM remains the same as in the periodic case if the coefficients are quasi-periodic or almost periodic subject to some conditions.

MsFEM for problems with scale separation

For periodic problems or problems with scale separation, multiscale finite element methods can take an advantage of scale separation. Basis functions can be approximated

$$\phi^i = \phi_0^i + N_\epsilon \cdot \nabla \phi_0^i,$$

where ϕ_i^0 is linear basis functions and N is the periodic solution of auxiliary problem in ϵ-size period

$$-div(k_\epsilon(x)(\nabla N + I)) = 0.$$

In this case, the coarse-scale equation will “exactly” correspond to solving

$$div(k^* \nabla p^*) = f,$$

where k^* is computed using classical homogenization procedure (cf. Durlofsky 1981, and etc.).
Note, the above procedure works **not only** for periodic heterogeneities, **but also** any heterogeneities when “homogenization by periodization” is applicable (e.g., random homogeneous case).

Various global formulations

- Once basis functions are constructed, various global formulation (mixed, control volume finite element, DG and etc) can be used to couple the subgrid effects.
- Control volume finite element: Find $p_h \in V_h$ such that

$$\int_{\partial V_z} k(x)\nabla p_h \cdot \mathbf{n}\, dl = \int_{V_z} q\, dx \quad \forall\, V_z \in Q,$$

  where V_z is control volume.
- Mixed finite element: In each coarse block K, we construct basis functions for the velocity field

$$\begin{aligned} div(k(x)\nabla w_i^K) &= \frac{1}{|K|} \quad \text{in} \quad K \\ k(x)\nabla w_i^K \mathbf{n}^K &= \begin{cases} \frac{1}{|e_i^K|} & \text{on } e_i^K \\ 0 & \text{else.} \end{cases} \end{aligned}$$

  For the pressure, the basis functions are taken to be constants.

MsFEM for problems with scale separation

For periodic problems or problems with scale separation, multiscale finite element methods can take an advantage of scale separation. Basis functions can be approximated

$$\phi^i = \phi_0^i + N_\epsilon \cdot \nabla \phi_0^i,$$

where ϕ_i^0 is linear basis functions and N is the periodic solution of auxiliary problem in ϵ-size period

$$-div(k_\epsilon(x)(\nabla N + I)) = 0.$$

In this case, the coarse-scale equation will “exactly” correspond to solving

$$div(k^* \nabla p^*) = f,$$

where k^* is computed using classical homogenization procedure (cf. Durlofsky 1981, HMM, and etc.).
Note, the above procedure works **not only** for periodic heterogeneities, **but also** any heterogeneities when “homogenization by periodization” is applicable (e.g., random homogeneous case).

Applications of MsFEM to subsurface flow simulations

Two-phase flow model.
Darcy's law for each phase

$\mathbf{v}_i = - \quad k \quad \frac{k_i(S_i)}{\mu_i} \nabla p_i$, i=1,2.

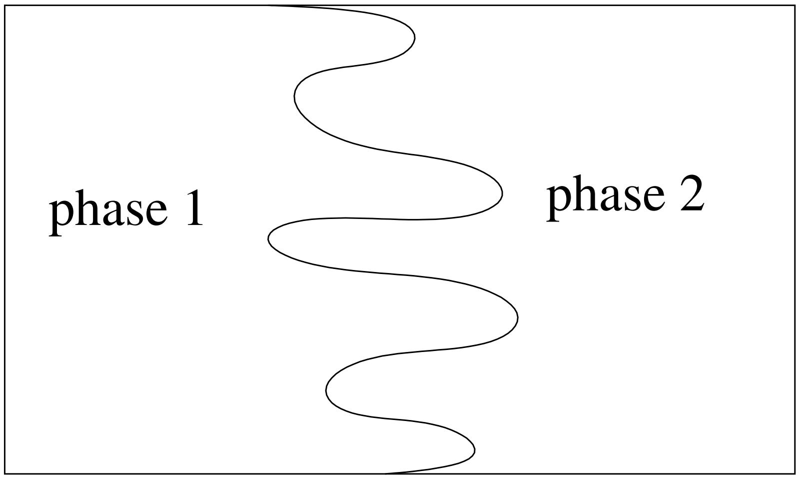

Applications of MsFEM to subsurface flow simulations

Two-phase flow model.
Darcy's law for each phase

$\mathbf{v}_i = -\, k \, \frac{k_i(S_i)}{\mu_i} \nabla p_i$, i=1,2.

k - permeability field representing the heterogeneities (micro-level information), p_i - the pressure, $\mathbf{v}_i$ - velocity, k_i - relative permeability, S_i -saturation, μ_i -viscosity

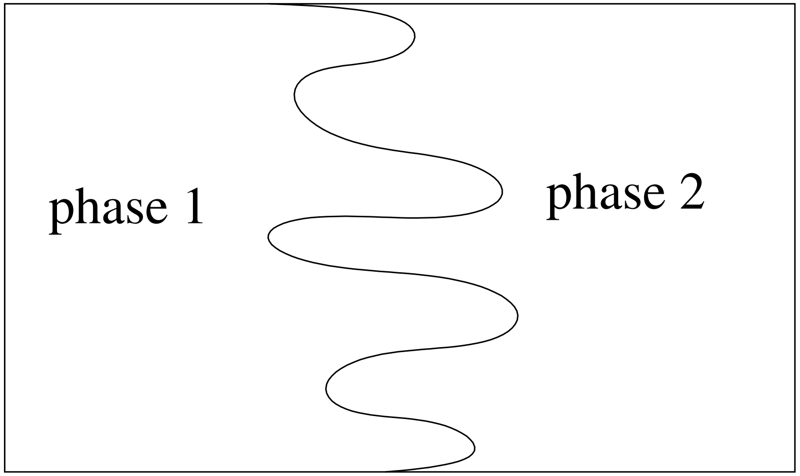

Two-phase flow model

- $p_1 = p_2 = p$ if the capillary effects are neglected. The total velocity v is given by

$$v = v_1 + v_2 = -\lambda(S) k \nabla p, \quad \lambda(S) = \frac{k_1(S)}{\mu_1} + \frac{k_2(S)}{\mu_2}.$$

  where $S = S_1$, $S_2 = 1 - S_1$.
- Incompressibility of the total velocity implies

$$div(\lambda(S) k \nabla p) = 0,$$

- From the conservation of mass $S_t + div(v_1) = 0$ we can derive

$$\frac{\partial S}{\partial t} + v \cdot \nabla f(S) = 0, \quad f(S) = \frac{\frac{k_1(S)}{\mu_1}}{\frac{k_1(S)}{\mu_1} + \frac{k_2(S)}{\mu_2}}$$

Requirements/Challenges

- Accuracy and Robustness
- Retain geological realism in flow simulation
- Valid for different types of subsurface heterogeneity

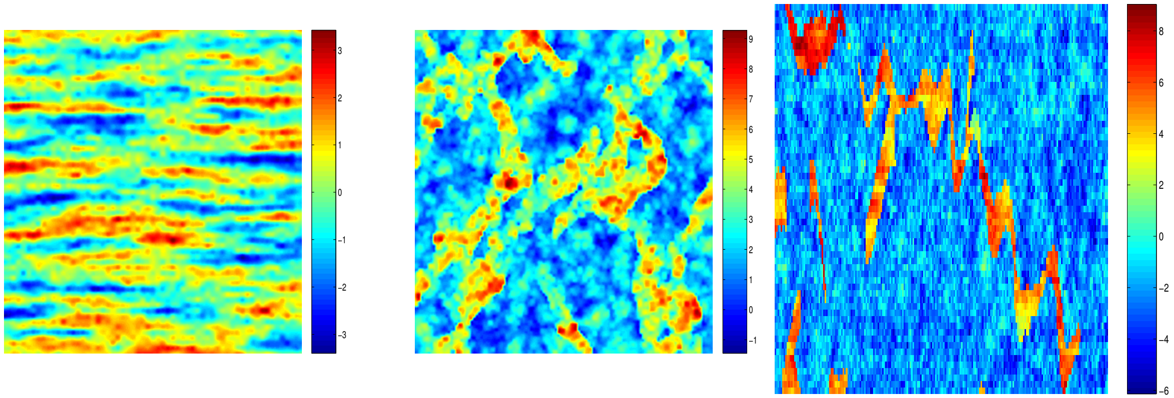

- Applicable for varying flow scenarios

Requirements/Challenges

- Accuracy and Robustness
- Retain geological realism in flow simulation
- Valid for different types of subsurface heterogeneity

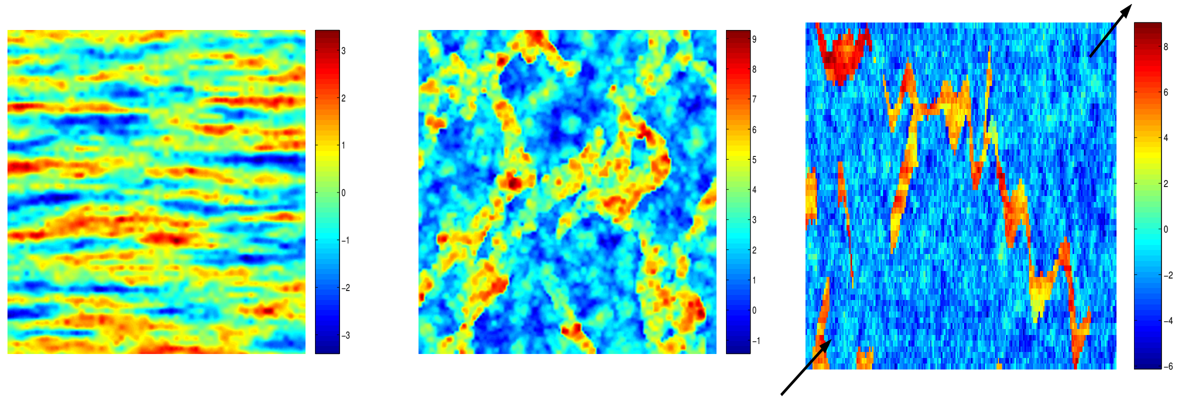

- Applicable for varying flow scenarios

Requirements/Challenges

- Accuracy and Robustness
- Retain geological realism in flow simulation
- Valid for different types of subsurface heterogeneity

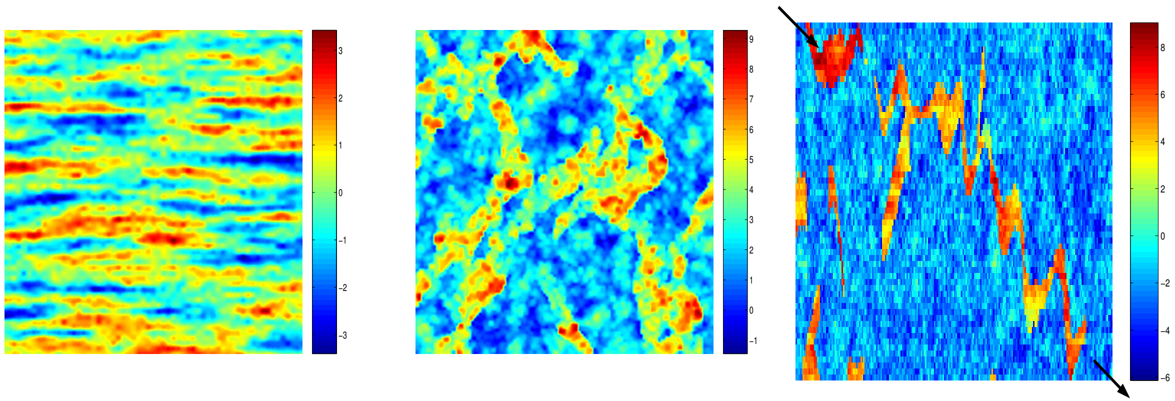

- Applicable for varying flow scenarios

Existing upscaling techniques

- $-div(\lambda(S)k\nabla p) = 0$, $S_t + v \cdot \nabla f(S) = 0$, $v = -\lambda(S)k\nabla p$.
- Single-phase upscaling: $(k \to k^*)$, $\mathbf{k}^* = \frac{\overline{\mathbf{k}\nabla p}}{\overline{\nabla p}}$.

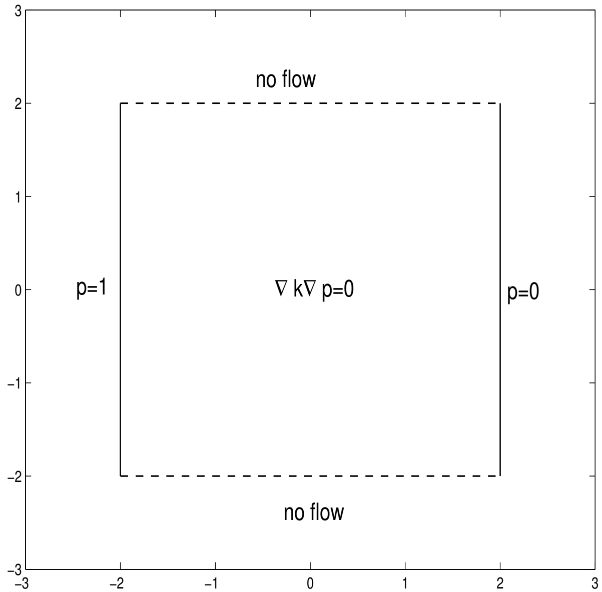

- Multiphase upscaling $\lambda \to \lambda^*$, $f \to f^*$.

Applications of MsFEM

At least two way one can apply MsFEM
1) Solve the pressure equation on the coarse-grid and solve the saturation equation on the fine-grid

$$-div(\lambda(S)k\nabla p) = 0$$

$$\frac{\partial}{\partial t}S + v \cdot \nabla f(S) = 0,$$

where $v = -\lambda(S)k\nabla p$. Basis functions are updated only near sharp fronts.

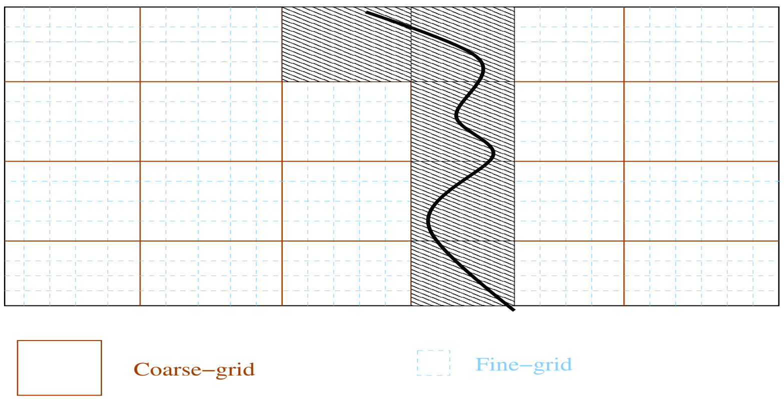

MsFVEM applied to two-phase flow problem

(IM)plicit (P)ressure (E)xplicit (S)aturation:

Given S^0, for $n = 1, 2, 3, \cdots$, do the following:

- find $p_h^{n-1} \in V_h$ such that

$$\int_{\partial V_z} \lambda(S^{n-1})k(x)\nabla p_h^{n-1} \cdot \mathbf{n}\, dl = \int_{V_z} q\, dx \quad \forall\, V_z \in Q$$

- compute $\mathbf{v}^{n-1} = -\lambda(S^{n-1})k(x)\nabla p_h^{n-1}$
- time march on the saturation equation:

$$\int_{c_z} \left(S^n - S^{n-1}\right)\, dx + \Delta t^{n-1} \int_{\partial c_z} f(S^{n-1})\mathbf{v}^{n-1} \cdot \mathbf{n}\, dl = \Delta t^{n-1} \int_{c_z} q\tilde{S}\, dx$$

Numerical Setting

- Rectangular domain is considered. The permeability field is generated using geostatistical libraries.
- The boundary conditions: no flow on top and bottom boundaries, a fixed pressure and saturation ($S = 1$) at the inlet (left edge), fixed pressure at the outlet (right edge).
- The production rate $F = q_0/q$, where q_0 the volumetric flow rate of oil produced at the outlet edge and q the volumetric flow rate of the total fluid produced at the outlet edge. The dimensionless time is defined as $PVI = qt/V_p$, where t is time, V_p is the total pore volume of the system.

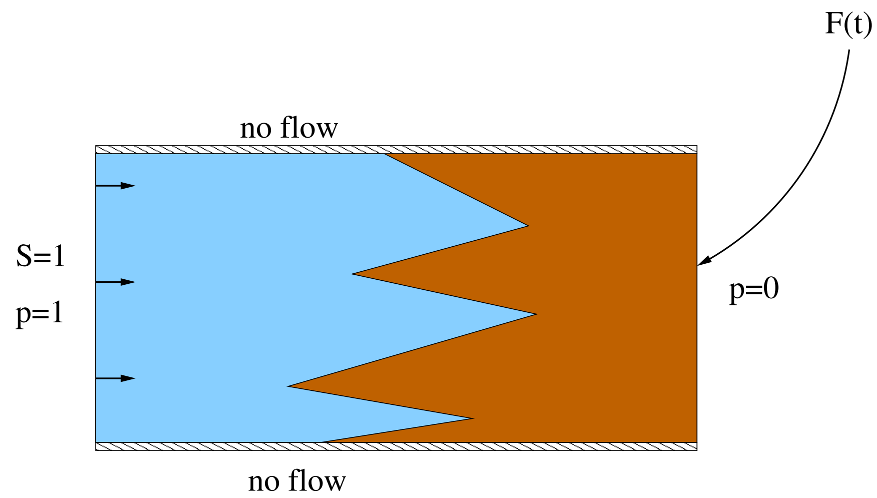

Two-point geostatistics

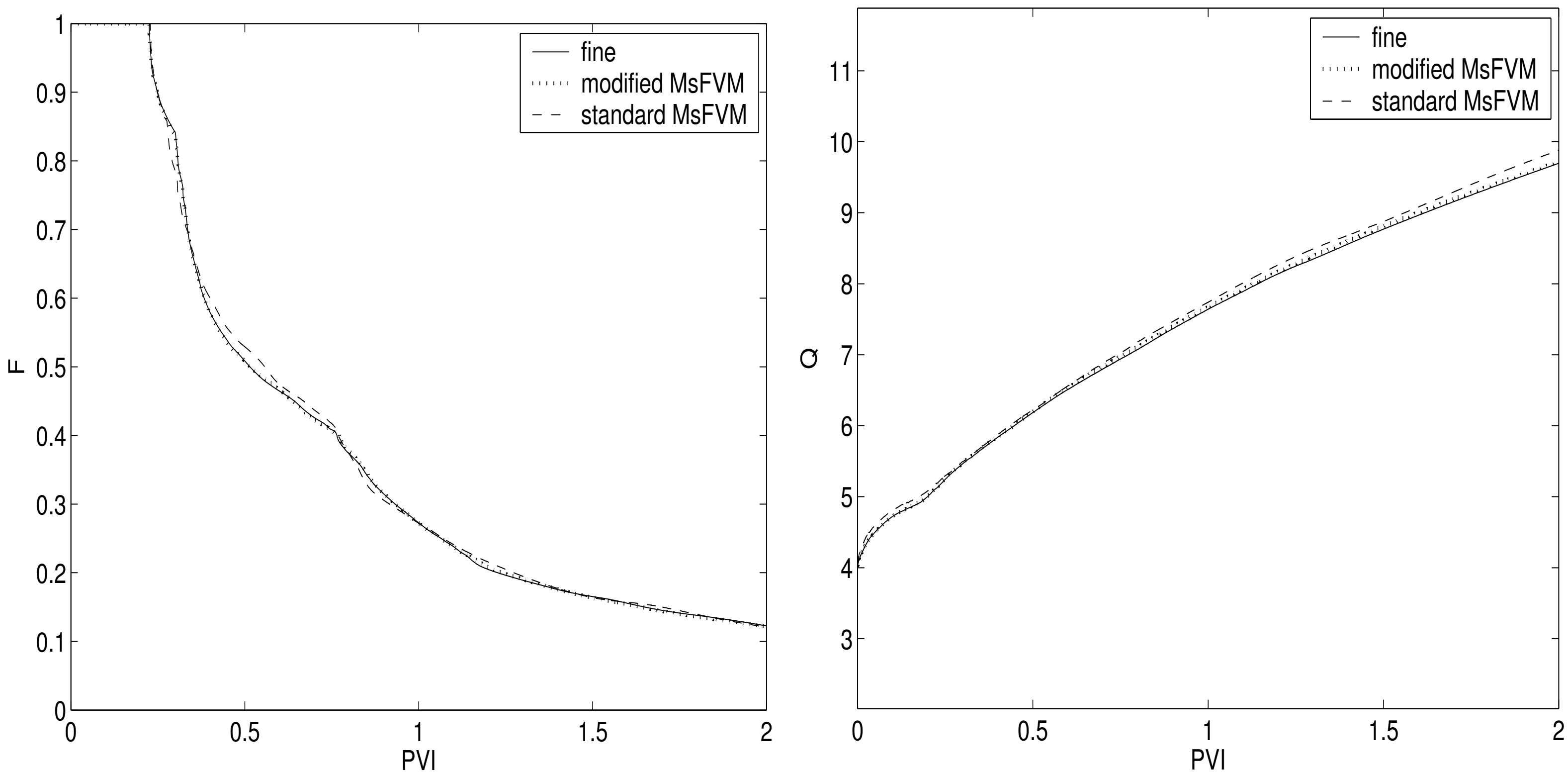

Fractional flow and total flow for a realization of permeability field with spherical variogram and $l_x = 0.4$, $l_z = 0.02$, $\sigma = 1.5$.

Two-point geostatistics

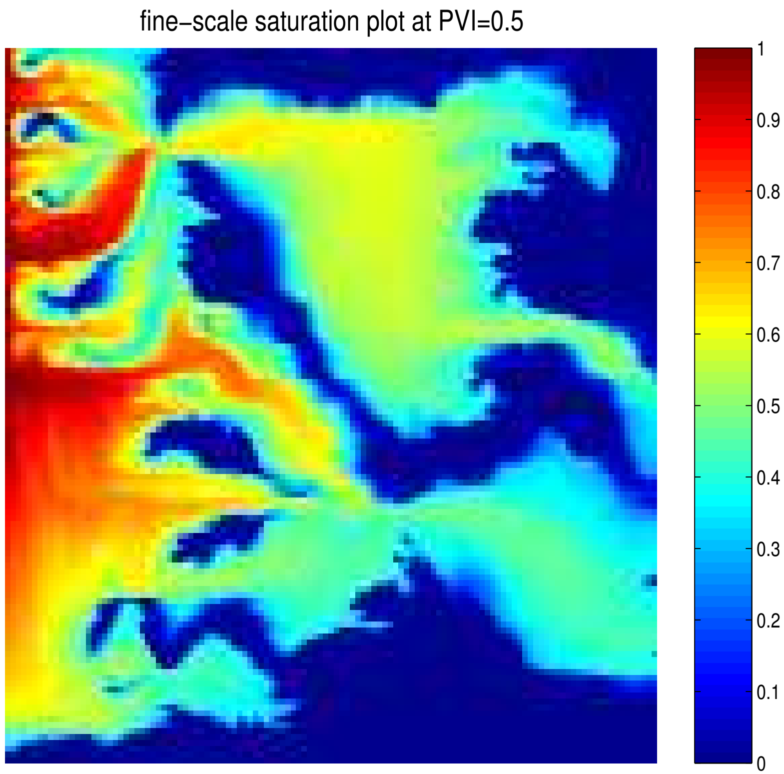

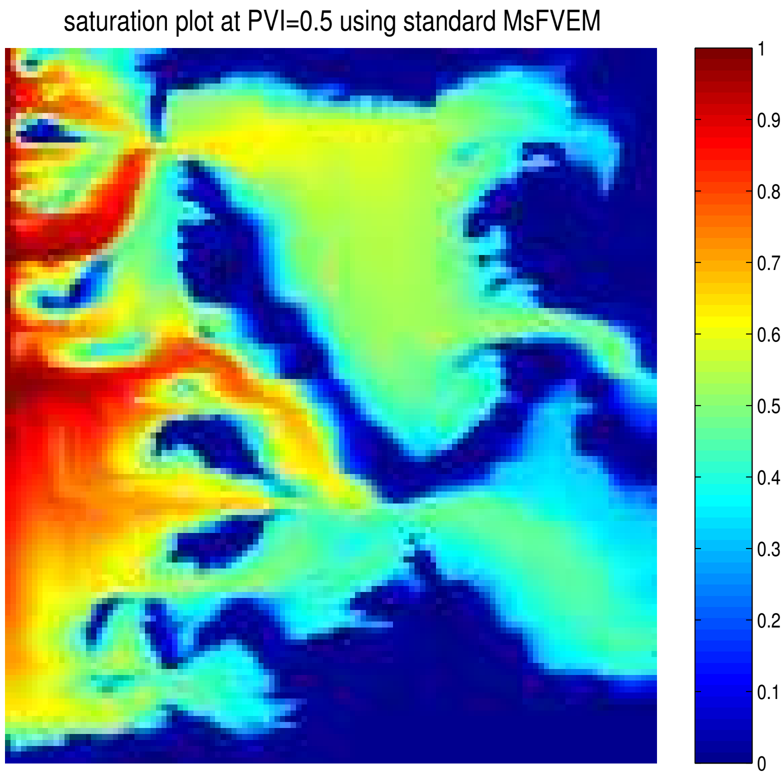

Applications of MsFEM

2) Obtain coarse-scale equations for the saturation equation. The approximate macro scale equation is (Efendiev et al., 2000, 2002, 2004)

$$\frac{\partial \overline{S}}{\partial t} + \overline{v} \cdot \nabla f(\overline{S}) = \nabla_i f'(\overline{S})^2 D^{ij} \nabla_j \overline{S}$$

- D^{ij} depends on two point correlation of the velocity field and $\overline{S}$.
- The overall approach is obtained by combining the saturation equation with the pressure equation in the form $div(\lambda(\overline{S})k\nabla p) = 0$.
- The multiscale base functions are constructed once. The two-point correlation of the velocity can be found using the multiscale base functions. This approach is very efficient and can predict the quantity of interest on a highly coarsened grid.

Multiscale finite element using limited global information

Channelized permeability fields

Benchmark tests: SPE 10 Comparative Project

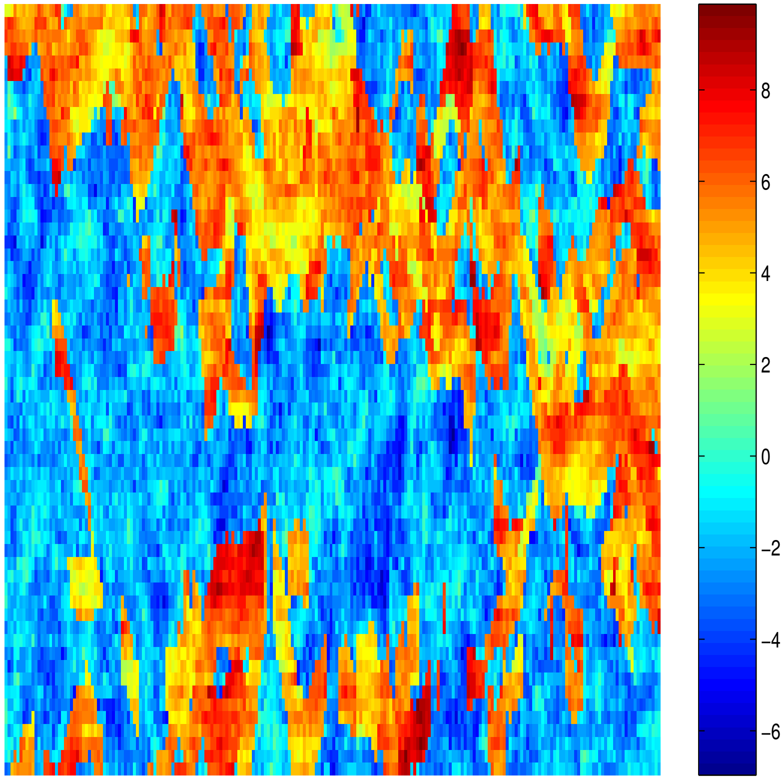

Channelized reservoir

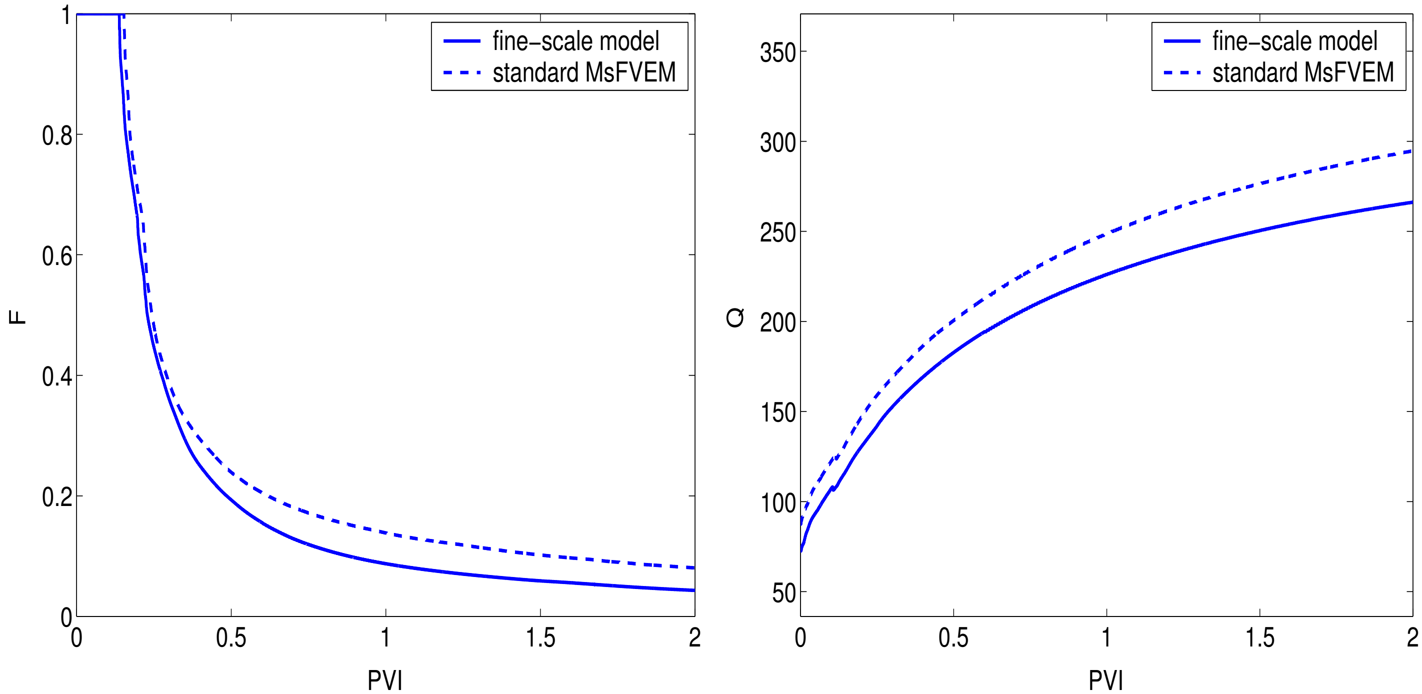

Comparison of upscaled quantities (Layer 43)

Channelized reservoir

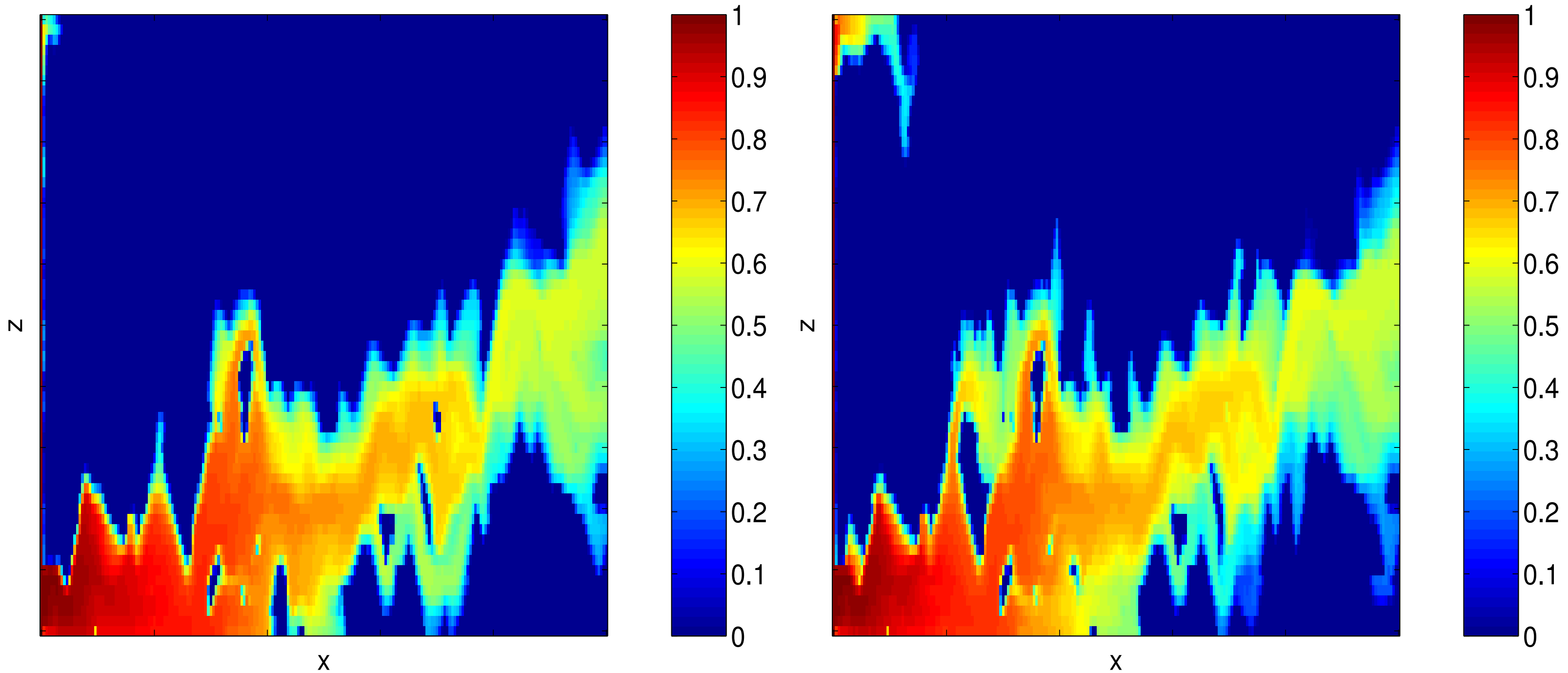

Comparison of saturation profile at PVI=0.5: (left) fine-scale model, (right) standard MsFVEM

MsFVEM utilizing global information

- The numerical tests using strongly channelized permeability fields (such as SPE 10 Comparative) show that local basis functions can not accurately capture the long-range information. There is a need to incorporate a global information.
- The main idea is to use the solution of the fine-scale problem at time zero, p^0, to determine the boundary conditions for the multiscale basis formulation.

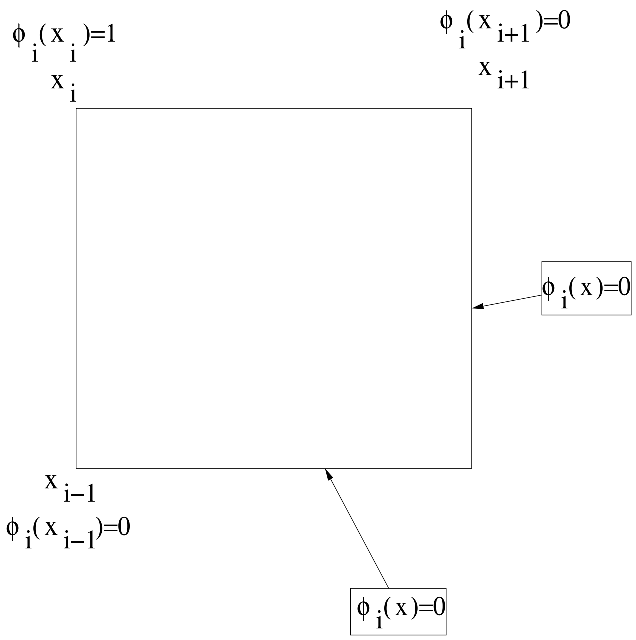

- These approach is different from oversampling technique.
- Previous related work: J. Aarnes; L. Durlofsky et al.

MsFVEM utilizing global information

- If $p^0(x_i) \neq p^0(x_{i+1})$

$$g_i(x)|_{[x_i,x_{i+1}]} = \frac{p^0(x) - p^0(x_{i+1})}{p^0(x_i) - p^0(x_{i+1})}, \quad g_i(x)|_{[x_i,x_{i-1}]} = \frac{p^0(x) - p^0(x_{i-1})}{p^0(x_i) - p^0(x_{i-1})}.$$

  If $p^0(x_i) = p^0(x_{i+1}) \neq 0$ then

$$g_i|_{[x_i,x_{i+1}]} = \psi_i(x) + \frac{1}{2p^0(x_i)}(p^0(x) - p^0(x_{i+1})),$$

  where $\psi_i(x)$ is a linear function on $[x_i, x_{i+1}]$ such that $\psi_i(x_i) = 1$ and $\psi_i(x_{i+1}) = 0$.
- The modified MsFVEM is exact for linear elliptic problem.
- When global boundary changes, then reevaluation of the basis might be needed.

Channelized reservoir

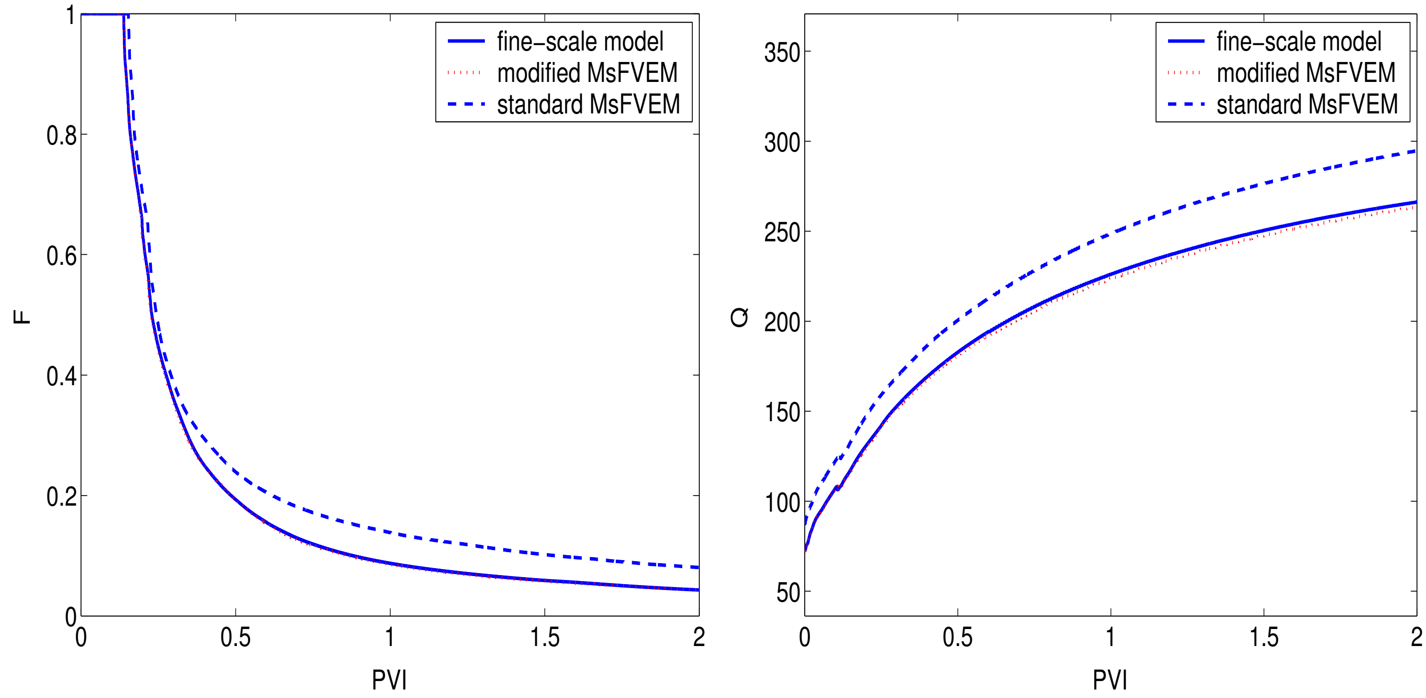

Comparison of upscaled quantities

Channelized reservoir

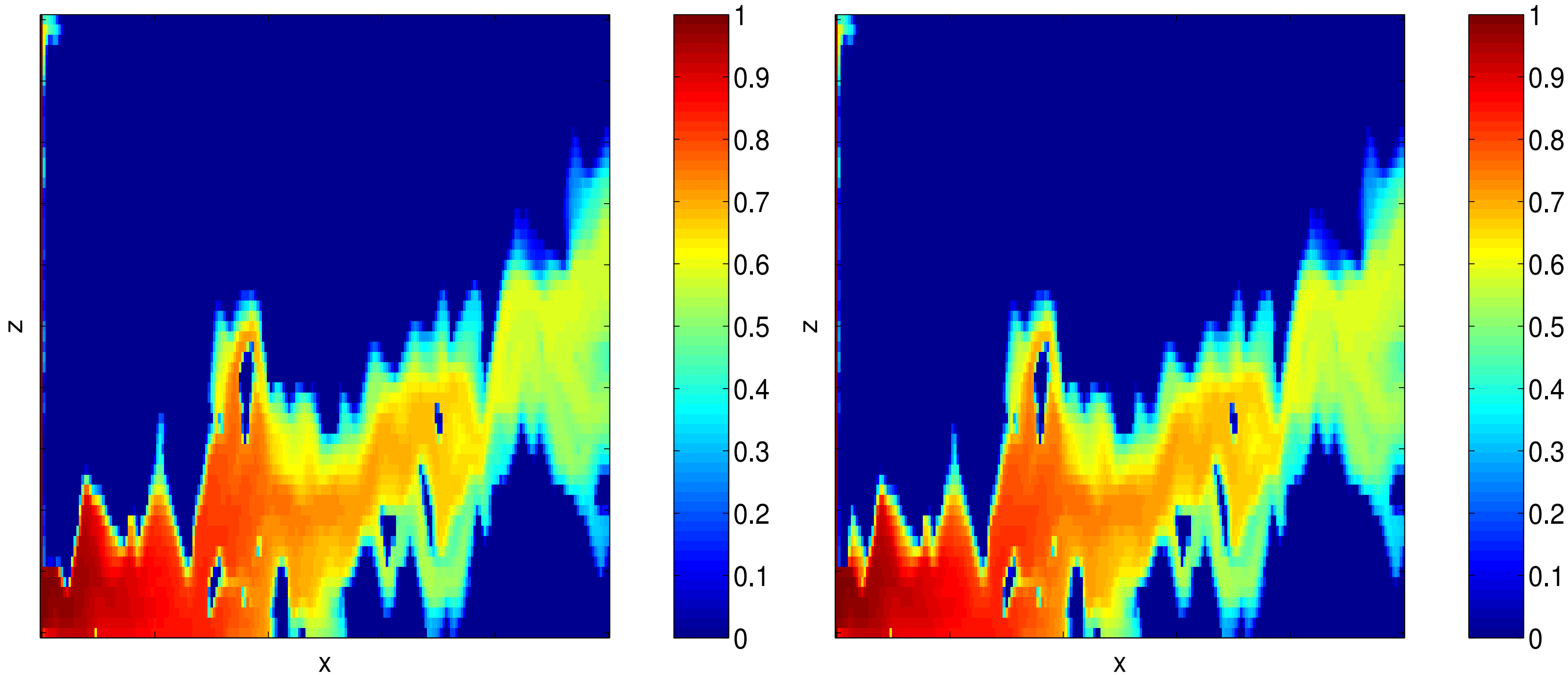

Comparison of saturation profile at PVI=0.5: (left) fine-scale model, (right) modified MsFVEM

Channelized reservoir

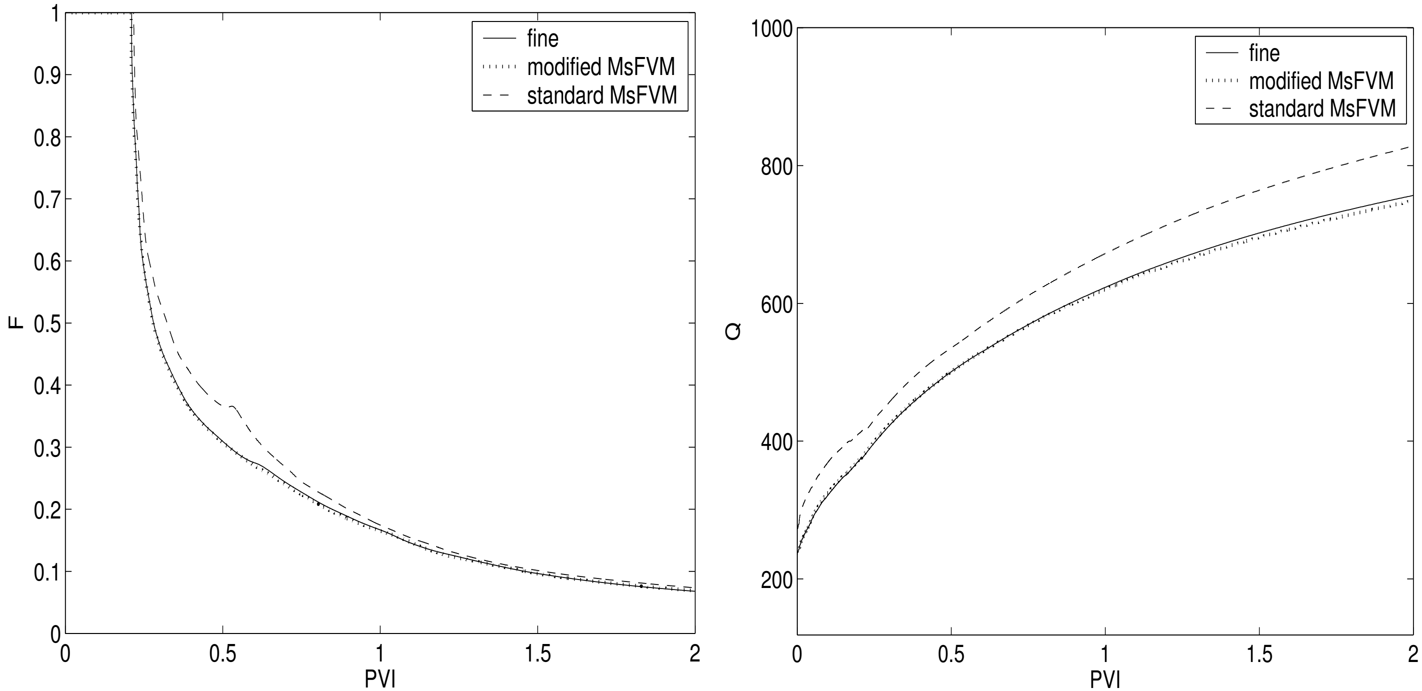

Comparison of upscaled quantities (Layer 59)

Channelized reservoir

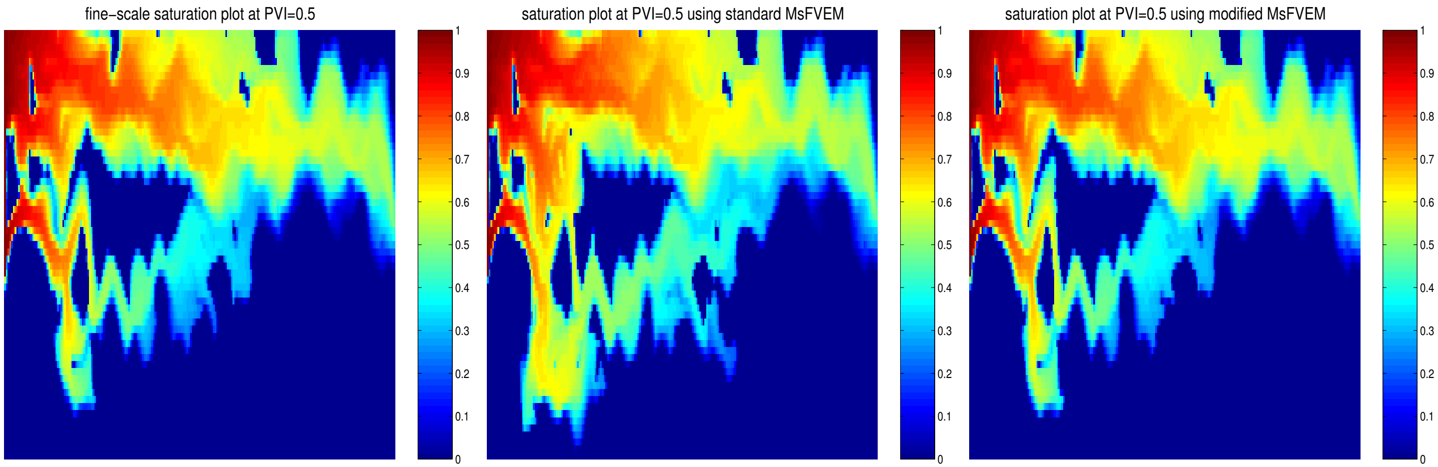

Comparison of saturation profile at PVI=0.5: (left) fine-scale model, (middle) standard MsFVEM (right) modified MsFVEM

Channelized reservoir

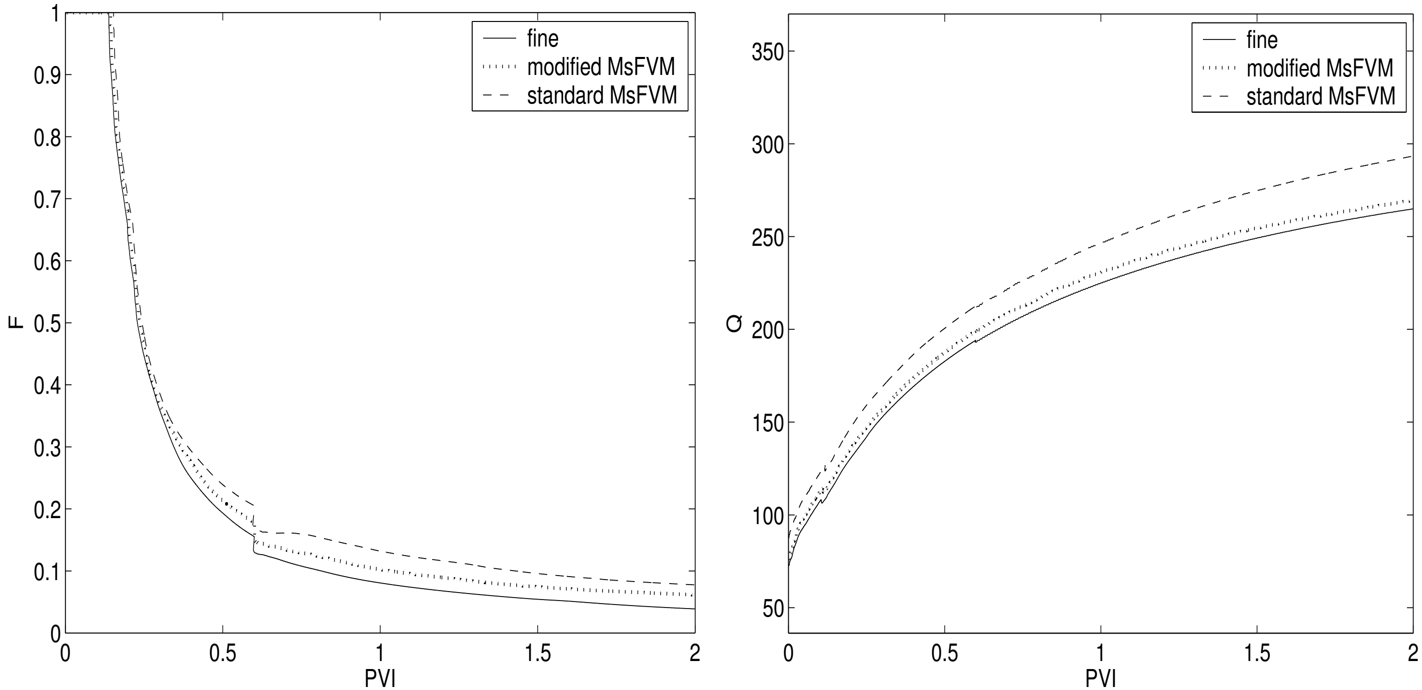

Comparison of upscaled quantities (Layer 43, changing boundary conditions)

Channelized reservoir

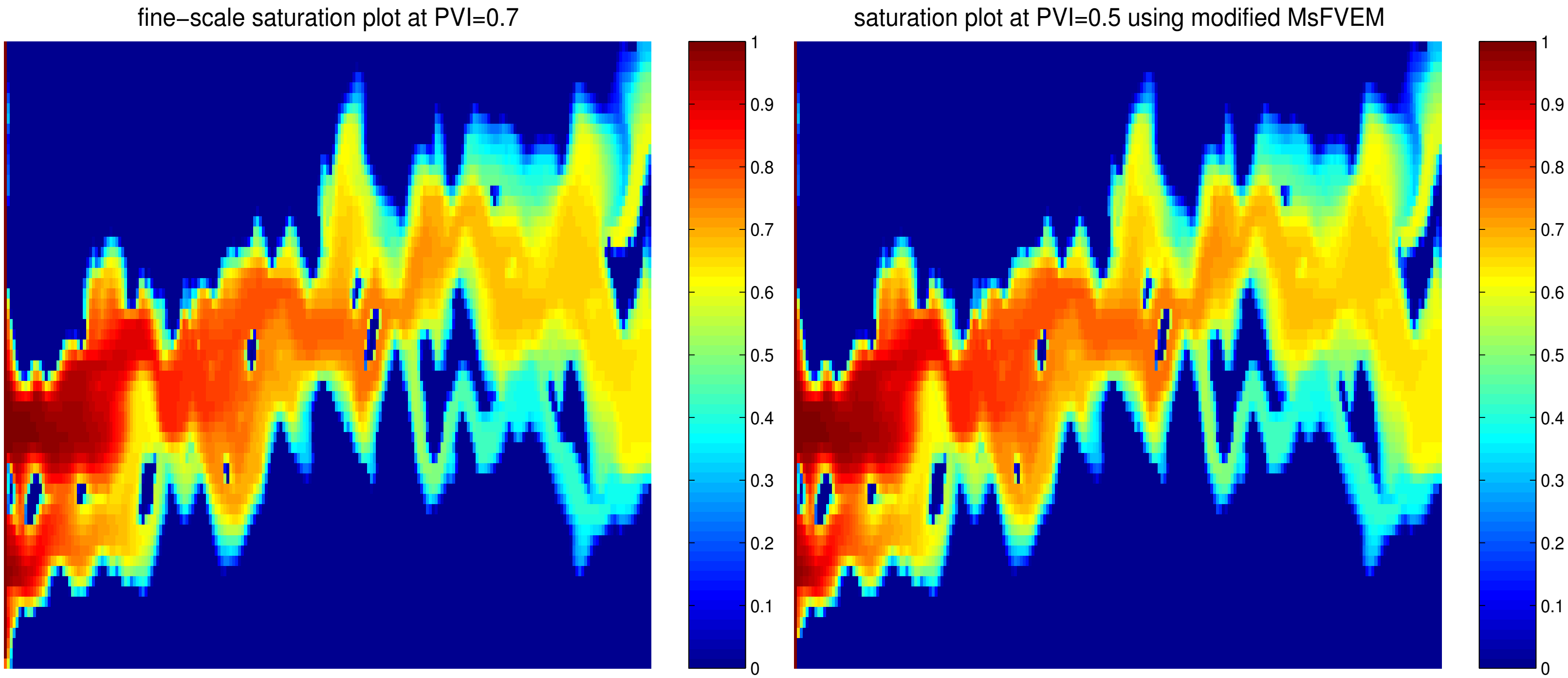

Comparison of saturation profile at PVI=0.5: (left) fine-scale model (right) modified MsFVEM (changing boundary condition)

Channelized reservoir

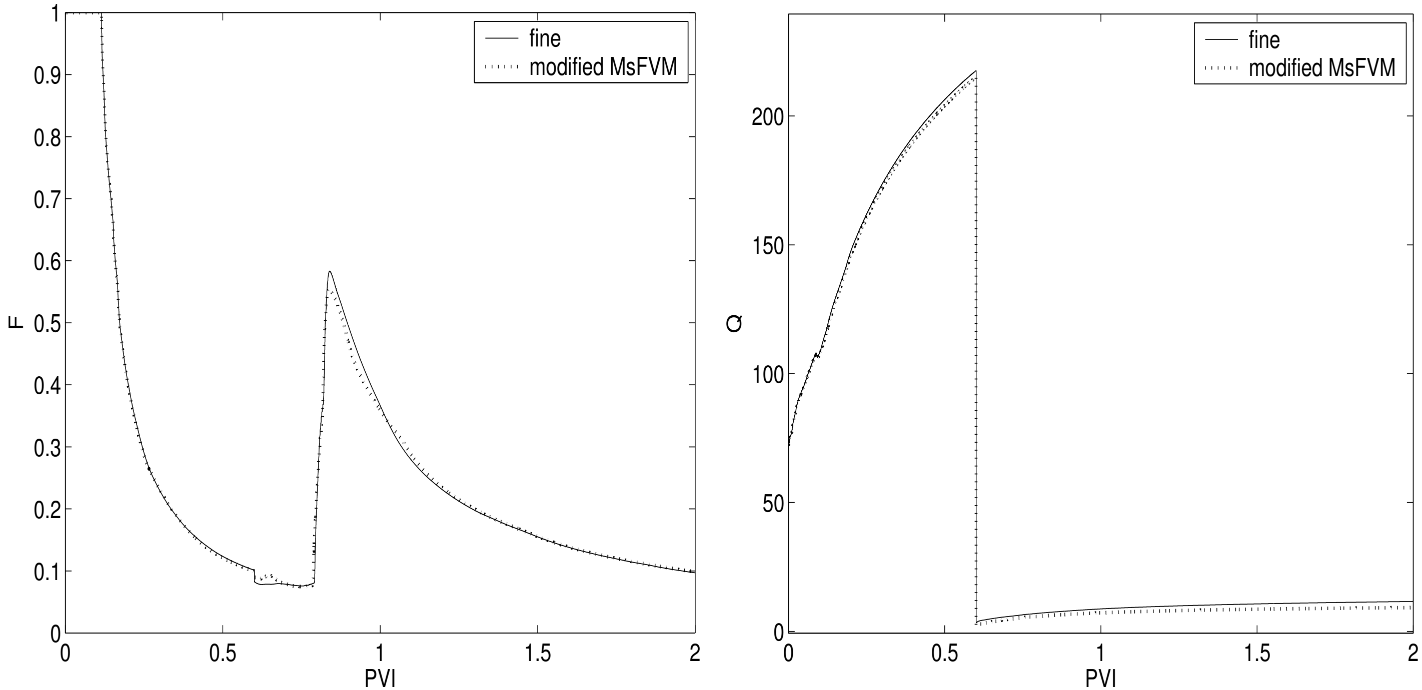

Comparison of upscaled quantities (Layer 43, changing boundary conditions)

Brief Analysis

- Main goal is to show that time-varying pressure is strongly influenced by the initial pressure field.
- Use the streamline-pressure coordinates:

$$\partial\psi/\partial x_1 = -v_2, \quad \partial\psi/\partial x_2 = v_1$$

- Set $\eta = \psi(x, t = 0)$ and $\zeta = p(x, t = 0)$ and transform as follows:

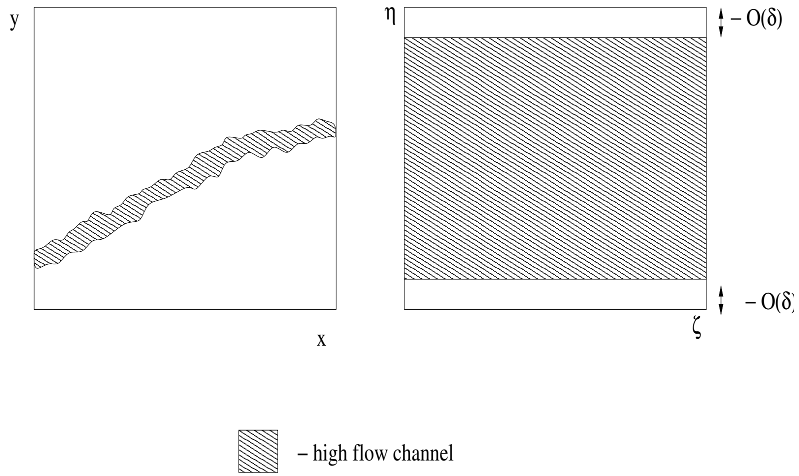

Brief Analysis

- The transformed pressure equation:

$$\frac{\partial}{\partial \eta}\left(|k|^2 \lambda(S) \frac{\partial p}{\partial \eta}\right) + \frac{\partial}{\partial \zeta}\left(\lambda(S) \frac{\partial p}{\partial \zeta}\right) = 0$$

- The transformed saturation equation:

$$\frac{\partial S}{\partial t} + (\mathbf{v} \cdot \nabla \eta) \frac{\partial f(S)}{\partial \eta} + (\mathbf{v} \cdot \nabla \zeta) \frac{\partial f(S)}{\partial \zeta} = 0$$

- $|k|^2 \lambda(S) = |k_0|^2 \lambda_0(\zeta, t) 1_{Q_{1-\delta}} + |k_1|^2 \lambda_1(\eta, \zeta, t) 1_{Q_\delta},\ \lambda(S) = \lambda_0(\zeta, t) 1_{Q_{1-\delta}} + \lambda_1(\eta, \zeta, t) 1_{Q_\delta}$.
- The pressure has the following expansion:

$$p(\eta, \zeta, t) = p_0(\zeta, t) + \delta p_1(\eta, \zeta, t) + \ldots,$$

$\frac{\partial}{\partial \zeta}\left(\lambda_0(\zeta, t) \frac{\partial p_0}{\partial \zeta}\right) = 0$.

- Modified basis functions can exactly recover the initial pressure.

Brief Analysis

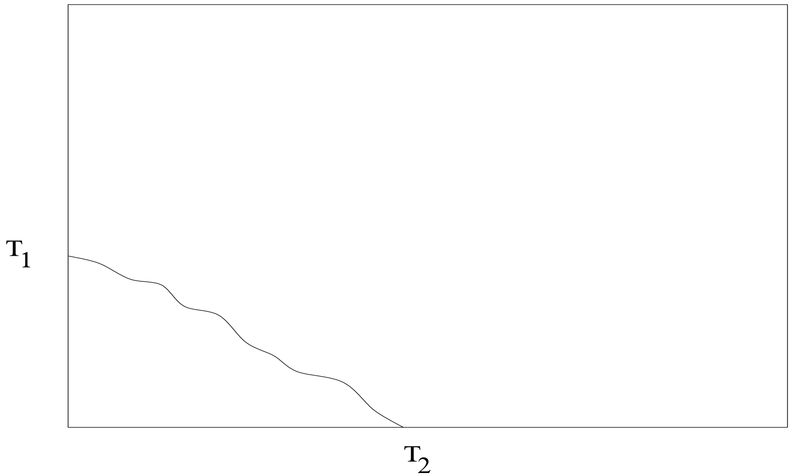

Consider

$$b_1(x) = \frac{p_{loc}^{init}(x) - p_{loc}^{init}(T_2)}{p_{loc}^{init}(T_1) - p_{loc}^{init}(T_2)}, \quad b_2(x) = \frac{p_{loc}^{init}(x) - p_{loc}^{init}(T_1)}{p_{loc}^{init}(T_2) - p_{loc}^{init}(T_1)}.$$

Because 1 and $p_{loc}^{init}(x)$ is in $span(\phi_1, ..., \phi_4)$, $b_1(x)$ and $b_2(x)$ are also in the span of ϕ_i, $i = 1, ..., 4$.
It can be shown that the linear approximation of $p_0(\zeta, t)$ in the span of b_1 and b_2.

Analysis

Assumption G. There exists a sufficiently smooth scalar valued function $G(\eta)$ ($G \in C^3$), such that

$$|p - G(p^{sp})|_{1,Q} \le C\delta,$$

where δ is sufficiently small.
Under Assumption G and $p^{sp} \in W^{1,s}(Q)$ ($s > 2$), multiscale finite element method converges with the rate given by

$$|p - p_h|_{1,Q} \le C\delta + Ch^{1-2/s}|p^{sp}|_{W^{1,s}(Q)} + Ch^{1-2/s}|p^{sp}|_{1,Q} + Ch\|f\|_{0,Q} \le C\delta + Ch^{1-2/s}.$$

Scale separation

Assumption G-S. There exists a sufficiently smooth scalar valued function $G(\eta)$ ($G \in C^3$) such that

$$|p_0 - G(p_0^{sp})|_{1,Q} \leq C\delta_0,$$

where δ_0 is sufficiently small.
Under Assumption G-S and the fact that $p_\epsilon^{sp} \in W^{1,s}$ ($s > 2$) and $|p_0|_{2,Q} + |p_0^{sp}|_{2,Q}$ is bounded, multiscale finite element method converges with the rate given by

$$|p_\epsilon - c_i\phi_i^K|_{1,Q} \leq C\sqrt{\epsilon}|p_0|_{2,Q} + C\delta_0 + C\epsilon(|p_\epsilon^{sp}|_{1,Q} + |p_0^{sp}|_{1,Q}) +$$
$$C\sqrt{\epsilon}|p_0^{sp}|_{2,Q} + Ch^{1-2/s} \leq C\delta_0 + C\sqrt{\epsilon} + Ch^{1-2/s}.$$

Mixed finite element methods

In each coarse block K, we construct basis functions for the velocity field

$$div(k(x)\nabla w_i^K) = \frac{1}{|K|} \quad \text{in} \quad K$$

$$k(x)\nabla w_i^K \mathbf{n}^K = \begin{cases} g_i^K & \text{on } e_i^K \\ 0 & \text{else,} \end{cases}$$

For the pressure, the basis functions are taken to be constants. In Chen and Hou, $g_i^K = \frac{1}{|e_i^K|}$ and e_i^K are the edges of K.

Mixed multiscale finite element methods using single-phase flow information is given in the following way (Aarnes, 2004).

Suppose that p^{sp} solves the single-phase flow equation. We set $b_i^K = (k\nabla p^{sp}|_{e_i^K}) \cdot \mathbf{n}^K$ and assume that b_i^K is uniformly bounded. Then the new basis functions for velocity is constructed by solving the following local problems with $g_i^K = b_i^K/\beta_i^K$, where $\beta_i^K = \int_{e_i^K} k\nabla p^{sp} \cdot \mathbf{n}^K ds$.

Lemma. Inf-sup condition holds.

Mixed finite element methods. Analysis

Assume

$$\|\mathbf{u} - A(x)\mathbf{u}^{sp}\|_{0,Q} \leq \delta$$

and

$$|\sum_i A_i \int_{\partial e_i^K} \mathbf{u}^{sp}\mathbf{n}^K ds| \leq C\delta_1 h^2.$$

Then

$$\|\mathbf{u} - \mathbf{u}_h\|_{H(div,Q)} + \|p - p_h\|_{0,Q} \leq C\delta + C\delta_1 + Ch^\gamma.$$

Multiscale finite element for nonlinear problems

Generalizations of multiscale finite element methods

- Homogenization of nonlinear pdes. Non-periodic homogenization.
- Generalizations of multiscale finite element methods to nonlinear partial differential equations.
- Convergence.
- Oversampling technique.
- Applications.
- (Efendiev and Pankov, SIAM MMS 2003, SIAM AP 2004, EJDE 2005, Appl. Anal., Efendiev, Hou and Ginting, Comm. Math. Sci. 2004).

Nonlinear elliptic and parabolic equations

$$\frac{\partial}{\partial t}u_\epsilon - div(a_\epsilon(x,t,u_\epsilon,\nabla u_\epsilon)) + a_{0,\epsilon}(x,t,u_\epsilon,\nabla u_\epsilon) = f.$$

Assumptions:

$$(a_\epsilon(\cdot,\cdot,\eta,\xi_1) - a_\epsilon(\cdot,\cdot,\eta,\xi_2), \xi_1 - \xi_2) \geq C|\xi_1 - \xi_2|^p$$

$$|a_\epsilon(\cdot,\cdot,\eta,\xi)| + |a_{0,\epsilon}(\cdot,\cdot,\eta,\xi)| \leq C(1 + |\eta| + |\xi|)^{p-1}$$

$$|a_\epsilon(\cdot,\cdot,\eta,\xi_1) - a_\epsilon(\cdot,\cdot,\eta,\xi_2)| \leq C(1 + |\eta|^{p-1-s} + |\xi_i|^{p-1-s})|\xi_1 - \xi_2|^s$$

$$|a_\epsilon(\cdot,\cdot,\eta_1,\xi) - a_\epsilon(\cdot,\cdot,\eta_2,\xi)| \leq C(1 + |\eta_i|^{p-1} + \xi|^{p-1})\nu(|\eta_1 - \eta_2|)$$

$$(a_\epsilon(\cdot,\cdot,\eta,\xi),\xi) + a_{0,\epsilon}(\cdot,\cdot,\eta,\xi)\eta \geq C|\xi|^p - C_0$$

$p > 1$, $s \in (0, \min(p-1, 1))$

Random homogeneous case

Extensions of periodic case: Quasiperiodic; Almost periodic; Random Homogeneous.

(Ω, Σ, μ) - a probability space. Assume $a(x, \omega)$ is strictly stationary field. Then it can be represented as $a(x, \omega) = a(T(x)\omega)$, $x \in R^d$ where $a(\omega)$ is a fixed r.v., $T(x) : \Omega \to \Omega$ is a measure preserving transformation, s.t., $T(0) = I$, and $T(x_1 + x_2) = T(x_1)T(x_2)$; 3) $T(x) : \Omega \to \Omega$ preserve the measure μ on Ω;
Assume $T(x)$ is ergodic (i.e., any invariant function is constant almost everywhere).
Birkhoff Ergodic Theorem:

$$f_\omega(x/\varepsilon) \to M\{f_\omega\}$$

as $\varepsilon \to 0$ weakly in $L^p_{loc}(\mathbb{R}^d)$.

Periodic and almost periodic cases are special cases.

Random case

Auxiliary problem.

Periodic: $div(a(y)(\xi + \nabla N_\xi)) = 0$, $N \in H^1_{per}$, $a^*\xi = \langle a(y)(\xi + \nabla N_\xi)\rangle$.

Random: $a(\omega)(\xi + v(\omega)) \in L^2_{sol}$, $v(\omega) \in L^2_{pot}$.

$$a^*\xi = E[a(\omega)(\xi + v(\omega))]$$

Homogenized solution

$$-div(a^*\nabla u^*) = f.$$

First order corrector: $u_{1,\epsilon} = u^* + N^\epsilon_k(x)\frac{\partial u^*}{\partial x_k}$, where

$$\nabla N^\epsilon_k(x) = v_k(x/\epsilon).$$

Note that $\|N^\epsilon_k\|_{L^2(Q)} = o(1)$ as $\epsilon \to 0$.

Nonlinear parabolic equations

$$A_\epsilon u_\epsilon = D_t u_\epsilon - div(a_\epsilon(x,t,u_\epsilon,D_x u_\epsilon)) + a_{0,\epsilon}(x,t,u_\epsilon,D_x u_\epsilon) = f.$$

$a(\cdot,\cdot,\eta,\xi)$ and $a_0(\cdot,\cdot,\eta,\xi)$ are Carathéodory functions on $Q \times \mathbb{R} \times \mathbb{R}^n$, with values in $\mathbb{R}^n$ and $\mathbb{R}$ respectively, satisfying:

$$(a_\epsilon(\cdot,\cdot,\eta,\xi_1) - a_\epsilon(\cdot,\cdot,\eta,\xi_2), \xi_1 - \xi_2) \geq C(1 + |\xi_1| + |\xi_2|)^{p-\beta}|\xi_1 - \xi_2|^\beta,$$

$$|a_\epsilon(\cdot,\cdot,\eta,\xi)| + |a_{0,\epsilon}(\cdot,\cdot,\eta,\xi)| \leq C(1 + |\eta| + |\xi|)^{p-1},$$

$$|a_\epsilon(\cdot,\cdot,\eta,\xi_1) - a_\epsilon(\cdot,\cdot,\eta,\xi_2)| \leq C(1 + |\eta,\xi_i|^{p-1-s})|\xi_1 - \xi_2|^s,$$

$$(a_\epsilon(\cdot,\eta,\xi),\xi) + a_{0,\epsilon}(\cdot,\eta,\xi)\eta \geq C|\xi|^p - C_0$$

$$|a_\epsilon(\cdot,\cdot,\eta_1,\xi) - a_\epsilon(\cdot,\cdot,\eta_2,\xi)| \leq C(1 + |\eta_i,\xi|^{p-1})\nu(|\eta_1 - \eta_2|)$$

It is known that up there exists a parabolic operator A^*, such that $A^\epsilon \overset{G}{\Longrightarrow} A^*$ (up to a subsequence). This means that $u_\epsilon \to u$ weakly in $L^p(W^{1,p})$, where $A^* u = f$.

G-convergence

Introduce

$$V = L^p(0,T,W_0^{1,p}(Q_0)), \quad \overline{V} = L^p(0,T,W^{1,p}(Q_0)),$$
$$W = \{u \in V, D_t u \in L^q(0,T,W^{-1,q}(Q_0))\},$$
$$\overline{W} = \{u \in \overline{V}, D_t u \in L^q(0,T,W^{-1,q}(Q_0))\}, \quad W_0 = \{u \in W, u(0) = 0\}$$

and $\mathcal{L}^1(u,v) = D_t u - div\big(a(x,t,v,D_x u)\big)$.
Let $L_k^1(u_k,v) = L^1(u,v)$. The sequence $\mathcal{L}_k$ is called G*-convergent* to $\mathcal{L}$ (in symbols, $\mathcal{L}_k \overset{G}{\Longrightarrow} \mathcal{L}$) if for every $v \in V$ and $u \in W_0$ we have that

$$\lim u_k = u$$

weakly in W_0 and

$$\begin{aligned} \lim \Gamma^k(u,v) &= \Gamma(u,v), \\ \lim \Gamma_0^k(u,v) &= \Gamma_0(u,v) \end{aligned}$$

weakly in $L^q(Q)^n$ and $L^q(Q)$, respectively, as $k \to \infty$. Here Γ's denote the nonlinear fluxes.

Homogenization in random media

(Ω, Σ, μ) - a probability space. Assume $a(\omega, \eta, \xi)$ is strictly stationary field for each $\eta \in R, \xi \in R^n$. Then it can be represented as $a(z, \omega, \eta, \xi) = a(T_z\omega, \eta, \xi)$, $z \in R^{d+1}$ where $a(\omega, \eta, \xi)$ is a fixed r.v., $T(z) : \Omega \to \Omega$ is a measure preserving transformation, s.t., $T(0) = I$, and $T(z_1 + z_2) = T(z_1)T(z_2)$; 3) $T(z) : \Omega \to \Omega$ preserve the measure μ on Ω; Periodic and almost periodic cases are special cases. Using Birkhoff Ergodic Theorem:

$$f_\omega(x/\varepsilon^\beta, t/\varepsilon^\alpha) \to M\{f_\omega\}$$

as $\varepsilon \to 0$ weakly in $L^p_{loc}(\mathbb{R}^{n+1})$.

$$D_t u_\epsilon = div\ a(T(x/\epsilon^\beta, t/\epsilon^\alpha)\omega, u_\epsilon, D_x u_\epsilon) - a_0(T(x/\epsilon^\beta, t/\epsilon^\alpha)\omega, u_\epsilon, D_x u_\epsilon) + f$$

in $Q = Q_0 \times [0, T]$.
$U(z)f(\omega) = f(T(z)\omega)$ defines a $(d+1)$-parameter group of isometries in the space of $L_p(\Omega)$. Denote by $\partial_{full} = (\partial_1, \cdots, \partial_{d+1})$ the collection of generators of the group $U(z)$.

Auxiliary problems

$$-div(a(x/\epsilon, u_\epsilon, D_x u_\epsilon)) = f,\ u_\epsilon \in W_0^{1,p}(Q_0)$$

Periodic case. The auxiliary problem: find $N_{\eta,\xi}(y)$ periodic for every η, ξ, such that

$$-div(a(y, \eta, \xi + D_y N_{\eta,\xi}(y))) = 0.$$

Then $u_\epsilon \rightarrow u$ weakly in $W^{1,p}$, where

$$-div(a^*(u, D_x u)) = f$$

and $a^*(\eta, \xi) = \langle a(y, \eta, \xi + D_x N_{\eta,\xi}(y)) \rangle$.
Random case. The auxiliary problem: find $w_{\eta,\xi} \in L^p_{pot}(\Omega)$, $\langle w_{\eta,\xi} \rangle = 0$, such that

$$a(\omega, \eta, \xi + w_{\eta,\xi}(\omega)) \in L^{p'}_{sol}(\Omega).$$

Then $a^*(\eta, \xi) = \langle a(\omega, \eta, \xi + w_{\eta,\xi}(\omega)) \rangle$.
Note that if we define N, such that $\partial N = w$, then N is no longer strictly stationary (periodic case is exception).

Auxiliary problem for nonlinear parabolic equations

$$\mu D_\tau N^\mu_{\eta,\xi} - div_y \; a(y, \tau, \eta, \xi + D_y N^\mu_{\eta,\xi}) = 0.$$

$\mu = \epsilon^{2\beta-\alpha}$. Depending on the relation between α and β, the auxiliary problem is different.
(1) Self-similar case $\alpha = 2\beta$:

$$D_\tau N_{\eta,\xi} - div_y \; a(y, \tau, \eta, \xi + D_y N_{\eta,\xi}) = 0.$$

(2) $\alpha < 2\beta$:

$$-diva(\tau, y, \eta, \xi + D_y N_{\eta,\xi}) = 0.$$

(3) $\alpha > 2\beta$:

$$-div\overline{a}(y, \eta, \xi + D_y N_{\eta,\xi}) = 0,$$

where $\overline{a}(y, \eta, \xi) = \langle a(y, \tau, \eta, \xi)\rangle_\tau$.
(4) $\alpha = 0$ - spatial homogenization:

$$-div_y a(t, y, \eta, \xi + N_{\eta,\xi}) = 0.$$

(5) $\beta = 0$ - temporal homogenization:

$$\hat{a}(x, \eta, \xi) = \langle a(\tau, x, \eta, \xi)\rangle_\tau.$$

Auxiliary problem for nonlinear parabolic equations

Efendiev and Pankov, Homogenization of nonlin. random parab. eq., Adv. Diff. Eq., 2005

$$\mu \sigma w^{\mu}_{\eta,\xi} - div\ a(\omega, \eta, \xi + \partial w^{\mu}_{\eta,\xi}) = 0.$$

$S \subset L_p(\Omega)$ that is contained in the domains of all operators $\partial^{\alpha}_{full} = \partial_1^{\alpha_1} \cdots \partial_{n+1}^{\alpha_{n+1}}$, $\alpha \in Z_+^{n+1}$.
$\mathcal{V} = \mathcal{V}^p$ the completion of S with respect to the semi-norm

$$\|f\|_{\mathcal{V}} = \left(\sum_{i=1}^{n} \|\partial_i f\|^p_{L_p(\Omega)} \right)^{1/p}.$$

By duality we define the operator $\mathbf{div} : L^{p'}(\Omega)^n \to \mathcal{V}'$ by

$$\langle \mathbf{div} u, w \rangle = -\langle u, \partial w \rangle, \ \forall w \in \mathcal{V}.$$

The operators ∂_i may be viewed as derivatives along trajectories of the dynamical system $T(z)$

$$(\partial_i f)(T(z)\omega) = \frac{\partial}{\partial z_i} f(T(z)\omega)$$

for a.e. $\omega \in \Omega$ and $f \in D(\partial_i, L^p(\Omega))$.

Auxiliary problem for nonlinear parabolic equations

Define an unbounded operator $\sigma = (D_t)$ from $\mathcal{V}$ into $\mathcal{V}'$ as follows. $\mathcal{V}_1$, defined as the image of operator ∂, is a closed subspace of $L^p(\Omega)^n$ and ∂ maps $\mathcal{V}$ onto $\mathcal{V}_1$ isomorphically. We say that $v \in \mathcal{V}_1$ belongs to the domain $D(\sigma_1)$ if there exists $f \in \mathcal{V}_1'$ such that

$$\langle v, \partial_{n+1}\varphi \rangle = -\langle f, \varphi \rangle, \; \forall \varphi \in S_1$$

and set $\sigma_1 v = f$. The (unbounded) operator σ_1 is a well-defined closed linear operator from $\mathcal{V}_1$ into $\mathcal{V}_1'$ and its domain is dense in $\mathcal{V}_1$. Using the mollifiers J^δ, it can be verified that $\sigma_1' = -\sigma_1$, where $\sigma_1' : \mathcal{V}_1 \to \mathcal{V}_1'$ is the adjoint operator to σ_1. Now we set

$$\sigma = \mathbf{div} \circ \sigma_1 \circ \partial \,.$$

Then σ is a closed linear operator from $\mathcal{V}$ into $\mathcal{V}'$, with domain $\mathcal{W} = D(\sigma)$.
We need so-called near solutions that approximate w by random fields with smooth realizations.
Near solutions are defined by $\mu\sigma N_\delta^\mu + A N_\delta^\mu = \partial\rho_\delta$. It can be shown that $\lim_{\delta\to 0}\langle|\rho_\delta|^p\rangle = 0$. **Lemma.** Assume $\rho_\delta \in L^p(\Omega)$ and $\langle|\rho|^p\rangle < s(\delta)$, where $s(\delta) \to 0$ as $\delta \to 0$. Then for any sequence $\delta \to 0$ there exists a sequence $\epsilon_0(\delta)$, such that $\epsilon_0(\delta) \to 0$ as $\delta \to 0$, and for any $Q \subset R^{n+1}$

$$\int_Q |\rho_\delta(T(x/\epsilon^\beta, t/\epsilon^\alpha)\omega)|^p dxdt < s(\delta), \; \forall \epsilon < \epsilon_0(\delta),$$

Homogenization result

The homogenized operator is defined for a.e. realization by

$$L^* u = D_t u - div(a^*(\omega, x, t, u, D_x u)) + a_0^*(\omega, x, t, u, D_x u).$$

a^* and a_0^* are defined as follows (Efendiev and Pankov 2005).
For self-similar case ($\alpha = 2\beta$),

$$a^*(\eta, \xi) = \langle a(\omega, \eta, \xi + \partial w_{\eta,\xi}) \rangle, {a_0}^*(\eta, \xi) = \langle a_0(\omega, \eta, \xi + \partial w_{\eta,\xi}) \rangle,$$

where $w_{\eta,\xi} = w^{\mu=1} \in \mathcal{W}$ is the unique solution of

$$\sigma w^{\mu=1} - div\ a(\omega, \eta, \xi + \partial w^{\mu=1}) = 0.$$

For non self-similar case ($\alpha < 2\beta$),

$$a^*(\eta, \xi) = \langle a(\omega, \eta, \xi + \partial w_{\eta,\xi}) \rangle, {a_0}^*(\eta, \xi) = \langle a_0(\omega, \eta, \xi + \partial w_{\eta,\xi}) \rangle,$$

where $w_{\eta,\xi} = w^0 \in \mathcal{V}$ is the unique solution of

$$-div\ a(\omega, \eta, \xi + \partial w^0) = 0.$$

Homogenization result

Denote $M_t\{f\} = \lim_{T\to\infty} \frac{1}{2T} \int_{-T}^{T} f(T(0,\tau)\omega)d\tau$,
$M_x\{f\} = \lim_{|K|\to\infty} \frac{1}{|K|} \int_K f(T(y,0)\omega)dy$

$$\overline{a}(\omega,\eta,\xi) = M_t(a(\omega,\eta,\xi)).$$

$\mathcal{V}_s$ is obtained by completing the elements of S

$$f(\omega) = M_t\{f(T_1(t)\omega\}.$$

with respect to the norm $\|f\| = (\sum_{i=1}^n \|\partial_i f\|^p_{L_p(\Omega)})^{1/p}$.
For spatial case ($\alpha = 0$),

$$a(\omega,\eta,\xi) = M_x\{a(T_2(x)\omega,\eta,\xi + \partial w_{\eta,\xi}(T_2(x)\omega))\},$$
$$a_0(\omega,\eta,\xi) = M_x\{a_0(T_2(x)\omega,\eta,\xi + \partial w_{\eta,\xi}(T_2(x)\omega))\},$$

where $w_{\eta,\xi} = w_x \in \mathcal{V}$

$$-div\ a(\omega,\eta,\xi + \partial w_x) = 0.$$

Homogenization result

For temporal case ($\beta = 0$), the homogenized fluxes are defined by

$$a^*(\omega, \eta, \xi) = P_1 a(\omega, \eta, \xi), a_0^*(\omega, \eta, \xi) = P_1 a_0(\omega, \eta, \xi).$$

Self-similar case $\alpha = 2$, $\beta = 1$

$$w^{\mu=1}_{\epsilon,\delta}(x,t,\omega) = \epsilon w^{\mu=1}_{\delta}(T(x/\epsilon, t/\epsilon^2)\omega).$$

$w^{\mu}_{\epsilon,\delta}$ satisfies in R^{n+1} for a.e. ω

$$D_t w^{\mu=1}_{\epsilon,\delta} - div(a(T(x/\epsilon, t/\epsilon^2)\omega, \eta, \xi + D_x w^{\mu=1}_{\epsilon,\delta})) = div_x \rho_\delta.$$

For every $\delta > 0$ $w^{\mu=1}_{\epsilon,\delta} \to 0$ weakly in $\overline{W}$ as $\epsilon \to 0$.

$$D_t w^{\mu=1}_{\epsilon,\delta} - div(a(T(x/\epsilon, t/\epsilon^2)\omega, \eta, \xi + D_x w^{\mu=1}_{\epsilon,\delta}) + a_0(T(x/\epsilon, t/\epsilon^2)\omega, \eta, \xi + D_x w^{\mu=1}_{\epsilon,\delta}) = h_{\epsilon,\delta}$$

$$+ div_x \rho_\delta,$$

where $h_{\epsilon,\delta} = a_0(T(x/\epsilon, t/\epsilon^2)\omega, \eta, \xi + D_x w^{\mu=1}_{\epsilon,\delta})$.

Self-similar case $\alpha = 2$, $\beta = 1$

It is possible to chose a generic sequence of $\delta_k \to 0$ as $k \to \infty$ and corresponding $\epsilon_k = \epsilon(\delta_k)$ such that $w_k^{\mu=1} = w_{\epsilon_k,\delta_k}^{\mu=1} \to 0$ weakly in $\overline{W}$, and $\rho_k = \rho_{\delta_k} \to 0$ in $L^{p'}(Q)^n$ as $k \to \infty$.
Consider for each $\omega \in \Omega$

$$L_k u = D_t u - div(a(T(x/\epsilon_k, t/\epsilon_k^2)\omega, \eta, \xi + D_x u) + a_0(T(x/\epsilon_k, t/\epsilon_k^2)\omega, \eta, \xi + D_x u).$$

It is known that L_k G-converges to $\tilde{L}$ (up to a subsequence),

$$\tilde{L}u = D_t u - div(\tilde{a}(\omega, t, x, \eta, \xi + D_x u)) + \tilde{a}_0(\omega, t, x, \eta, \xi + D_x u).$$

On the other hand using Ergodic Theorem

$$a(T(x/\epsilon_k, t/\epsilon_k^2)\omega, \eta, \xi + D_x w_k^{\mu=1}) \to \langle a(\omega, \eta, \xi + \partial w^{\mu=1})\rangle$$

$$a_0(T(x/\epsilon_k, t/\epsilon_k^2)\omega, \eta, \xi + D_x w_k^{\mu=1}) \to \langle a_0(\omega, \eta, \xi + \partial w^{\mu=1})\rangle,$$

as $k \to \infty$ weakly in $L^{p'}(Q)^n$ and $L^{p'}(Q)$.

Individual homogenization

Let $C_b(R^{n+1})$ be the Banach space of all bounded and continuous functions on R^{n+1}. The closure of the space $Trig(R^{n+1})$ in $C_b(R^{n+1})$ is called the space of Bohr almost periodic (a.p.) functions and is denoted by $CAP(R^{n+1})$.

Bohr compactification of R^{n+1}. There exist a compact Abelian group R_B^{n+1} and a continuous group monomorphism

$$i_B : R^{n+1} \longrightarrow R_B^{n+1}$$

with the following property: $f \in C_b(R^{n+1})$ *is almost periodic if and only if there exists a unique function* $\tilde{f} \in C(R_B^{n+1})$ *such that* $f(z) = \tilde{f}(i_B z)$. Such a couple (R_B^{n+1}, i_B) is unique up to a natural equivalence and is called the Bohr compactification. $CAP(R_B^{n+1})$ may be isometrically identified with $C(R_B^{n+1})$.

We define a dynamical system $T(z)$ on R_B^{n+1} by

$$T(z)\omega = \omega + z, \quad \omega \in R_B^{n+1}, \; z \in R^{n+1}.$$

Denote by μ the Haar measure on R_B^{n+1} normalized by $\mu(R_B^{n+1}) = 1$.

Individual homogenization

Besicovitch almost periodicity. For a function

$$f \in L^p_{loc}(R^{n+1}), \quad 1 \leq p < \infty,$$

we set

$$\|f\|^p_{B^p} = \limsup_{t \to \infty} \frac{1}{|K_t|} \int_{K_t} |f(z)|^p dz, \tag{-15}$$

where $K_t = \{z \in R^{n+1} : |z_i| \leq t, \ i = 1, 2, \dots, n+1\}$. A function $f \in L^p_{loc}(R^{n+1})$ is said to be Besicovitch almost periodic with the exponent p if there is a sequence $f_k \in Trig(R^{n+1})$ such that

$$\lim_{k \to \infty} \|f - f_k\|_{B^p} = 0.$$

Bohr compactification: One can extend, by continuity, the isomorphism $f \longmapsto \tilde{f}$ between $CAP(R^{n+1})$ and $C(R_B^{n+1})$ to the map from $B^p(R^{n+1})$ into $L^p(R_B^{n+1})$. The density of $C(R_B^{n+1})$ in $L^p(R_B^{n+1})$ implies that this map is onto and $\|\tilde{f}\|_{p, R_B^{n+1}} = \|f\|_{B^p}$. The map $f \longmapsto \tilde{f}$ induces an isometric isomorphism between $\overline{B}^p(R^{n+1})$ and $L^p(R_B^{n+1})$.

Individual homogenization

Comparison estimate (Efendiev, Jiang and Pankov 2006)

Suppose $\mathcal{A}_k$ and $\mathcal{B}_k$ are sequences of operators of the class Π, $\mathcal{A}_k \xRightarrow{G} \mathcal{A}$, and $\mathcal{B}_k \xRightarrow{G} \mathcal{B}$. There exists $\alpha > 0$ such that given $R > 0$

$$g(t,x,R) \le \overline{g}(t,x,r) + K\left[\varphi(r)^{1/q} + \varphi^{\gamma}(r) + (1+r)^{\gamma}\overline{g}(t,x,r)^{\gamma}\right]$$

for a constant $K = K(R)$ and almost all $x \in Q$ and for all $r > 0$, where $\gamma = \frac{s}{q^2(\beta-1)}$,

$$\varphi(r) = r^{-p} + r^{-\alpha p/(p+\alpha)}, \quad r > 0.$$

Here

$$g(t,x,r) = \sup_{|\xi|,|\eta|\le r} |a(t,x,\eta,\xi) - b(t,x,\eta,\xi)|$$

$$g^k(t,x,r) = \sup_{|\xi|,|\eta|\le r} |a^k(t,x,\eta,\xi) - b^k(t,x,\eta,\xi)|,$$

$$\overline{g}(t,x,r) = \limsup_{\rho\to 0}\limsup_{k\to\infty} \frac{1}{|U_\rho(t,x)|}\int_{U_\rho(t,x)} g^k(t,y,r)dydt$$

Individual homogenization

We shall say that a sequence $\mathcal{A}_k \in \Pi$ converges to $\mathcal{A} \in \Pi$ *component-wise* in L^1 (c.-w. in L^1), if for any $r \geq 0$

$$\lim_{k\to\infty} \sup_{|\xi|,|\eta|\leq r} |a^k(t,x,\eta,\xi) - a(t,x,\eta,\xi)| =$$

$$= \lim_{k\to\infty} \sup_{|\xi|,|\eta|\leq r} |a_0^k(t,x,\eta,\xi) - a_0(t,x,\eta,\xi)| = 0$$

strongly in $L^1(Q)$.

Corollary. Let $\mathcal{A}_k^l$ be a double sequence of operators of the class Π such that $\mathcal{A}_k^l \xrightarrow{G} \mathcal{A}^l$ for any $l \in \mathbf{N}$, as $k \to \infty$. Assume that $\mathcal{A}_k^l \to \mathcal{A}_k$ c.-w. in L^1 uniformly with respect to $k \in \mathbf{N}$ and $\mathcal{A}^l \to \mathcal{A}$ c.-w. in L^1, as $l \to \infty$. Then $\mathcal{A}_k \xrightarrow{G} \mathcal{A}$.

Individual homogenization

Individual homogenization takes place for the operator

$$\mathcal{L}_\varepsilon^m u = D_t u - div\, a^m(\frac{t}{\epsilon^\alpha}, \frac{x}{\epsilon^\beta}, u, D_x u) + a_0^m(\frac{t}{\epsilon^\alpha}, \frac{x}{\epsilon^\beta}, u, D_x u),$$

we have $\mathcal{L}_\varepsilon^m \overset{G}{\Longrightarrow} \hat{\mathcal{L}}^m$.
Consider

$$g(t,x,r) = \sup_{|\eta|,|\xi|\le r} |a^m(t,x,\eta,\xi) - a(t,x,\eta,\xi)|,$$

$$\hat{g}(t,x,r) = \sup_{|\eta|,|\xi|\le r} |\hat{a}^m(\eta,\xi) - b(t,x,\eta,\xi)|.$$

We set

$$\overline{g}(t,x,r) = \limsup_{\rho\to 0} \limsup_{\varepsilon\to 0} \frac{1}{|K_\rho(t,x)|} \int_{K_\rho(t,x)} g(\varepsilon^{-\alpha}\tau, \varepsilon^{-\beta}y, r)\, dy d\tau$$

It follows from comparison theorem
$\hat{g}(t,x,R) \le \overline{g}(t,x,r) + c(R)\left[\varphi(r)^{1/q} + \varphi^\gamma(r) + (1+r)^\gamma \overline{g}(t,x,r)^\gamma\right]$. Pass to the limit as $m\to\infty$, then $r\to\infty$ gives $b(t,x,\eta,\xi) = \hat{a}(\eta,\xi)$.

Multiscale finite element methods for nonlinear problems

Consider $u_\epsilon \in W_0^{1,p}(Q)$, $-div(a_\epsilon(x, u_\epsilon, \nabla u_\epsilon)) + a_{0,\epsilon}(x, u_\epsilon, \nabla u_\epsilon) = f$.
Let S^h be "usual" finite dimensional space defined on a coarse-grid ($1 \gg h \gg \epsilon$).
Multiscale map: Define $E : S^h \to V_\epsilon^h$ such that for any $u_h \in S^h$, $u_{\epsilon,h} = Eu_h$ is defined by

$$-div(a_\epsilon(x, \eta^{u_h}, \nabla u_{\epsilon,h})) = 0 \text{ in } K,$$

$\eta^{u_h} = 1/|K| \int_K u_h dx$ and $u_{\epsilon,h} - u_h \in W_0^{1,p}(K)$ in each K.
For the linear case, V_ϵ^h is a linear space whose basis can be obtained by mapping the basis of S^h. This is precisely MsFEM for linear problems.

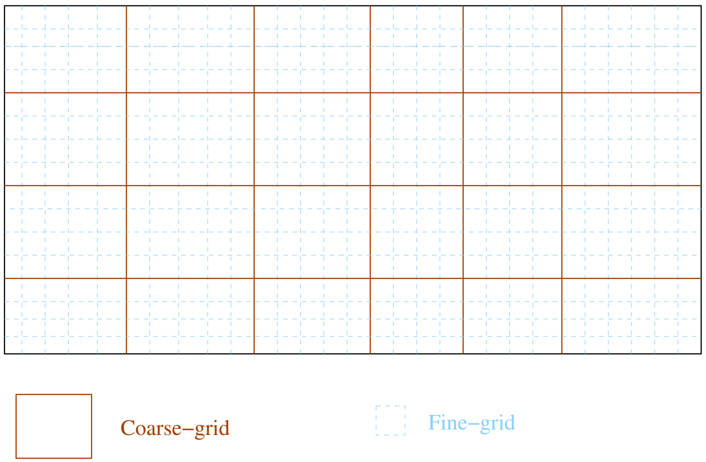

Multiscale finite element methods for nonlinear problems

Multiscale Formulation

MsFEM

Find $u_h \in S^h$ ($u_{\epsilon,h} = E u_h \in V_\epsilon^h$) such that

$$A(u_h, v_h) = \int_Q f v_h dx, \ \forall v_h \in S^h,$$

where

$$A(u_h, v_h) = \sum_K \int_K ((a_\epsilon(x, \eta^{u_h}, \nabla u_{\epsilon,h}), \nabla v_h) + a_{0,\epsilon}(x, \eta^{u_h}, \nabla u_{\epsilon,h}) v_h) dx.$$

Multiscale finite element methods for nonlinear problems

Multiscale Formulation

MsFEM

Find $u_h \in S^h$ ($u_{\epsilon,h} = Eu_h \in V_\epsilon^h$) such that

$$A(u_h, v_h) = \int_Q f v_h dx, \ \forall v_h \in S^h,$$

where

$$A(u_h, v_h) = \sum_K \int_K ((a_\epsilon(x, \eta^{u_h}, \nabla u_{\epsilon,h}), \nabla v_h) + a_{0,\epsilon}(x, \eta^{u_h}, \nabla u_{\epsilon,h}) v_h) dx.$$

MsFVEM

$$-\int_{\partial V_z} a_\epsilon \left(x, \eta^{u_h}, \nabla u_{\epsilon,h}\right) \cdot n \, dS + \int_{V_z} a_{0,\epsilon} \left(x, \eta^{u_h}, \nabla u_{\epsilon,h}\right) \, dx = \int_{V_z} f,$$

where V_z is control volume.

Convergence Theorems

(1) General heterogeneities (up to a subsequence) (Efendiev and Pankov, 2004)

$$\lim_{h \to 0} \lim_{\epsilon \to 0} \|u_h - u\|_{W^{1,p}(Q)} = 0$$

(2) Periodic heterogeneities (up to a subsequence) (Efendiev, Hou and Ginting, 2004)

$$\lim_{\epsilon/h \to 0} \|u_h - u\|_{W^{1,p}(Q)} = 0$$

Explicit convergence rates for strongly monotone operators are obtained.

Proof. Periodic Case

Consider, $u_\epsilon \in W_0^{1,p}(Q)$, $-div(a(\frac{x}{\epsilon}, u_\epsilon, \nabla u_\epsilon)) = f$.

Homogenization. For each $\eta \in R$, $\xi \in R^d$, $N_{\eta,\xi} \in W_{per}^{1,p}(Y)$

$$-div(a(y, \eta, \xi + \nabla_y N_{\eta,\xi}(y))) = 0.$$

The homogenized fluxes are computed by $a^*(\eta, \xi) = \langle a(y, \eta, \xi + \nabla_x N_{\eta,\xi}(y)) \rangle$, and the homogenized equation is given by $-div(a^*(u, \nabla_x u)) = f$.

Proof. Periodic Case

Theorem.

$$\lim_{\epsilon/h \to 0} \|u_h - u\|_{W^{1,p}(Q)} = 0,$$

where $h = h(\epsilon) \gg \epsilon$, and $h(\epsilon) \to 0$, as $\epsilon \to 0$.
Lemma. Coercivity: $\|u_h\|_{W^{1,p}(Q)} \le C$.

Proof. Periodic Case

Theorem.

$$\lim_{\epsilon/h\to 0}\|u_h-u\|_{W^{1,p}(Q)}=0,$$

where $h=h(\epsilon)\gg\epsilon$, and $h(\epsilon)\to 0$, as $\epsilon\to 0$.
Lemma. Coercivity: $\|u_h\|_{W^{1,p}(Q)}\le C$.

$$\langle A_{\epsilon,h}u_h,v_h\rangle=\sum_K\int_K(a(\frac{x}{\epsilon},\eta^{u_h},\nabla u_{\epsilon,h}),\nabla v_h)dx=\langle f,v_h\rangle$$

$$\langle A^*u_h,v_h\rangle=\sum_K\int_K(a^*(u_h,\nabla u_h),\nabla v_h)dx$$

$$\begin{aligned}\langle A^*u_h-A^*P_hu,u_h-P_hu\rangle&=\langle A^*u_h-A_{\epsilon,h}u_h,u_h-P_hu\rangle+\langle A_{\epsilon,h}u_h-A^*P_hu,u_h-P_hu\rangle\\&=\langle A^*u_h-A_{\epsilon,h}u_h,u_h-P_hu\rangle,\end{aligned}$$

where P_hu is a Galerkin solution, $\langle A^*P_hu,v_h\rangle=\langle f,v_h\rangle$, $\forall v_h\in S^h$.

Proof. Periodic Case

Introduce $\mathcal{P} = \nabla_x u_h + \nabla_y N_{\eta^{u_h}, \nabla u_h}(y)$ in each K, where $-div_y a(y, \eta^{u_h}, \mathcal{P}) = 0$.

$$\langle A_{\epsilon,h} u_h - A^* u_h, v_h \rangle = \sum_K \int_K (a(\frac{x}{\epsilon}, \eta^{u_h}, \nabla u_{\epsilon,h}) - a(\frac{x}{\epsilon}, \eta^{u_h}, \mathcal{P}), \nabla v_h) dx +$$

$$\sum_K \int_K (a(\frac{x}{\epsilon}, \eta^{u_h}, \mathcal{P}) - a^*(\eta^{u_h}, \nabla u_h), \nabla v_h) dx +$$

$$\sum_K \int_K (a^*(\eta^{u_h}, \nabla u_h) - a^*(u_h, \nabla u_h), \nabla v_h) dx = I + II + III$$

Lemma. $\|\nabla u_{\epsilon,h} - \mathcal{P}\|_{p,Q} \leq C \left(\frac{\epsilon}{h}\right)^{\frac{1}{p(p-s)}} \left(|Q| + \|u_h\|_{p,Q}^p + \|\nabla u_h\|_{p,Q}^p\right)^{\frac{1}{p}}$
Lemma. $III \to 0$ as $h \to 0$ if $\|u_h\|_{W^{1,p+\alpha}(Q)} \leq C$, for some $\alpha > 0$ (Meyers type estimate, Efendiev and Pankov, Num.Math., 2004).

Proof. Periodic Case

$$\langle A^* u_h - A^* P_h u, u_h - P_h u\rangle \le c\left(\left(\frac{\epsilon}{h}\right)^{\frac{s}{p(p-s)}} + \frac{\epsilon}{h}\right)\left(|Q| + \|u_h\|_{p,Q}^p + \|\nabla u_h\|_{p,Q}^p\right)^{\frac{1}{q}} \times$$
$$\|\nabla(u_h - P_h u)\|_{p,Q} + e(h)\|\nabla(u_h - P_h u)\|_{p,Q}.$$

Proof. Periodic Case

$$\langle A^* u_h - A^* P_h u, u_h - P_h u \rangle \leq c \left(\left(\frac{\epsilon}{h} \right)^{\frac{s}{p(p-s)}} + \frac{\epsilon}{h} \right) \left(|Q| + \|u_h\|_{p,Q}^p + \|\nabla u_h\|_{p,Q}^p \right)^{\frac{1}{q}} \times$$
$$\|\nabla (u_h - P_h u)\|_{p,Q} + e(h) \|\nabla (u_h - P_h u)\|_{p,Q}.$$

If A^* is a monotone operator, explicit convergence rate can be obtained.

Proof. Periodic Case

$$\langle A^* u_h - A^* P_h u, u_h - P_h u\rangle \le c\left(\left(\frac{\epsilon}{h}\right)^{\frac{s}{p(p-s)}} + \frac{\epsilon}{h}\right)\left(|Q| + \|u_h\|_{p,Q}^p + \|\nabla u_h\|_{p,Q}^p\right)^{\frac{1}{q}} \times$$
$$\|\nabla(u_h - P_h u)\|_{p,Q} + e(h)\|\nabla(u_h - P_h u)\|_{p,Q}.$$

If A^* is a monotone operator, explicit convergence rate can be obtained.

Approximation of the gradients

Theorem. If u_h is a MsFEM solution, then $u_{\epsilon,h} = Eu_h$ converges to u_ϵ in $W^{1,p}(Q)$ as $\epsilon/h \to 0$.

Multiscale finite element methods of parabolic eqns

For any $u_h \in S^h$ define $u_{\epsilon,h}(x,t) = Eu_h$ such that $E : S^h \to V_\epsilon^h$ and

$$\frac{\partial}{\partial t} u_{\epsilon,h} = div(a_\epsilon(x,t,\eta^{u_h}, \nabla u_{\epsilon,h}))\ in\ K \times [t_n, t_{n+1}],$$

$u_{\epsilon,h}(x, t = t_n) = u_h(x)$, $u_{\epsilon,h} = u_h$ on ∂K.
Find $u_h \in S^h$ such that

$$\int_Q (u_h(t = t_{n+1}) - u_h(t = t_n)) v_h dx + A_{\epsilon,h}(u_h, v_h) = \int_{t_n}^{t_{n+1}} f v_h dx dt$$

where

$$A_{\epsilon,h}(u_h, v_h) = \int_{t_n}^{t_{n+1}} [(a_\epsilon(x,t,\eta^{u_h}, \nabla u_{\epsilon,h}), \nabla v_h) dx dt +$$

$$a_{0,\epsilon}(x,t,\eta^{u_h}, \nabla u_{\epsilon,h}) v_h] dx dt$$

Explicit if $u_{\epsilon,h} = Eu_h(t = t_n)$
Implicit if $u_{\epsilon,h} = Eu_h(t = t_{n+1})$

Convergence result

Theorem. (General heterogeneities [Efendiev and Pankov, SIAM MMS 2004])

$$\lim_{h\to 0}\lim_{\epsilon\to 0}\|u_h - u\|_{L^p(0,T,W_0^{1,p}(Q))} = 0$$

(up to a subsequence).
Proof uses homogenization of random nonlinear parabolic operators (Efendiev and Pankov, Adv. PDE).

Remarks

- In the periodic case the problem in a period can be solved to approximate the solution of the local problem by periodicity. Solve

$$-div(a_\epsilon(x, \eta^{u_h}, \nabla u_{\epsilon,h})) = 0 \quad \text{in a period}$$

  $\eta^{u_h} = 1/|K| \int_K u_h dx$ and $u_{\epsilon,h} - u_h \in W^{1,p}_{per}$.

- Oversampling techniques both in space and time. The local problems are solved in S ($K \subset S$, K - target coarse block) to avoid "pollution" from artificial boundary conditions.
- If $a_\epsilon(x, t, \eta, \xi) = k_\epsilon(x) k_r(\eta) \xi$ then the local problems are solved only once.
- In general one can avoid solving the local parabolic problems in $K \times [t_n, t_{n+1}]$. Assume $a_\epsilon(x, t, \eta, \xi) = a_\epsilon(x/\epsilon^\beta, t/\epsilon^\alpha, \eta, \xi)$. 1) if $a_\epsilon(x, t, \eta, \xi) = a_\epsilon(x, \eta, \xi)$, then the following local problems can be considered: for each $v_h \in S^h$, $div(a_\epsilon(x, \eta^{v_h}, \nabla v_{\epsilon,h})) = 0$ in K. 2) if $\alpha < 2\beta$, $-div(a(x/\epsilon^\beta, t/\epsilon^\alpha, \eta^{v_h}, \nabla v_\epsilon)) = 0$ in K.

Oversampling technique

In general, given $v^h \in S^h$, where v^h is defined in K, we want to find $v_{\epsilon,h}$ that satisfies

$$div(a_\epsilon(x, \eta^{v_h}, \nabla v_{\epsilon,h})) = 0 \quad \text{in} \quad S$$

such that $v_{\epsilon,h}(z_i) = v^h(z_i)$, where z_i are the nodal points of the target coarse element K.

Special cases: $a_\epsilon(x,\eta,\xi) = a_\epsilon(x,\eta)\xi$. Given $v^h \in S^h$, we define

$$v_{\epsilon,h} = \sum_{i=1}^{3} c_i \, \phi_\epsilon^i,$$

where ϕ_ϵ^i satisfies

$$div(a(x/\epsilon, \eta^{v_h}) \, \nabla \phi_\epsilon^i) = 0 \quad \text{in} \quad S, \; \phi_\epsilon^i = \phi^i \quad \text{on} \quad \partial S.$$

The constants c_i, $i = 1,2,3$ are determined by imposing the conditions $v_{\epsilon,h}(z_j) = v^h(z_j) \qquad j = 1,2,3.$

Oversampling. Illustration

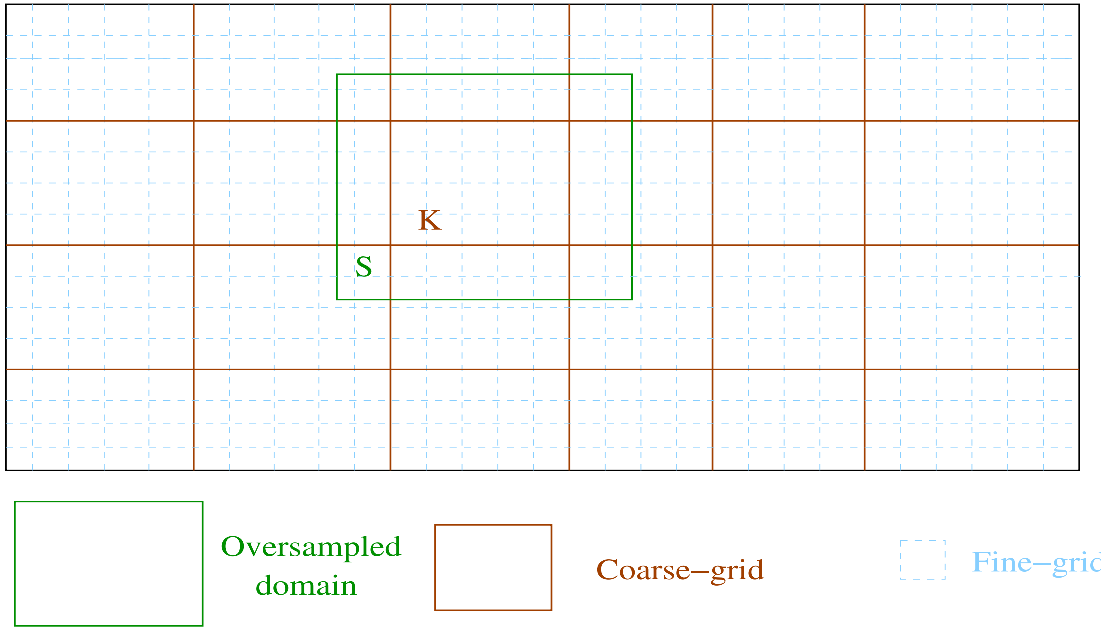

Numerical Examples

- Enhanced diffusion due to nonlinear heterogeneous convection

$$\frac{\partial}{\partial t} u_\epsilon - \frac{1}{\epsilon} v_\epsilon(x,t)) \cdot \nabla F(u_\epsilon) - d\Delta_{xx} u_\epsilon = f,$$

  where $div(v) = 0$.
- $-div(a_\epsilon(x, u_\epsilon)\nabla u_\epsilon) = f$.
- Richards' equation

Enhanced diffusion

$$D_t u_\epsilon - \frac{1}{\epsilon}\mathbf{v}(T(x/\epsilon^\beta, t/\epsilon^\alpha)\omega) \cdot D_x F(u_\epsilon) - d\Delta_{xx} u_\epsilon = f,$$

where $div\mathbf{v} = 0$. Assuming that there exists homogeneous stream function $\mathbf{H}(T(x/\epsilon^\beta, t/\epsilon^\alpha)\omega)$, $div\mathbf{H} = \mathbf{v}$.

$$D_t u_\epsilon - div(\mathbf{a}((x/\epsilon^\beta, t/\epsilon^\alpha)\omega, u_\epsilon) D_x u_\epsilon) = f,$$

where

$$\mathbf{a} = \left(\begin{array}{ll} d & H((x/\epsilon^\beta, t/\epsilon^\alpha)\omega)F'(u) \\ -H((x/\epsilon^\beta, t/\epsilon^\alpha)\omega)F'(u) & d \end{array} \right).$$

Enhanced diffusion

$$D_t u = div(\mathbf{a}^*(u) D_x u),$$

$a^*_{ij}(\eta) = d\delta_{ij} + \langle H_{ik} F'(\eta) W^{kj}_\eta \rangle$, where $w^i_\eta = W^{ij}_\eta \xi_i$, $w_\eta = \partial N_\eta$.
Numerical examples:$H = 0.5(\sin(t/\epsilon^\alpha) + \sin(t\sqrt{(}2)/\epsilon^\alpha))(\sin(2\pi y/\epsilon) + \sin(2\sqrt{(}2)\pi y/\epsilon))$, $\epsilon = 0.1$ and $d = 0.1$ (molecular diffusion) and vary α, $\alpha = 1, 2$. The flux function is chosen to be Buckley-Leverett function $F(u) = u^2/(u^2 + 0.2(1-u)^2))$, also the case - H is a Gaussian field is considered.

Numerical Results

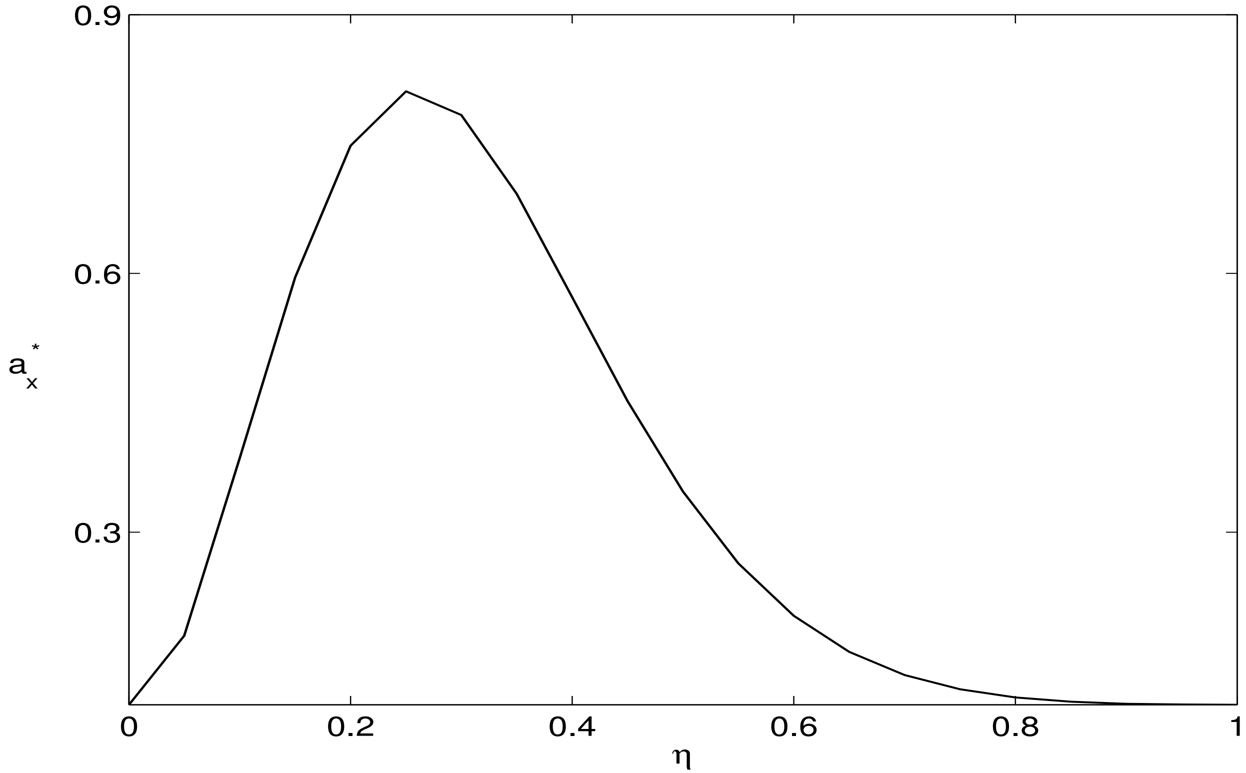

Enhanced diffusion for horizontal and vertical directions, quasi periodic layered flow, $\alpha = \beta = 1$.

Numerical Results

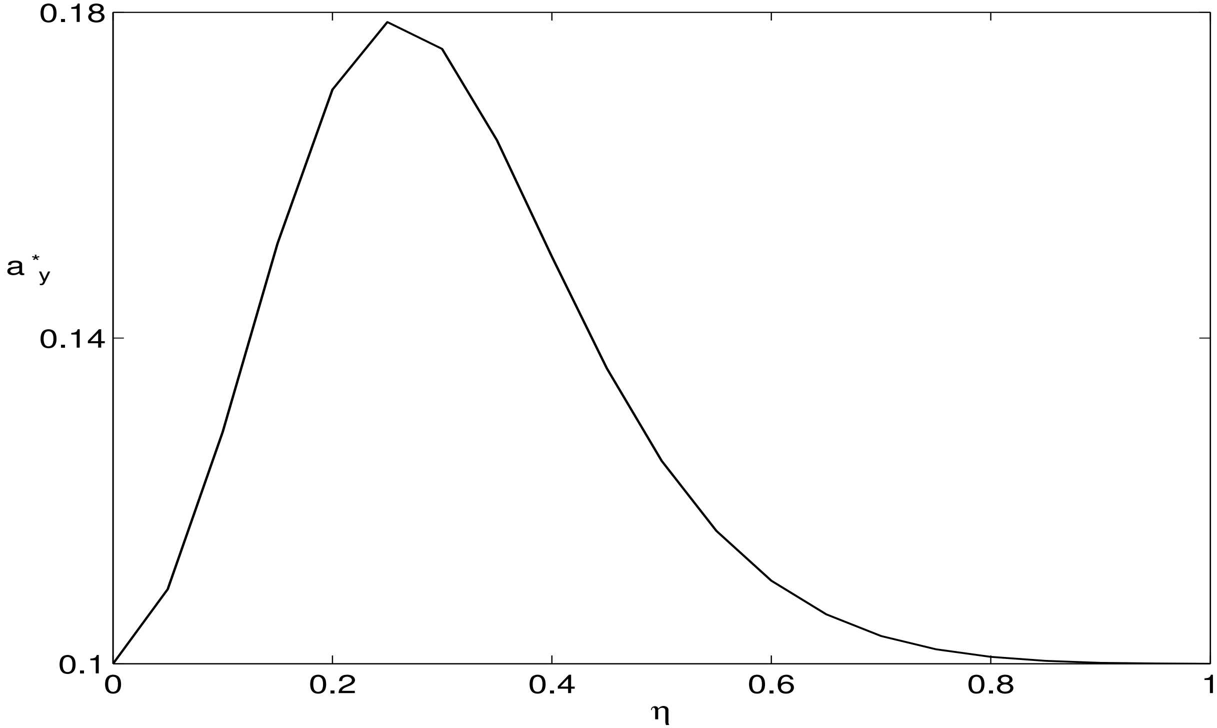

Enhanced diffusion for horizontal and vertical directions, quasi periodic layered flow

Numerical Results

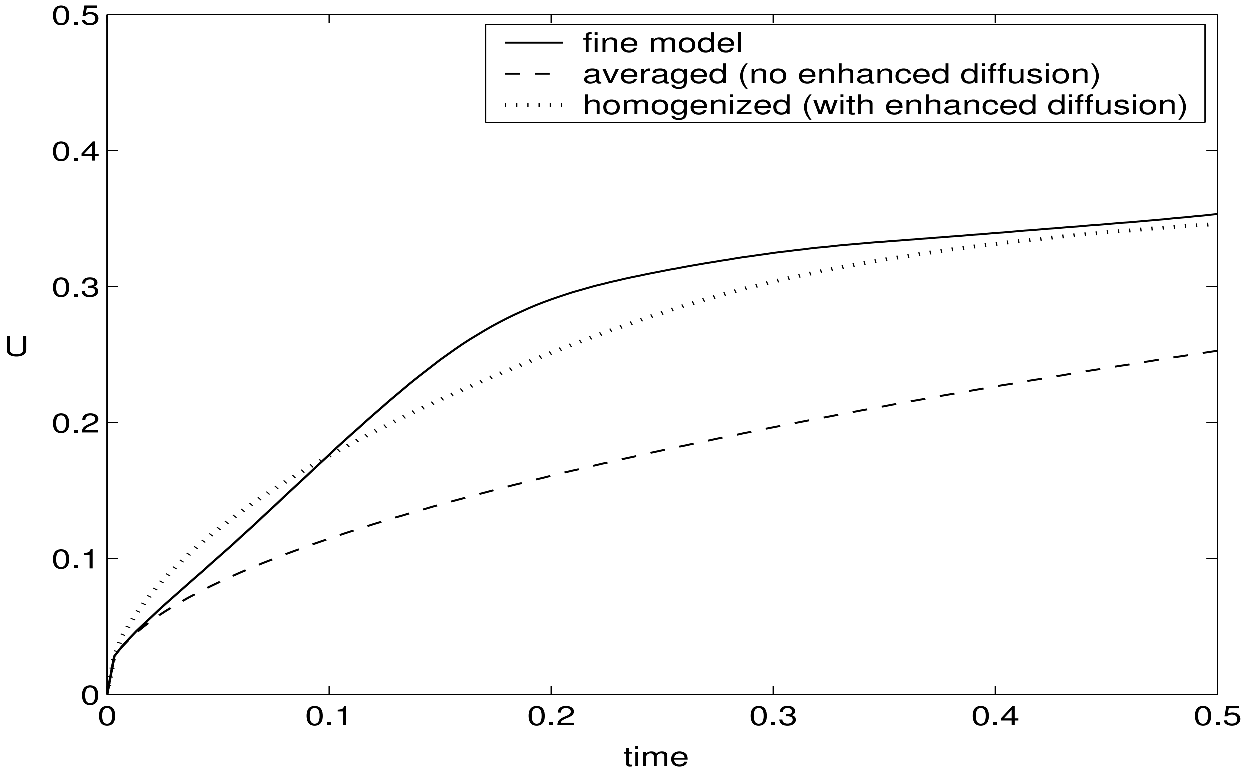

The solution comparison

Numerical Results

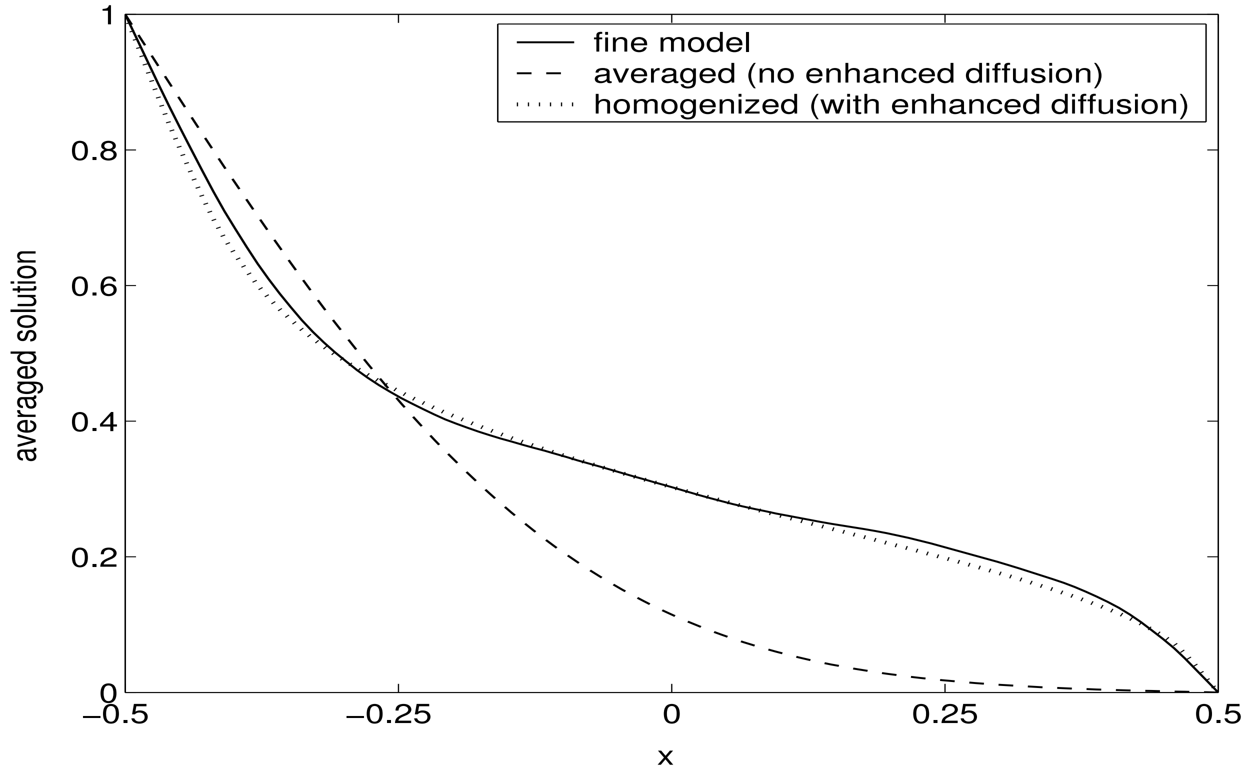

The solution comparison

Numerical Results

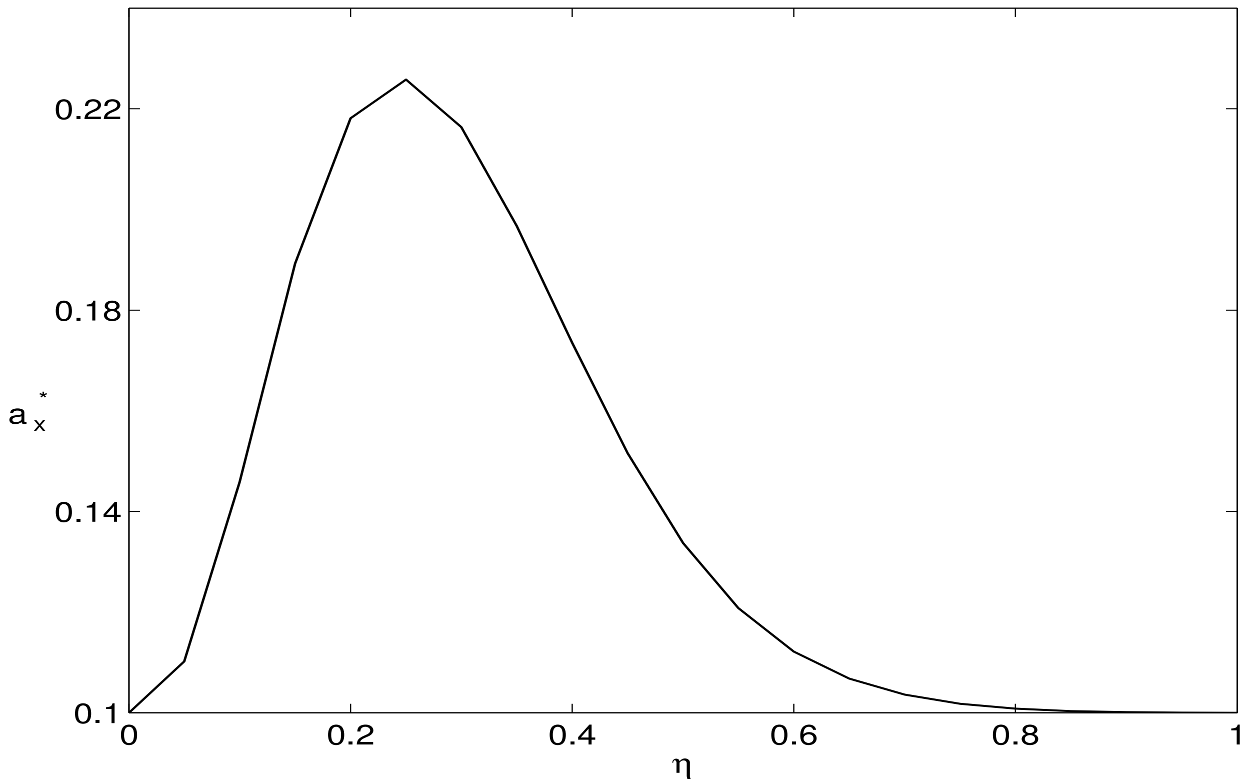

Enhanced diffusion for horizontal and vertical directions, Gaussian spatial field, $\alpha = 2$, $\beta = 1$.

Numerical Results

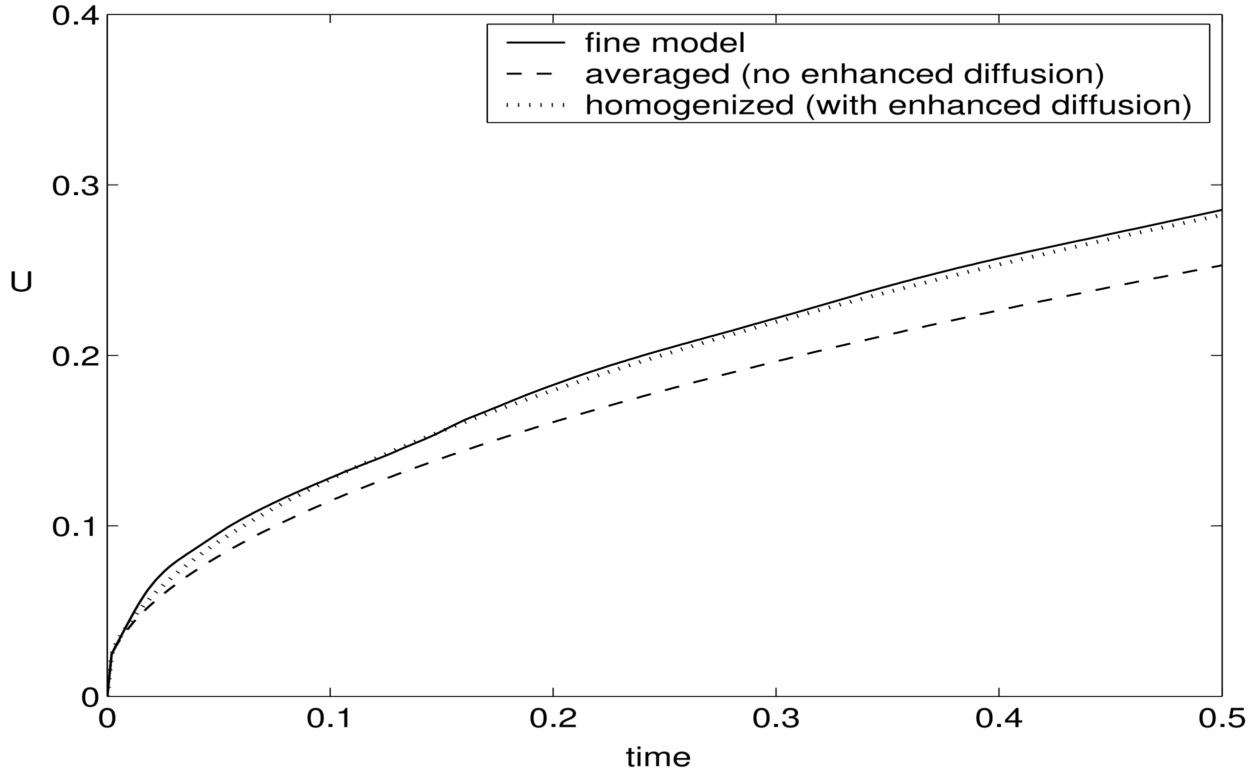

The solution comparison

Numerical Results

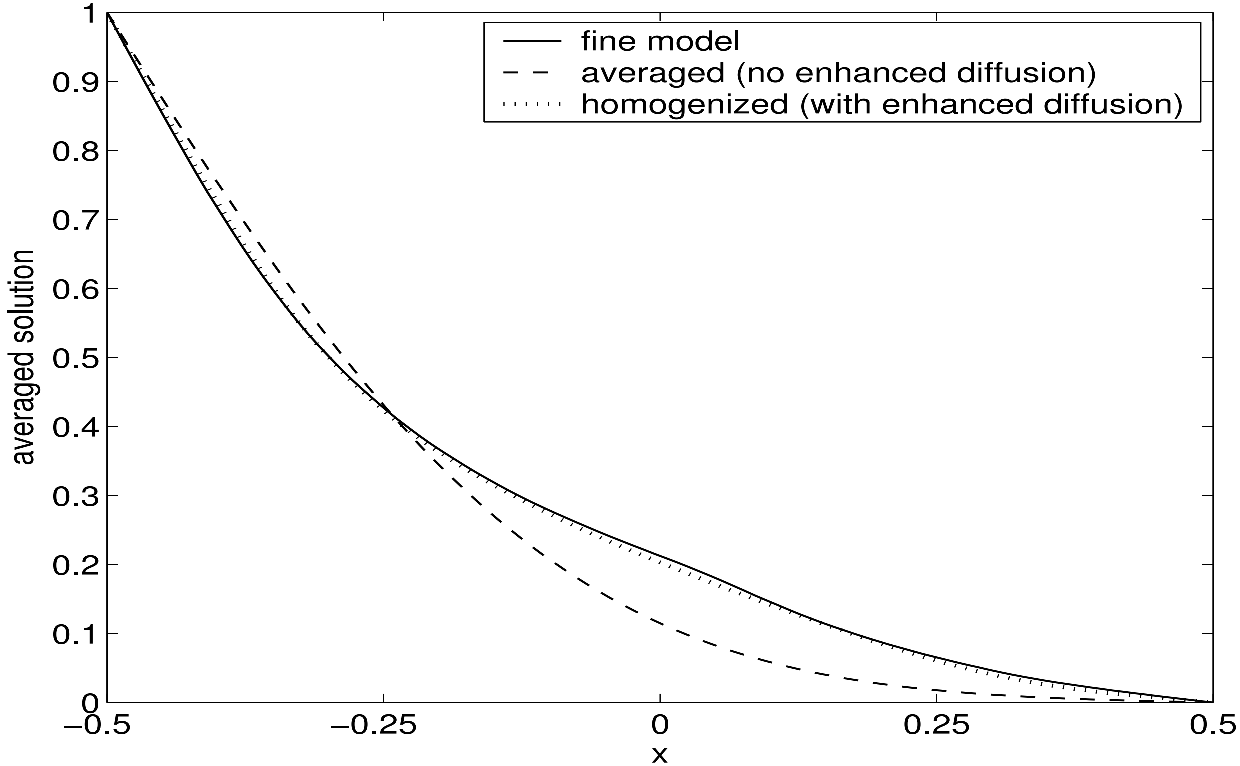

The solution comparison

Elliptic case

$$-div(a_\epsilon(x, u_\epsilon)\nabla u_\epsilon) = f.$$

$a_\epsilon(x, \eta) = k_\epsilon(x)/(1+\eta)^{\alpha_\epsilon(x)}$. $k_\epsilon(x) = \exp(\beta_\epsilon(x))$ is chosen such that $\beta_\epsilon(x)$ is a realization of a random field.

Convergence

Table 1: Relative MsFEM Errors without Oversampling

N	L^2-norm		H^1-norm		L^∞-norm	
	Error	Rate	Error	Rate	Error	Rate
32	0.029		0.115		0.03	
64	0.053	-0.85	0.156	-0.44	0.0534	-0.94
128	0.10	-0.94	0.234	-0.59	0.10	-0.94

Table 1: Relative MsFEM Errors with Oversampling

N	L_2-norm		H^1-norm		L_∞-norm	
	Error	Rate	Error	Rate	Error	Rate
32	0.002		0.038		0.005	
64	0.003	-0.43	0.021	0.87	0.003	0.72
128	0.001	1.10	0.009	1.09	0.001	1.08

Convergence

Table 1: Relative MsFEM Errors for random heterogeneities, spherical variogram, $l_x = 0.20$, $l_z = 0.02$, $\sigma = 1.0$

N	L_2-norm		H^1-norm		L_∞-norm		hor. flux	
	Error	Rate	Error	Rate	Error	Rate	Error	Rate
32	0.0006		0.0515		0.0025		0.027	
64	0.0002	1.58	0.029	0.81	0.0013	0.94	0.018	0.58
128	0.0001	1	0.016	0.85	0.0005	1.38	0.012	0.58

Richards' Equation

$$\frac{\partial}{\partial t}\theta(u) - div K(x,u)\nabla(u + x_3) = 0,$$

where $\theta(u)$ is volumetric water content (soil moisture) and u is the pressure.

Haverkamp model - $\theta(u) = \frac{\alpha(\theta_s - \theta_r)}{\alpha + |u|^\beta} + \theta_r$, $K(x,u) = K_s(x)\frac{A}{A+|u|^\gamma}$;

van Genuchten model (M. T. van Genuchten, 1980) - $\theta(u) = \frac{\alpha(\theta_s - \theta_r)}{[1+(\alpha|u|)^n]^m} + \theta_r$,

$K(x,u) = K_s(x)\frac{\{1-(\alpha|u|)^{n-1}[1+(\alpha|u|)^n]^{-m}\}^2}{[1+(\alpha|u|)^n]^{m/2}}$;

Exponential model (A. W. Warrick, 1976) - $\theta(u) = \theta_s\, e^{\beta u}$, $K(x,u) = K_s(x)\, e^{\alpha u}$.

Numerical setting

Exponential model

- BC: no flow on the lateral sides and $u_B = -10$ on the bottom. The top boundary is divided into three equal parts with prescribed u_T in the middle and no flow on other two.
- The other parameters: $\beta = 0.01$, $\theta_s = 1$, $\overline{Ks} = 1$, and $\overline{\alpha} = 0.01$.
- The heterogeneity comes from $K_s(x)$ and $\alpha(x)$.
- Isotropic and anisotropic heterogeneities are considered with $l_x = l_z = 0.1$ and $l_x = 0.20$, $l_z = 0.01$, respectively.
- Backward Euler scheme is used with $\Delta t = 2$.

Numerical results

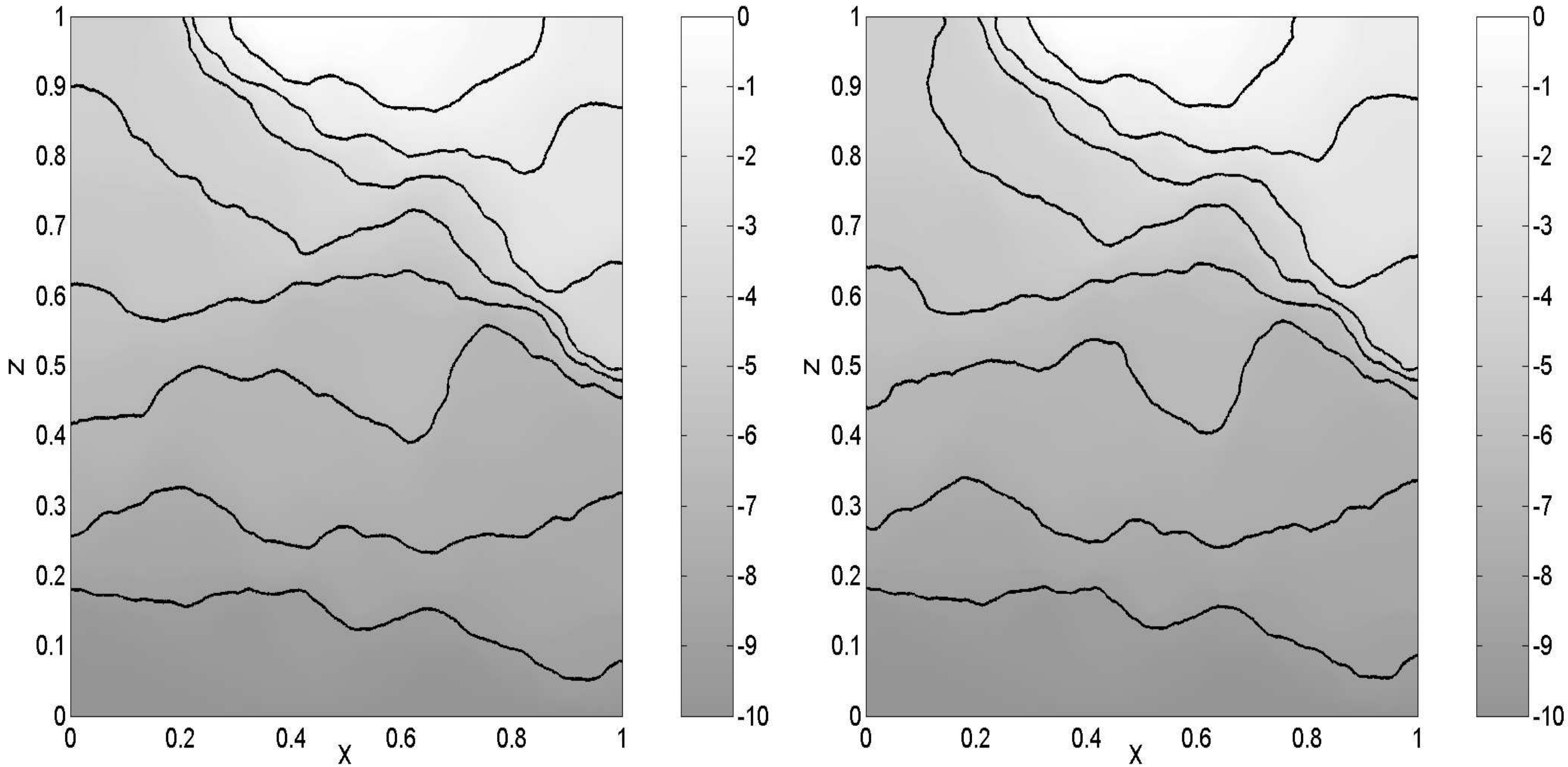

Exponential model with isotropic heterogeneity. Comparison of water pressure between the fine model (left) and the coarse model (right).

Numerical results

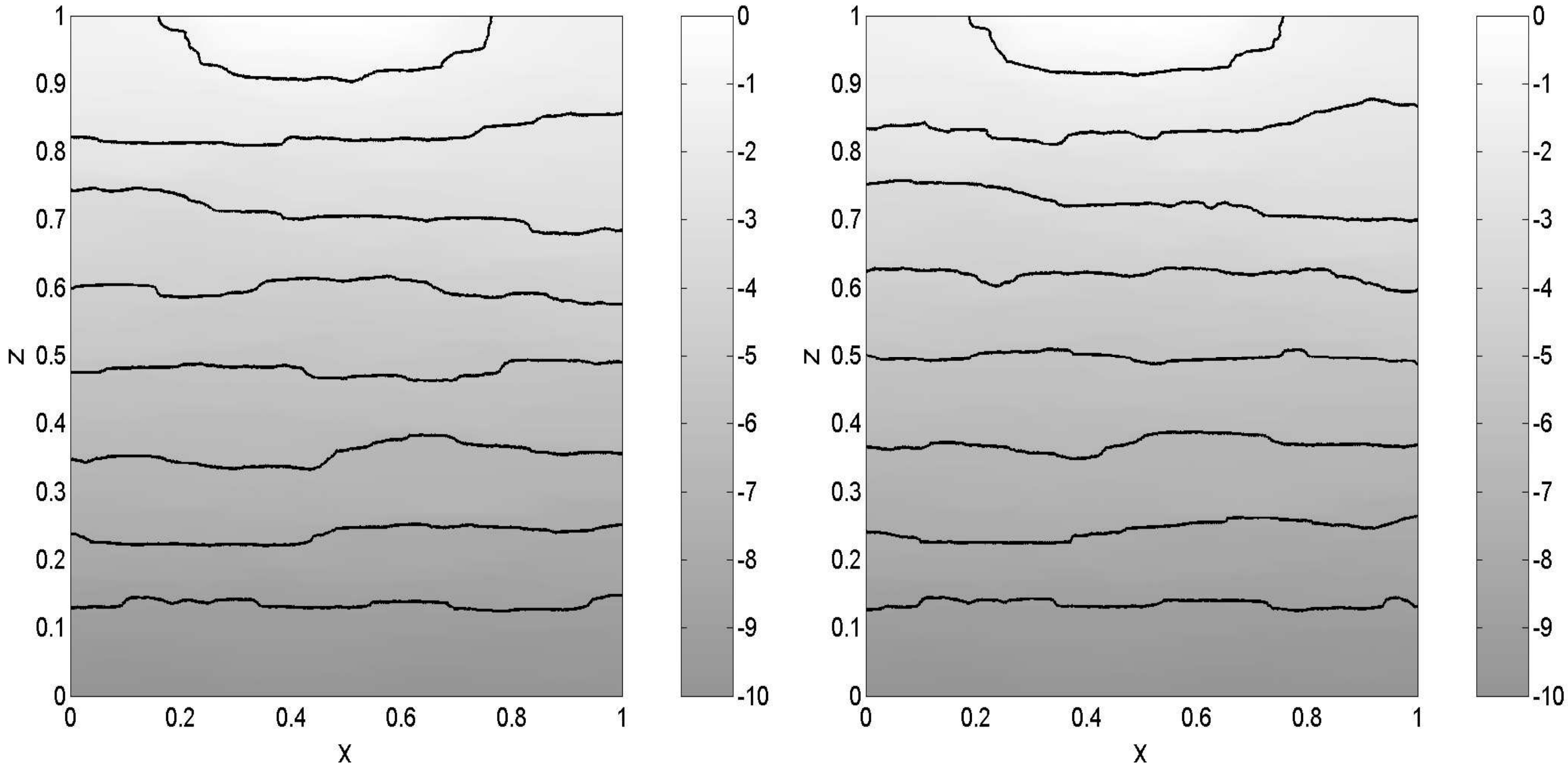

Exponential model with anisotropic heterogeneity. Comparison of water pressure between the fine model (left) and the coarse model (right).

Numerical Results

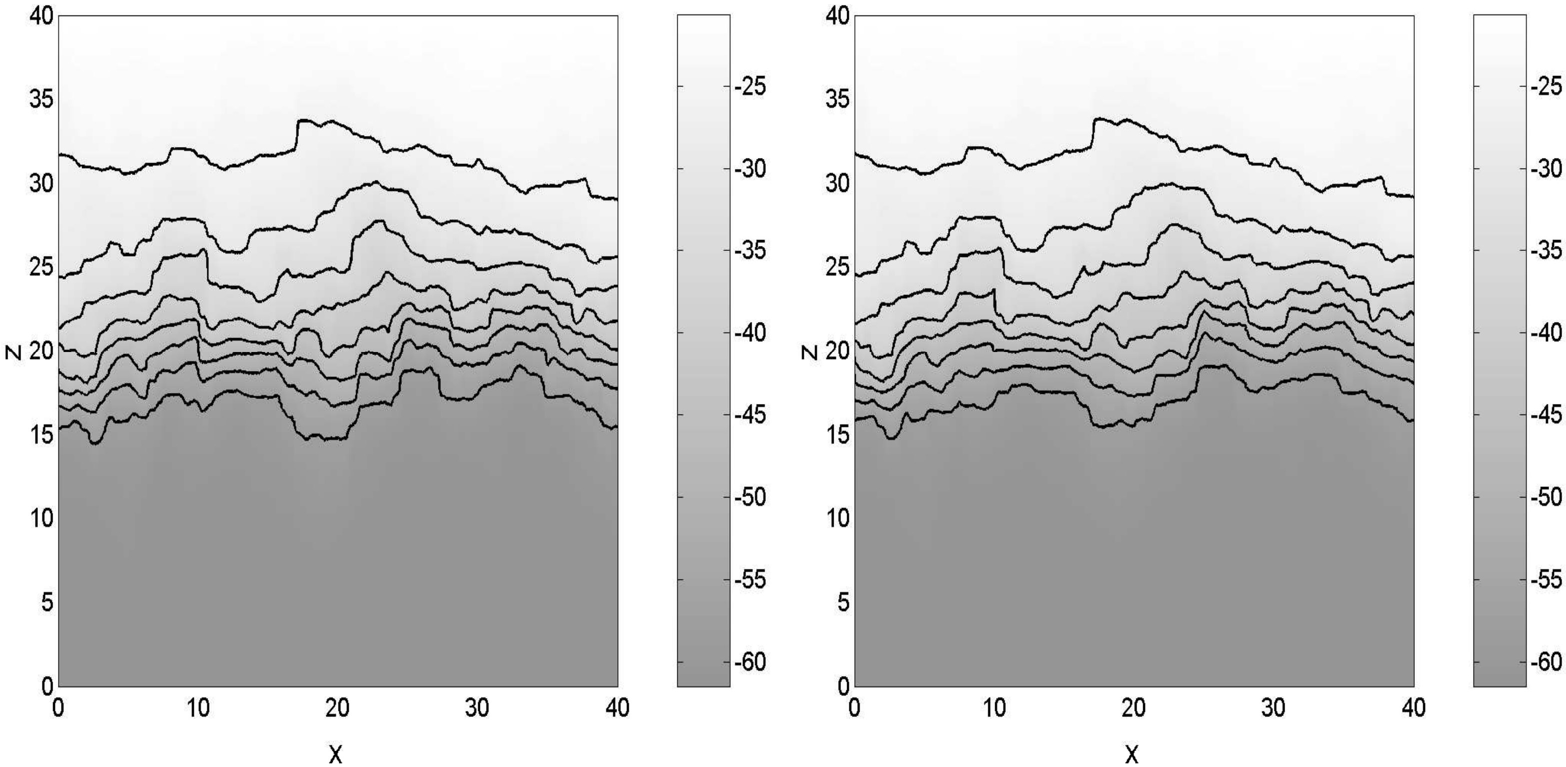

Figure 0: Haverkamp model

The use of limited global information for strongly channelized media.

Upscaling of transport equations

Homogenization of hyperbolic equations

- Hyperbolic equation with oscillatory velocity field

$$\frac{\partial S^\epsilon}{\partial t} + \mathbf{v}^\epsilon \cdot \nabla f(S^\epsilon) = 0$$

- Homogenized (macro-scale) equation is a non-local equation with memory effects.
- Consider the linear equation, $\frac{\partial S^\epsilon}{\partial t} + \mathbf{v}^\epsilon \cdot \nabla S^\epsilon = 0$, in a layered media, $\mathbf{v}^\epsilon = (v^\epsilon(y), 0)$.
- Assume the velocity $v^\epsilon(y)$ has finite number of distinct values v_i, $m_i = P\{v(y) = v_i\}$. Then the homogenized equation (Tartar, 89, Hou and Xin, 92)

$$\overline{S}_t + \overline{v}\,\overline{S}_x = \sum_k \int_0^t \beta_k \overline{S}_{xx}(x - u_k(t-\tau), \tau) d\tau.$$

Homogenization of hyperbolic equations, continued

- Homogenization of nonlinear hyperbolic equations in layered media.
- Main idea: the use of piece-wise linear discretization of the flux and piece-wise constant discretization of the initial condition (Dafermos, 72).
- $\|S_k(\cdot,t) - S(\cdot,t)\|_{L_1} \leq \|S_k(\cdot,0) - S(\cdot,0)\|_{L_1} + Ct\|f_k - f\|_{Lip}$.
- Homogenized equation (Efendiev and Popov, 2005)

$$\overline{S}_t + U\overline{S}_x = \sum_{k=1} \int_0^t \beta_k \overline{S}_{xx}(x - u_k(t-\tau), \tau) d\tau,$$

where β_k and u_k depend only on one point correlations of v, $f'(S)$ and are defined from (Riemann problem)

$$\sum_k \frac{\beta_k}{u_k - z} = \left(\sum_{i,j} \frac{m_i \Delta_j}{z - v_i f'(S_j)} \right)^{-1} - z + U, \quad \forall z \in C.$$

Perturbation technique

- Consider
$$\frac{\partial S^\epsilon}{\partial t} + \mathbf{v}^\epsilon \cdot \nabla S^\epsilon = 0$$
Expand the velocity and the saturation
$$\mathbf{v}_\epsilon = \overline{\mathbf{v}} + \mathbf{v}', \quad S^\epsilon = \overline{S} + S^{'}$$
- The fluctuations can be neglected on the scale of a coarse grid block (not on the scale of the entire domain!).
- Substituting the expansion into the equation and taking “average”
$$\frac{\partial \overline{S}}{\partial t} + \overline{\mathbf{v}} \cdot \nabla \overline{S} + \overline{\mathbf{v}' \cdot \nabla S'} = 0.$$
Here we have used $\overline{S'} = 0$, $\overline{\mathbf{v}'} = 0$.

Perturbation technique, continued

- $\overline{\mathbf{v}' \cdot \nabla S'}$ represent the macro scale effects associated with the small scales. To approximate it the equation for the fluctuating components is used

$$\frac{\partial S^{'}}{\partial t} + \overline{\mathbf{v}} \cdot \nabla S^{'} + \mathbf{v}^{'} \cdot \nabla \overline{S} + \mathbf{v}^{'} \cdot \nabla S^{'} = \overline{\mathbf{v}' \cdot \nabla S'}.$$

- Solving for $S^{'}$ along the streamline $d\mathbf{x}/dt = \overline{\mathbf{v}}$ we get

$$v_k^{'} S^{'} = -\int_0^t v_k^{'}(\mathbf{x}) v_j^{'}(\mathbf{x}(\tau)) \nabla_j \overline{S} d\tau + H.O.T$$

• Then $\overline{\mathbf{v}' S'}$ is given by

$$\overline{v_k^{'} S^{'}} = -\int_0^t \overline{v_k^{'}(x) v_j^{'}(x(\tau))} d\tau \nabla_j \overline{S}$$

Perturbation technique, continued

- The coarse scale equation is (Efendiev et al., WRR, 2000)

$$\frac{\partial \overline{S}}{\partial t} + \overline{v} \cdot \nabla \overline{S} = \nabla_i D^{ij} \nabla_j \overline{S},$$

  where $D^{ij} = \int_0^t \overline{v_j^{\prime}(\mathbf{x}) v_k^{\prime}(\mathbf{x}(\tau))} d\tau$

- The correlation of the velocity appears as a diffusivity

Perturbation technique for nonlinear saturation equation

- The approximate macro scale equation is (Efendiev et al., WRR, 2002)

$$\frac{\partial \overline{S}}{\partial t} + \overline{\mathbf{v}} \cdot \nabla f(\overline{S}) = \nabla_i f'(\overline{S})^2 D^{ij} \nabla_j \overline{S}$$

- D^{ij} depends on two point correlation of the velocity field and $\overline{S}$.
- The overall approach is obtained by combining the saturation equation with the pressure equation in the form $\nabla \cdot \lambda(\overline{S})\mathbf{k}\nabla p = 0$.
- The multiscale base functions are constructed once. The two-point correlation of the velocity can be found using the multiscale base functions. This approach is very efficient and can predict the quantity of interest on a highly coarsened grid.

The essence of the derivation

- Expand $\mathbf{v}_\epsilon = \overline{\mathbf{v}} + \mathbf{v}'$, $S^\epsilon = \overline{S} + S'$, and $f = \overline{f} + f'$. Substitute the expansions into the original equation and take average

$$\frac{\partial \overline{S}}{\partial t} + \overline{\mathbf{v}} \cdot \nabla f(\overline{S}) + \overline{\nabla \cdot f_S(\overline{S}) \mathbf{v}' S'} + \frac{1}{2} \nabla \cdot \overline{\mathbf{v}} f_{SS}(\overline{S}) \overline{S'^2} = 0.$$

- We need to model the coarse scale quantities, velocity-saturation covariance ($\overline{\mathbf{v}' S'}$), and saturation-saturation covariance ($\overline{S' S'}$). Their modeling is based on the equation for fluctuating components

$$\frac{\partial S'}{\partial t} + \overline{v}_j S' f_{SS}(\overline{S}) \nabla_j \overline{S} + \overline{v}_j f_S(\overline{S}) \nabla_j S' + v_j' f_S(\overline{S}) \nabla_j \overline{S} = \Phi(\mathbf{x}, t),$$

where $\Phi(\mathbf{x}, t)$ is a coarse scale function.

The essence of the derivation, continued

- Solving for S' along the coarse trajectories $d\mathbf{x}/dt = \overline{\mathbf{v}} f_S(\overline{S})$,

$$S^{'}(\mathbf{x},t) = \int_0^t -v_j^{'}(\mathbf{x}(\tau),\tau) f_S(\overline{S}(\tau,\mathbf{x}(\tau)))\nabla_j \overline{S}(\tau,\mathbf{x}(\tau)) \exp\left(-\int_\tau^t L(\mathbf{x}(\mu),\mu) d\mu\ \right) d\tau,$$

  where $L(\mathbf{x}(\mu),\mu)$ is a coarse scale function. From here $\overline{\mathbf{v}'(\mathbf{x},t)S'(\mathbf{x},t)}$ and $\overline{S'(\mathbf{x},t)S'(\mathbf{x},t)}$ can be evaluated.
- Further we simplify the expression showing that $d\overline{S}(\mathbf{x}(t),t)/dt = O(v'^2)$, if $f'(0) = f'(1) = 0$.

Nonlinear equation

• We propose an alternative way to calculate the diagonal components of two-point correlation of the velocity

$$v_i^{'}(\mathbf{x},t)v_i^{'}(\mathbf{x}(\tau),\tau) \approx \alpha(\sigma,l_x,l_z)\text{std}(v_i(\mathbf{x},t))\overline{v}_i(\mathbf{x}(\tau),\tau).$$

Coarse grid equation in FV framework

- Coarse grid transport equation:

$$\frac{\partial \overline{S}}{\partial t} + \overline{v} \cdot \nabla \overline{S} = \nabla \cdot \left\{ D(x,t) \nabla \overline{S}(x,t) \right\} \qquad \text{(single-phase),}$$

$$\frac{\partial \overline{S}}{\partial t} + \overline{v} \cdot \nabla f(\overline{S}) = \nabla \cdot \left\{ f_S(\overline{S})^2 \, D(x,t) \nabla \overline{S}(x,t) \right\} \qquad \text{(multi-phase)}$$

where

$$D_{ij}(x,t) = \int_{V_x i} \left[\int_0^t v_i'(x) v_j'(x(\tau)) d\tau \right] dA.$$

- First order approximation: $D_{ij}(x,t) = \int_{V_x i} v_i'(x) L_j dA$,

Numerical Results. Exponential variogram

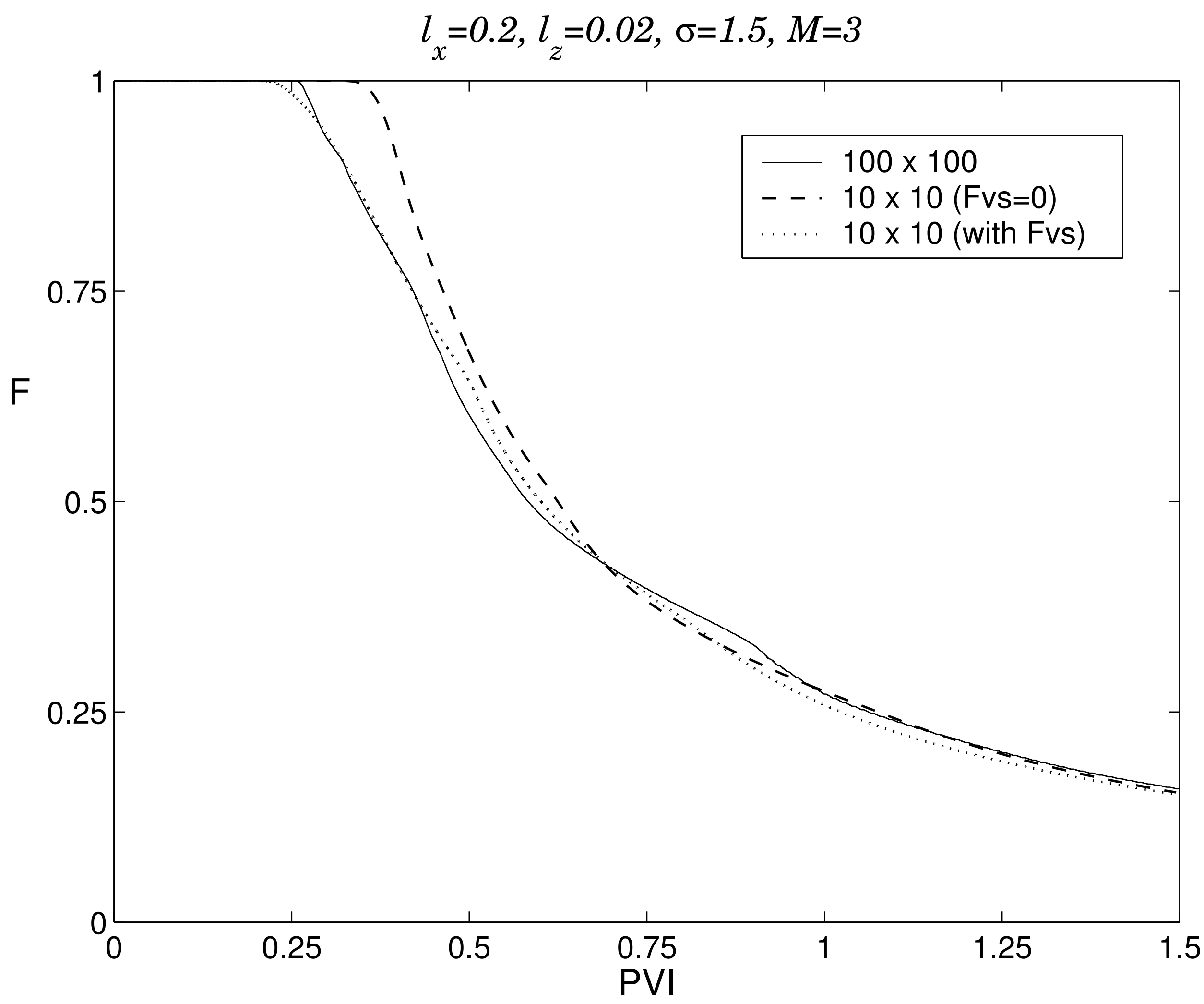

Numerical Results. Exponential variogram

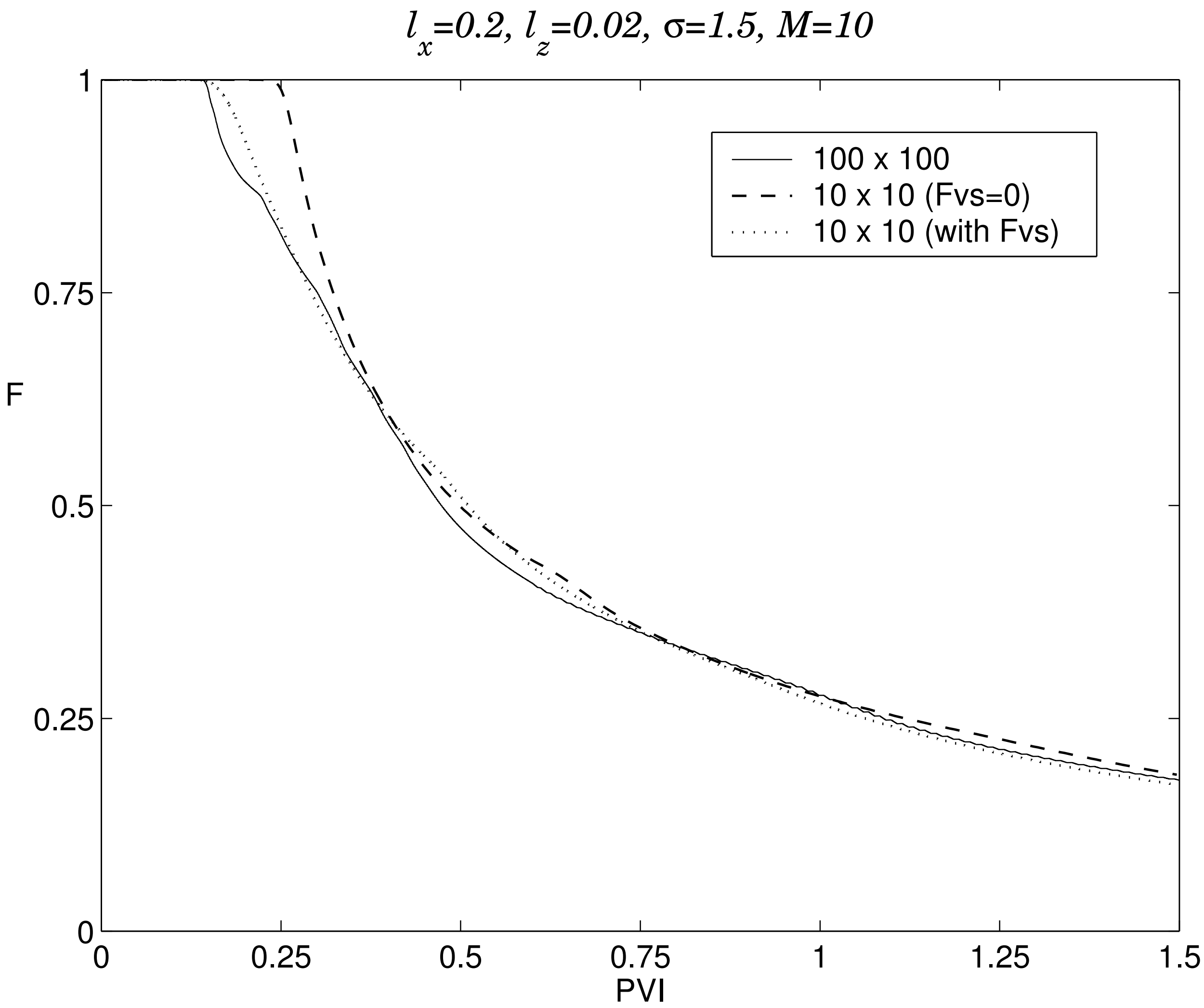

Numerical Results. Spherical variogram

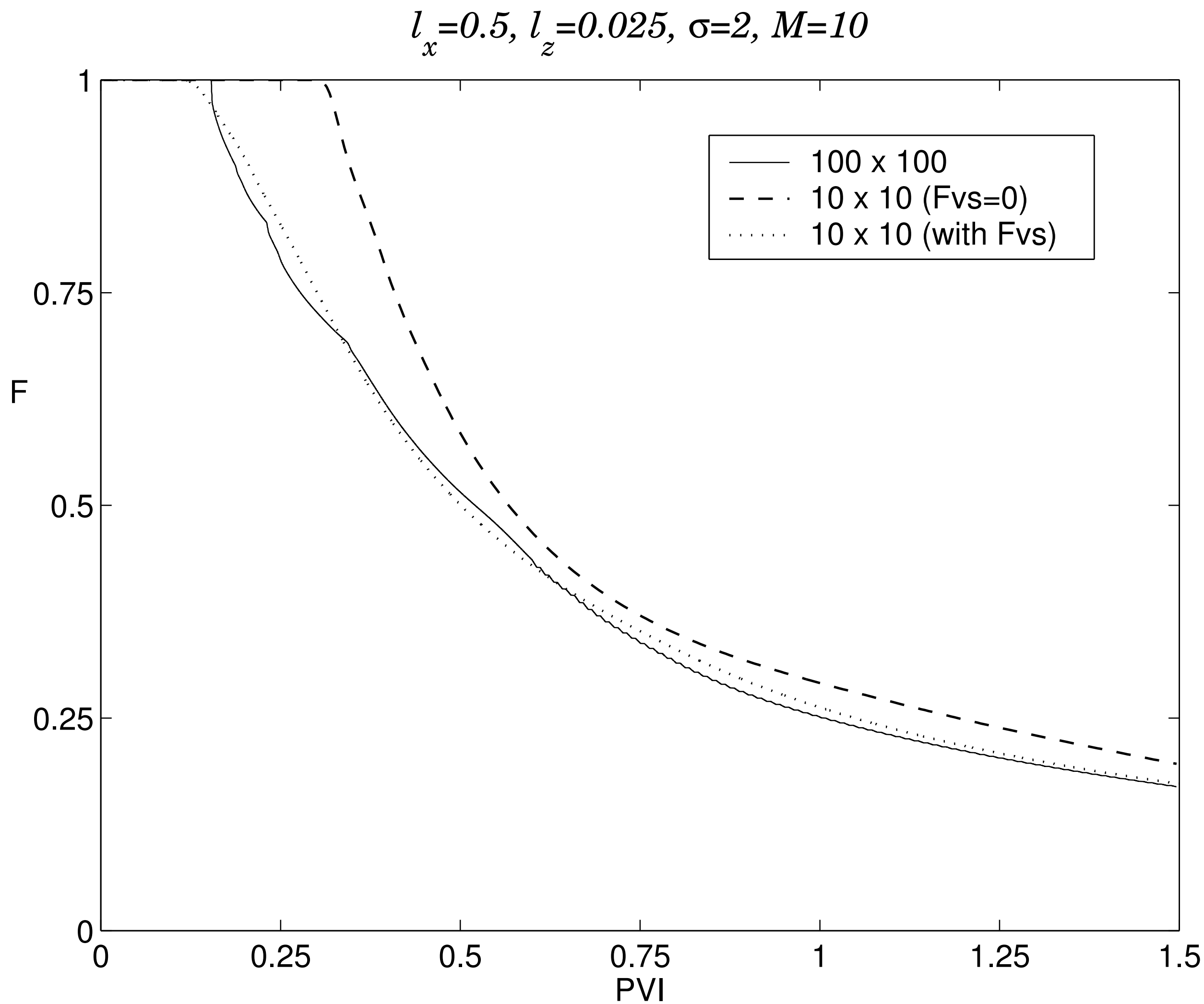

Numerical Results. Spherical variogram

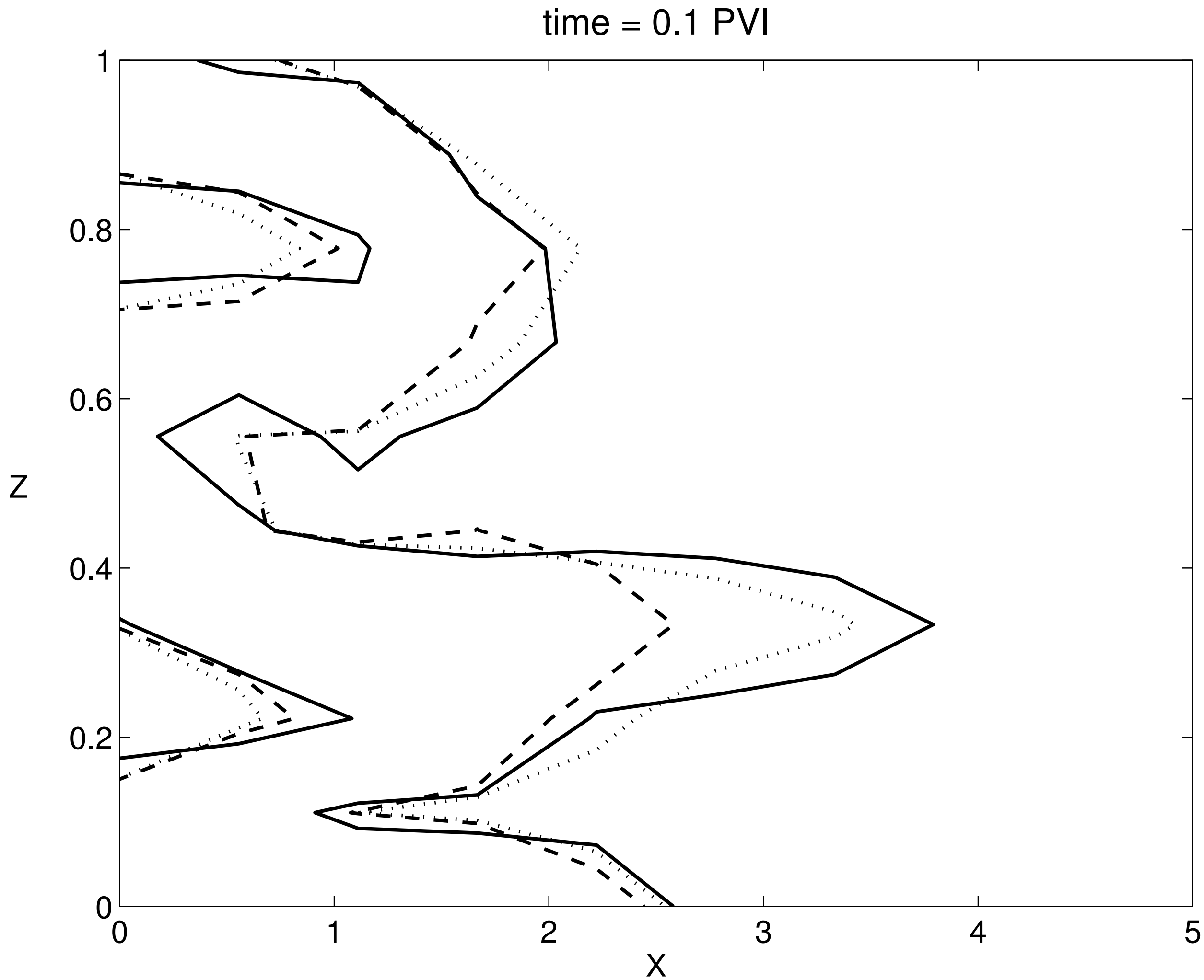

Numerical Results. Spherical variogram

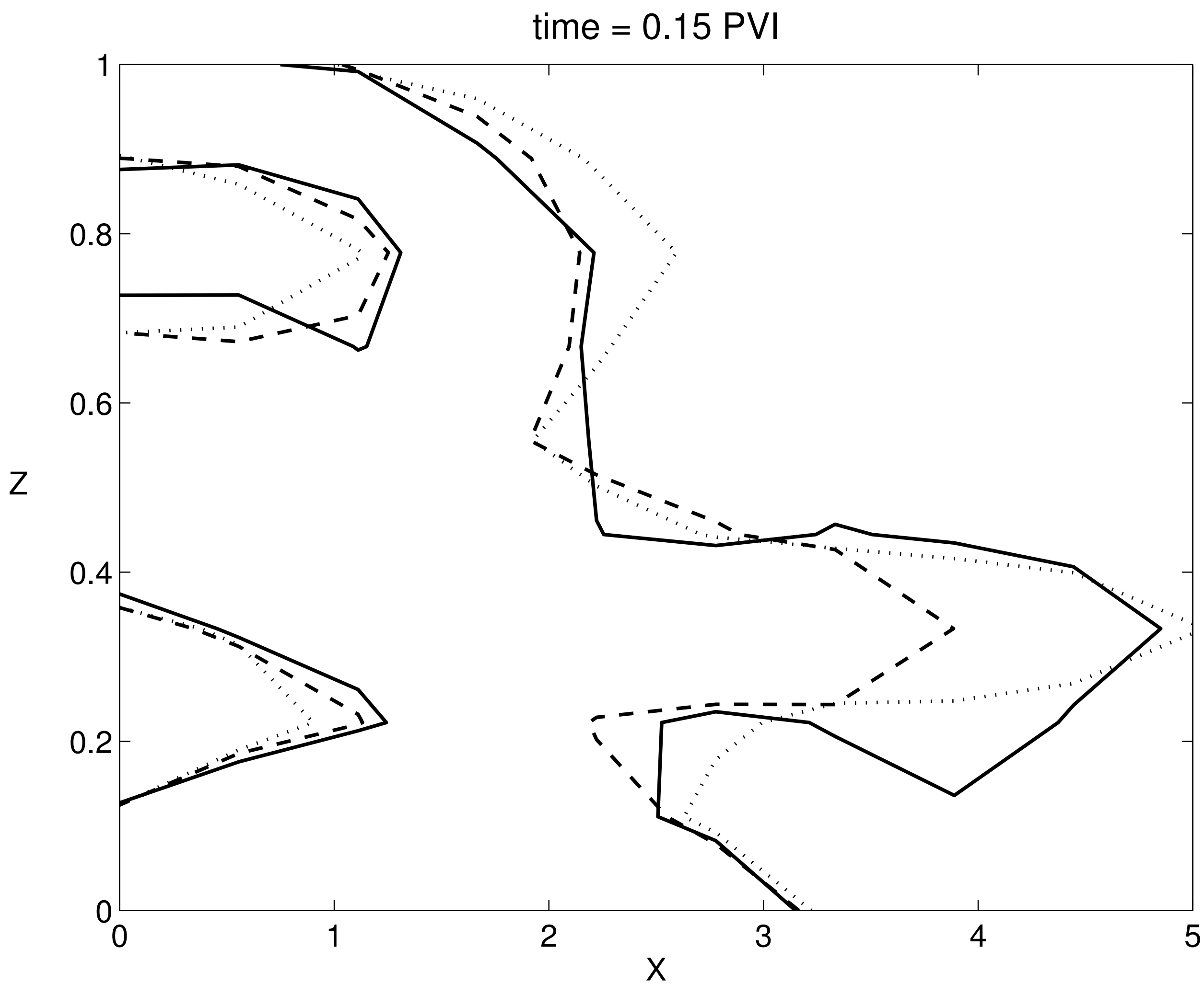

Two-component miscible flow

- $$-\nabla \cdot \left\{ \frac{k(x)}{\mu(C)} \nabla p \right\} = q$$
$$\frac{\partial C}{\partial t} + v \cdot \nabla C = (\tilde{C} - C)q.$$

- $$\mu(C) = \frac{\mu(0)}{\left(1 - C + M^{\frac{1}{4}} C\right)^4},$$

- The pressure equation is solved using the MsFVEM.

Two-component miscible flow

- Perturbation technique for the transport equation: $v = \overline{v} + v', \quad C = \overline{C} + C'$
  Result in *macrodiffusion* representing the subgrid effect on the coarse grid
- Coarse grid transport equation:

$$\frac{\partial \overline{C}(x,t)}{\partial t} + \overline{v} \cdot \nabla \overline{C}(x,t) - \nabla \cdot (D(x,t) \nabla \overline{C}(x,t)) = (\tilde{C} - \overline{C}(x,t))q,$$

  where

$$D_{ij}(x,t) = e^{-qt} \int_0^t e^{q\tau} \, \overline{v_i'(x,t) \, v_j'(x(\tau),\tau)} \, d\tau.$$

- Approximation of D_{ij}.
  Let

$$L_j(x,t) = \int_0^t e^{q\tau} \, v_j'(x(\tau),\tau) \, d\tau.$$

  Then

$$D_{ij}(x,t) \approx e^{-qt} \, \overline{v_i'(x,t) \, L_j(x,t)}.$$

- Numerical computation of $L_j(x,t)$:
  Let $t_p < t$ and y_p denotes the particle location at time t_p.
  Then $L_j(x,t) \approx L_j(y_p, t_p) + e^{qt} \, (t - t_p) \, v_j'(x,t)$.

Numerical results (two-phase flow)

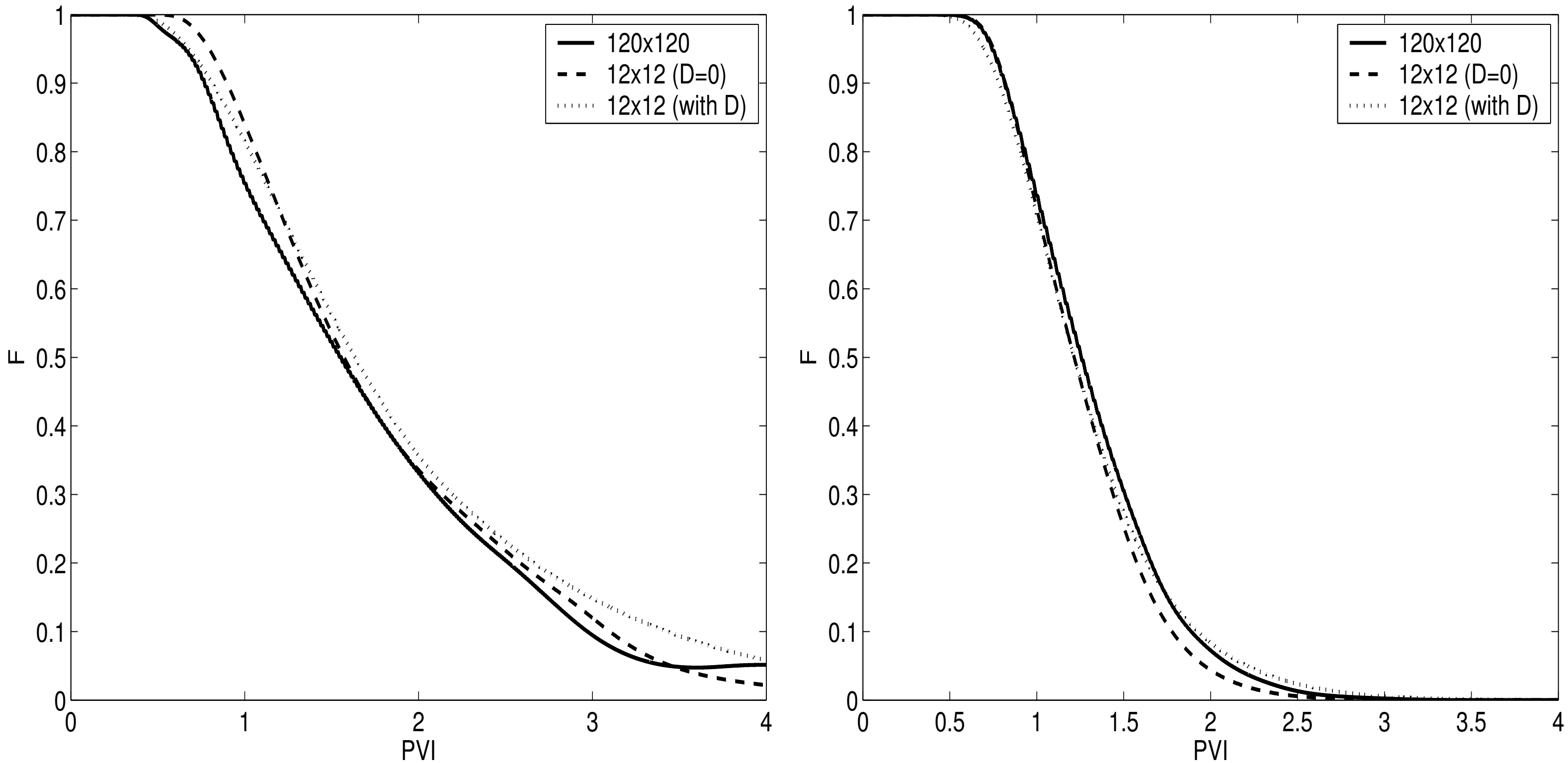

Two-component miscible flow

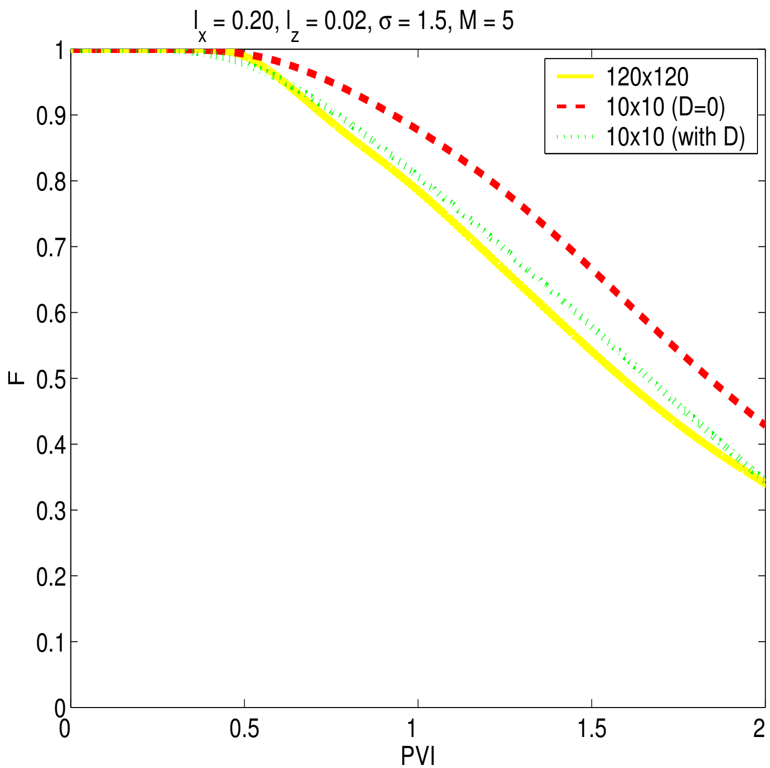

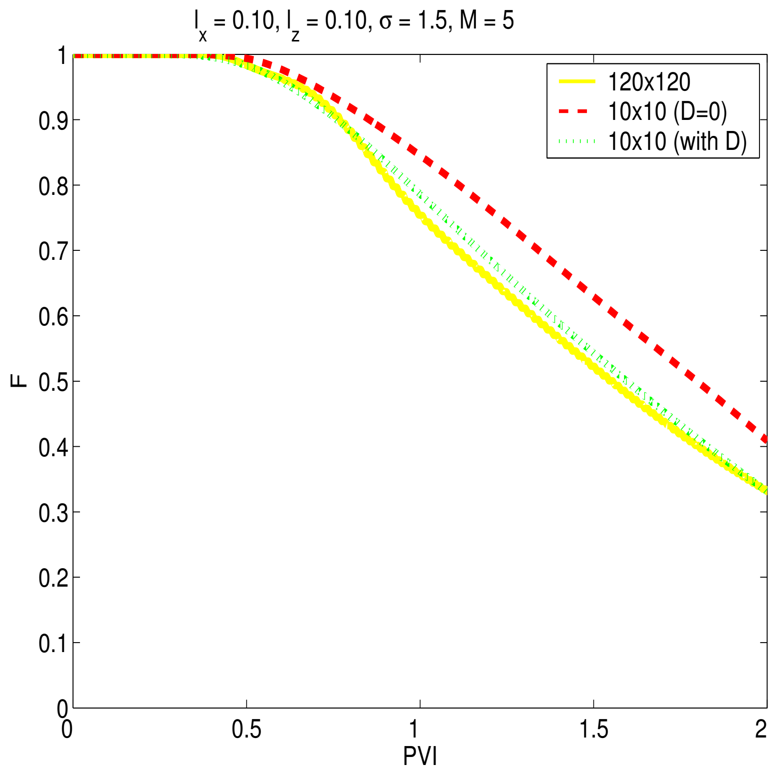

Comparison of fractional flow of displaced fluid at the production edge for anisotropic case (left) and isotropic case (right). The mobility ratio, $M = 5$.

Two-component miscible flow

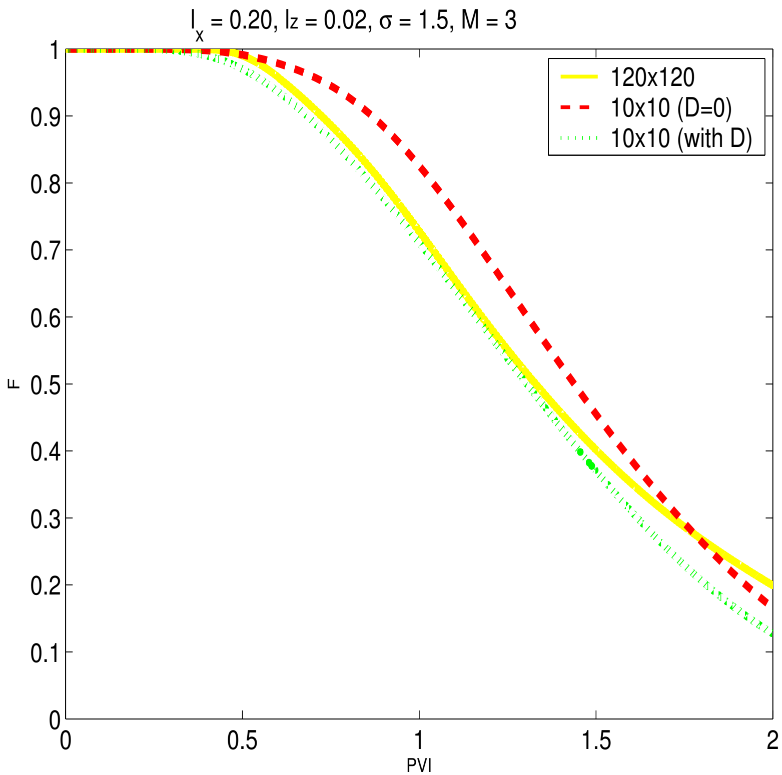

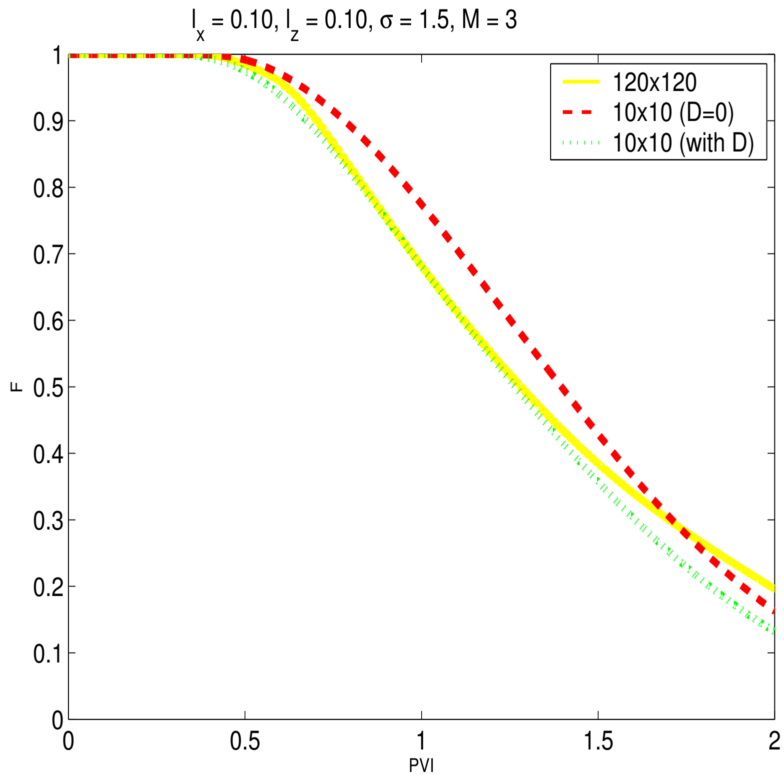

Comparison of fractional flow of displaced fluid at the production edge for anisotropic case (left) and isotropic case (right). The mobility ratio, $M = 3$.

Multiscale methods for two-phase flow in flow-based coordinate system

Two-phase flow equations in flow-based coor.

$$\frac{\partial}{\partial \psi}\left(k^2 \lambda(S) \frac{\partial P}{\partial \psi}\right) + \frac{\partial}{\partial p}\left(\lambda(S) \frac{\partial P}{\partial p}\right) = 0.$$

$$\frac{\partial S}{\partial t} + (\mathbf{v} \cdot \nabla \psi) \frac{\partial f(S)}{\partial \psi} + (\mathbf{v} \cdot \nabla p) \frac{\partial f(S)}{\partial p} = 0.$$

Consider $\lambda(S) = 1$. Homogenization of hyperbolic equations.

$$\begin{aligned} S_t^\epsilon + v_0^\epsilon f(S^\epsilon)_p &= 0 \\ S(p, \psi, t = 0) &= S_0, \end{aligned}$$

$$v_0^\epsilon(p) = v_0(p, \frac{p}{\epsilon}).$$

Homogenization of transport

Then, for each ψ, it can be shown that $S^\epsilon(p,\psi,t) \to \tilde{S}(p,\psi,t)$ in $L^1((0,1)\times(0,T))$, where $\tilde{S}$ satisfies

$$\tilde{S}_t + \tilde{v}_0 f(\tilde{S})_p = 0,$$

where $\tilde{v}_0$ is harmonic average of v_0^ϵ, i.e.,

$$\frac{1}{v_0^\epsilon} \to \frac{1}{\tilde{v}_0} \quad \text{weak} * \text{ in } L^\infty(0,1).$$

Theorem.

$$\|S^\epsilon - \tilde{S}\|_n \le G\epsilon^{1/n}.$$

Note. $\tilde{S}$ can be considered as an upscaled S^ϵ along streamlines. Can we average across streamlines?

Homogenization across streamlines

If the velocity field does not depend on p inside the cells, that is, $\tilde{v}(\psi, \frac{\psi}{\epsilon})$, then the homogenized solution, $\overline{\tilde{S}}$, (weak* limit of $\tilde{S}$, which will be denoted by $\overline{S}$), satisfies

$$\overline{S}_t + \overline{\tilde{v}}_0 \overline{S}_p = \int_0^t \int \overline{S}_{pp}(p - \lambda(t-\tau), \psi, \tau) d\mu_{\frac{\psi}{\epsilon}}(\lambda) d\tau.$$

Here, $d\nu_{\frac{\psi}{\epsilon}}$ the Young measure associated with the sequence $\tilde{v}_0(\psi, \cdot)$ and $d\mu_{\frac{\psi}{\epsilon}}$ is a Young measure that satisfies

$$\left(\int \frac{d\nu_{\frac{\psi}{\epsilon}}(\lambda)}{\frac{s}{2\pi i q} + \lambda} \right)^{-1} = \frac{s}{2\pi i q} + \overline{\tilde{v}}_0 - \int \frac{d\mu_{\frac{\psi}{\epsilon}}(\lambda)}{\frac{s}{2\pi i q} + \lambda}.$$

We have denoted by $\overline{\tilde{v}}_0$ the weak limit of the velocity. This equation has no dependence on the small scale and we consider it to be the full homogenization of the fine saturation equation.
Efendiev and Popov (CPAA, 2005) have extended this method for the Riemann problem in the case of nonlinear flux.

Numerical Averaging across Streamlines

$$\tilde{S} = \overline{S}(p,\psi,t) + S'(p,\psi,\zeta,t)$$
$$\tilde{v}_0 = \overline{\tilde{v}_0}(p,\psi,t) + \tilde{v}_0'(p,\psi,\zeta,t).$$

First, consider $f(S) = S$. Averaging fine-scale equations with respect to ψ we find an equation for the mean of the saturation

$$\overline{S}_t + \overline{\tilde{v}_0}\,\overline{S}_p + \overline{\tilde{v}_0' S_p'} = 0.$$

An equation for the fluctuations is

$$S_t' + (\tilde{v}_0 - \overline{\tilde{v}_0})\overline{S}_p + \tilde{v}_0 S_p' - \overline{\tilde{v}_0' S_p'} = 0.$$

Together, the equations for the saturation are

$$\begin{aligned} \overline{S}_t + \overline{\tilde{v}_0}\,\overline{S}_p + \overline{\tilde{v}_0' S_p'} &= 0 \\ S_t' + \tilde{v}_0'\overline{S}_p + \tilde{v}_0 S_p' - \overline{\tilde{v}_0' S_p'} &= 0. \end{aligned} \qquad (-28)$$

$$\frac{dP}{dt} = \overline{\tilde{v}_0}, \text{ with } P(p,0) = p.$$

$$S' = -\int_0^t \left(\tilde{v}_0'(P(p,\tau),\psi)\overline{S}_p(P(p,\tau),\psi,\tau) + \tilde{v}_0'(P(p,\tau),\psi)S_p'(P(p,\tau),\psi,\tau) + \overline{\tilde{v}_0' S_p'} \right) d\tau.$$

$$\frac{dP}{dt} = \overline{\tilde{v}_0}, \text{ with } P(p,0) = p.$$

$$S' = -\int_0^t \left(\tilde{v}_0'(P(p,\tau),\psi)\overline{S}_p(P(p,\tau),\psi,\tau) + \tilde{v}_0'(P(p,\tau),\psi)S_p'(P(p,\tau),\psi,\tau) + \overline{\tilde{v}_0' S_p'} \right) d\tau.$$

$$\overline{\tilde{v}_0' S'} = -\int_0^t \overline{\tilde{v}_0' \tilde{v}_0(P(p,\tau),\psi)\overline{S}_p(P(p,\tau),\psi,\tau)} d\tau.$$

It can be easily shown that $\overline{S}_p(P(p,\tau)$ depends weakly on time. Then

$$\overline{\tilde{v}_0' S'} = -\int_0^t \overline{\tilde{v}_0' \tilde{v}_0'(P(p,\tau),\psi)} d\tau \overline{S}_p.$$

Nonlinear case

$$\begin{aligned}\overline{S}_t + \overline{\tilde{v}_0} f(\overline{S})_p + \overline{\tilde{v}_0'(f_S(\overline{S})S')_p} &= 0 \\ S_t' + \tilde{v}_0' f_S(\overline{S})\overline{S}_p + \tilde{v}_0 f_S(\overline{S})S_p' - \overline{\tilde{v}_0' S_p'} &= 0.\end{aligned}$$

The macrodispersion is discretized as

$$\overline{\tilde{v}_0'(f_S(\overline{S})S')_p} = \frac{\overline{\tilde{v}_0' f_S(\overline{S})S'}^{i+1} - \overline{\tilde{v}_0' f_S(\overline{S})S'}^{i}}{\Delta p} + O(\Delta p).$$

We solve the second equation on the coarse characteristics defined by

$$\frac{dP}{dt} = \overline{\tilde{v}_0} f_S(\overline{S}), \text{ with } P(p,0) = p$$

and form the terms that appear in the macrodispersion

$$\overline{\tilde{v}_0' f_S(\overline{S})S'} = -\int_0^t \overline{\tilde{v}_0' f_S(\overline{S})\tilde{v}_0'(P(p,\tau),\psi) f_S(\overline{S}(P(p,\tau),\psi,\tau))\overline{S}_p(P(p,\tau),\psi,\tau)}d\tau.$$

Nonlinear case

We have dropped terms that are second-order in fluctuating quantities. It can be shown that $f_S(\overline{S}(P(p,\tau),\psi,\tau))\overline{S}_p(P(p,\tau),\psi,\tau)$ does not vary significantly along the streamlines and it can be taken out of the integration in time:

$$\overline{\tilde{v}_0' f_S(\overline{S}) S'} = -\int_0^t \overline{\tilde{v}_0' \tilde{v}_0'(P(p,\tau),\psi)} d\tau f_S(\overline{S})^2 \overline{S}_p.$$

This expression is similar to the one obtained in the linear case, however the macrodispersion depends on the past saturation through the equation for the coarse characteristics.

Numerical results

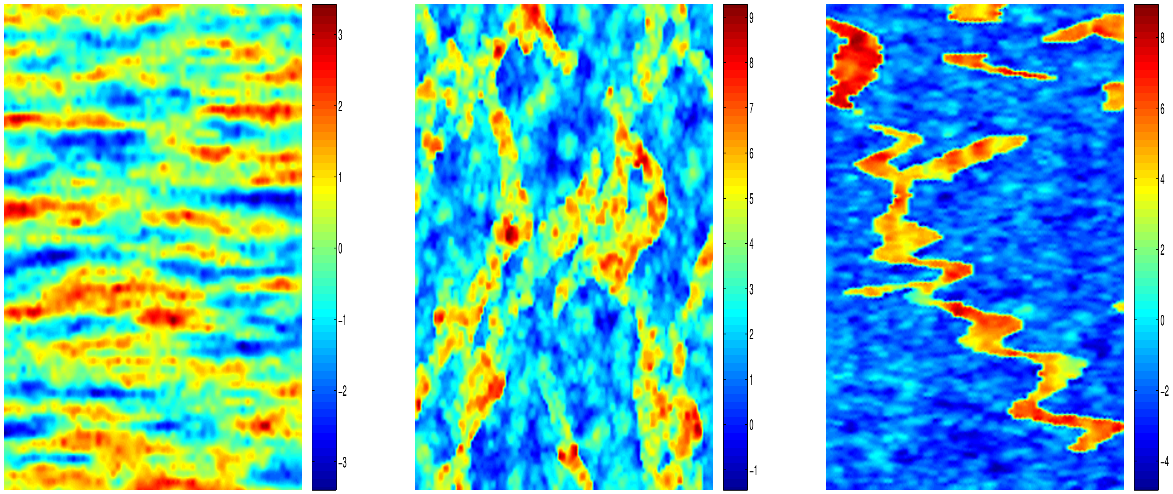

Permeability fields used in the simulations. Left - permeability field with exponential variogram, middle - synthetic channelized permeability field, right - layer 36 of SPE comparative project

Numerical results

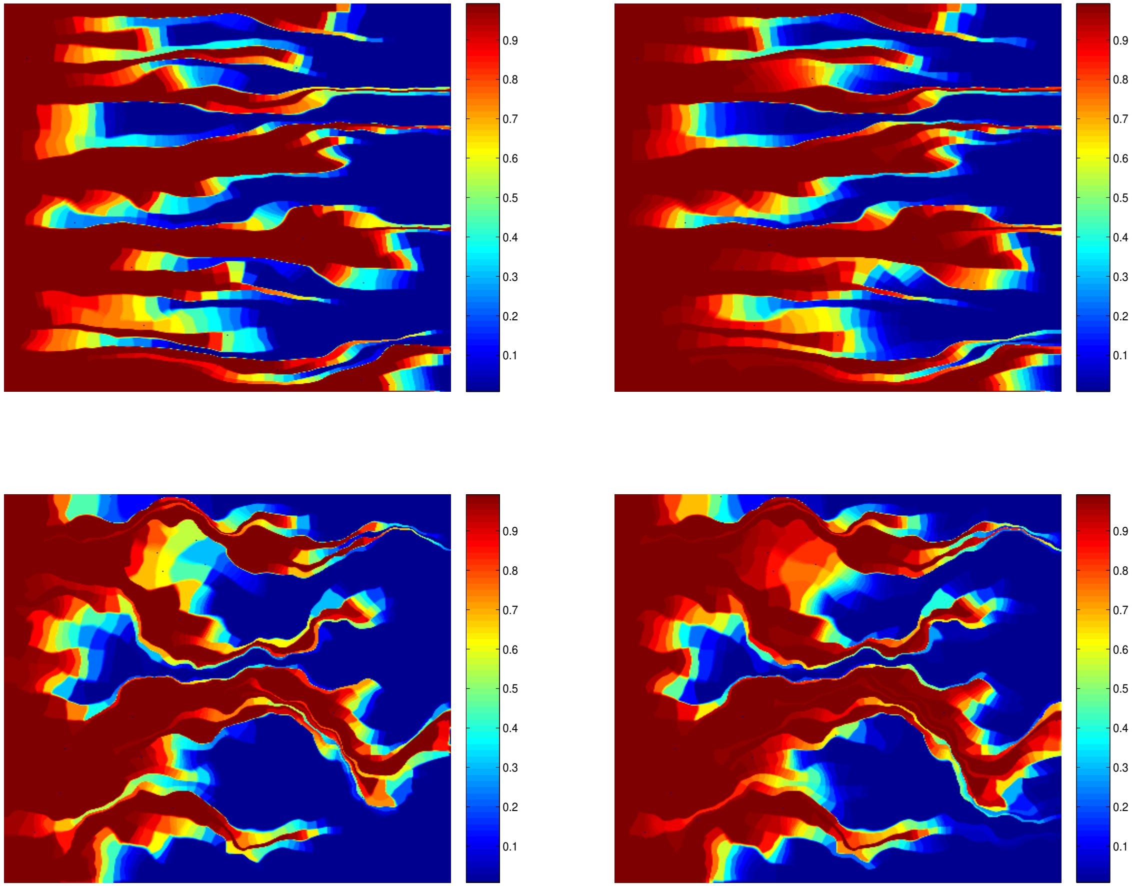

Saturation snapshots for variogram based permeability field (top) and synthetic channelized permeability field (bottom). Linear flux is used. Left figures represent the upscaled saturation plots and the right figures represent the fine-scale saturation plots.

Numerical results

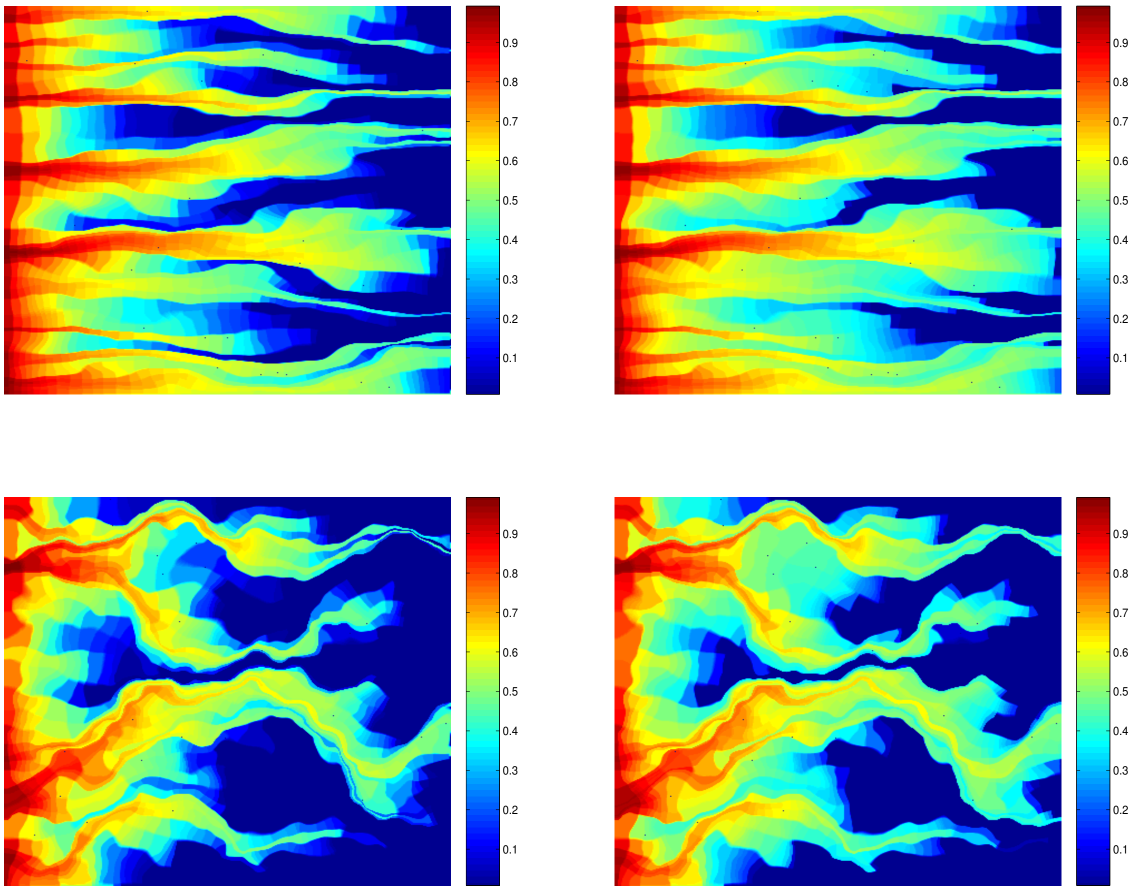

Saturation snapshots for variogram based permeability field (top) and synthetic channelized permeability field (bottom). Nonlinear flux is used. Left figures represent the upscaled saturation plots and the right figures represent the fine-scale saturation plots.

Numerical results

Upscaling error for permeability generated using two-point geostatistics

LINEAR FLUX	25x25	50x50	100x100	200x200
L_1 error of $\tilde{S}$	0.0021	$6.57e-4$	$2.15e-4$	$8.75e-5$
L_1 error of $\overline{S}$ with macrodispersion	0.115	0.0696	0.0364	0.0135
L_1 error of $\overline{S}$ fine without macrodispersion	0.1843	0.0997	0.0505	0.0191

NONLINEAR FLUX	25x25	50x50	100x100	200x200
L_1 error of $\tilde{S}$	0.0023	$8.05e-4$	$2.89e-4$	$1.29e-4$
L_1 error of $\overline{S}$ with macrodispersion	0.116	0.0665	0.0433	0.0177
L_1 error of $\overline{S}$ fine without macrodispersion	0.151	0.0805	0.0432	0.0186

Numerical results

Upscaling error for SPE 10, layer 36

LINEAR FLUX	25x25	50x50	100x100	200x200
L_1 error of $\tilde{S}$	0.0128	0.0093	0.0072	0.0042
L_1 error of $\overline{S}$ with macrodispersion	0.0554	0.0435	0.0307	0.0176
L_1 error of $\overline{S}$ fine without macrodispersion	0.123	0.0798	0.0484	0.0258

NONLINEAR FLUX	25x25	50x50	100x100	200x200
L_1 error of $\tilde{S}$	0.0089	0.0064	0.0054	0.0033
L_1 error of $\overline{S}$ with macrodispersion	0.0743	0.0538	0.0348	0.0189
L_1 error of $\overline{S}$ fine without macrodispersion	0.0924	0.0602	0.0395	0.0202

Numerical results

Total error for SPE10 layer 36

LINEAR FLUX	25x25	50x50	100x100	200x200
L_1 upscaling error of $\tilde{S}$	0.0128	0.0093	0.0072	0.0042
L_1 error of $\tilde{S}$ computed on coarse grid	0.023	0.0095	0.0069	0.0052
L_1 upscaling error of $\overline{S}$	0.0554	0.0435	0.0307	0.0176
L_1 error of $\overline{S}$ computed on coarse grid	0.0683	0.052	0.0361	0.0205

NONLINEAR FLUX	25x25	50x50	100x100	200x200
L_1 upscaling error of $\tilde{S}$	0.0089	0.0064	0.0054	0.0033
L_1 error of $\tilde{S}$ computed on coarse grid	0.0338	0.0148	0.0074	0.0037
L_1 upscaling error of $\overline{S}$	0.0743	0.0538	0.0348	0.0189
L_1 error of $\overline{S}$ computed on coarse grid	0.115	0.0720	0.0406	0.0204

Numerical results

Computational cost

	fine $x.y$	fine p, ψ	$\tilde{S}$	$\overline{S}$
layered, linear flux	5648	257	9	1
layered, nonlinear flux	14543	945	28	4
percolation, linear flux	8812	552	12	1
percolation, nonlinear flux	23466	579	12	1
SPE10 36, linear flux	40586	1835	34	2
SPE10 36, nonlinear flux	118364	7644	25	2

Numerical results

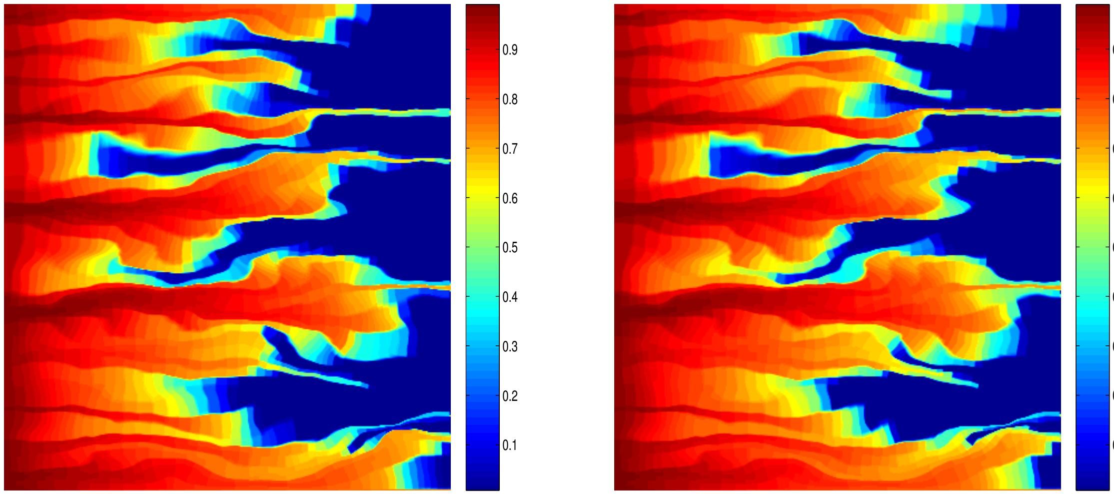

Left: Saturation plot obtained using coarse-scale model. Right: The fine-scale saturation plot. Both plots are on coarse grid. Variogram based permeability field is used. $\mu_o/\mu_w = 5$.

Numerical results

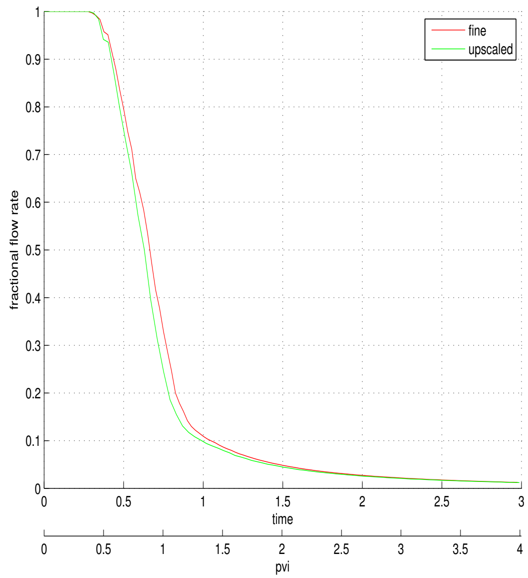

Comparison of fractional flow for coarse- and fine-scale models. Variogram based permeability field is used. $\mu_o/\mu_w = 5$.

Numerical results

Convergence of the upscaling method for two-phase flow for variogram based permeability

with $\tilde{S}$	50x50	100x100	200x200
L_2 pressure error at $t = \frac{3T_{final}}{4}$	0.0014	0.007	0.004
L_2 velocity error at $t = \frac{3T_{final}}{4}$	0.0235	0.0137	0.0072
L_1 saturation error $t = T_{final}$	0.0105	0.0052	0.0027

with $\overline{S}$	50x50	100x100	200x200
L_2 pressure error at $t = \frac{3T_{final}}{4}$	0.0046	0.0021	0.0008
L_2 velocity error at $t = \frac{3T_{final}}{4}$	0.0530	0.0335	0.0246
L_1 saturation error $t = T_{final}$	0.0546	0.0294	0.0134

Multiscale methods for transport equation

Adaptive Multiscale Algorithm

For each $T \in \mathcal{T}^n_{\mathrm{tr}}$, do

- For $K_i \subset T^E$, compute

$$S_i^{n+1/2} = S_i^n + \frac{\triangle t}{\int_{K_i} \phi\, dx} \left[\int_{K_i} q_w(S^{n+1/2}) - \sum_{j \neq i} V^*_{ij} \right],$$

where $V^*_{ij} = \begin{cases} V_{ij}(S^n) & \text{if } \gamma_{ij} \subset \partial T^E \text{ and } v_{ij} < 0. \\ V_{ij}(S^{n+1/2}) & \text{otherwise.} \end{cases}$

- Set $S^{n+1}|_T = S^{n+1/2}|_T$.

For each $T \notin \mathcal{T}^n_{\mathrm{tr}}$, do

- Set $S^{n+1}|_T = S^n|_T$.
- While $\sum_j \triangle_j t \leq \triangle t$, compute

$$\bar{S}_T^{n+1} = \bar{S}_T^{n+1} + \frac{\triangle_j t}{\int_T \phi\, dx} \left[\int_T q_w(S^{n+1})\, dx - \sum_{\gamma_{ij} \subset \partial T} V_{ij}(S^{n+1}) \right],$$

and set $S^{n+1}|_T = I_T(\bar{S}_T^{n+1})$.

Multiscale interpolation

The basis functions $\Phi_i^k = \chi_i(x, \tau_k)$ represent snapshots of the solution of the following equation:

$$\phi \frac{\partial \chi_i}{\partial t} + \nabla \cdot (f_w(\chi_i) v) = q_w \quad \text{in } T_i.$$

The multiscale interpolation is chosen as

$$I_{T_i}(\bar{S}_i^n) = \omega \Phi_i^k + (1-\omega)\Phi_i^{k+1},$$

where $\omega \in [0,1]$ is chosen such that the interpolation preserves mass, i.e., such that

$$\int_{T_i} I_{T_i}(\bar{S}_i^n)\phi \, dx = \bar{S}_i^n \int_{T_i} \phi \, dx.$$

The relation to pseudo type of approaches

$$\frac{\partial \overline{S}}{\partial t} + \nabla \cdot F^*(x, \overline{S}) = 0,$$

where $F^*(x, \overline{S}) = \overline{v} f_w^*$, $\overline{v}$ is the upscaled velocity field.
The pseudofunctions are computed from local fine scale problems such that they provide the same average response as the fine grid model for the prescribed boundary conditions. Assuming that the pseudofunctions have been computed, the corresponding coarse scale equation takes the following form:

$$\overline{S}^{n+1} = \overline{S}^n + \frac{\Delta t}{\int_T \phi dx} \left[\int_T q_w(S^n) dx - \sum_{\Gamma_{ij} \subset \partial T} V_{ij}^*(S^n) \right],$$

where $V_{ij}^*(S) = \max\{\overline{v}_{ij} f_{w,i}^*(\overline{S}_i), -\overline{v}_{ij} f_{w,j}^*(\overline{S}_j)\}$.
Advantages: (1) adaptivity; (2) ability to downscale; (3) avoid no flow boundaries.

Analysis

$$
\begin{aligned}
G_f(S) &= -\frac{1}{\int_T \phi\, dx} \int_{\partial T} f_w(S)(v \cdot n)\, ds, \\
G_c(\overline{S}) &= -\frac{1}{\int_T \phi\, dx} \int_{\partial T} f_w(I(\overline{S}))(v \cdot n)\, ds.
\end{aligned}
$$

Let

$$
\delta^n = \overline{S}^n - \overline{S}^n_h.
$$

It can be shown that

$$
|\delta^n| \leq o(\Delta t) + \Delta t \sum_{k=0}^{n-1} (1 + C\Delta t)^k |G_f(S^{n-k}) - G_c(\overline{S}^{n-k})| \leq o(\Delta t) + \left[\frac{e^{C(n\Delta t)} - 1}{C} \right] \left[\max_{1 \leq i \leq n} |G_f(S^i) - G_c(\overline{S}^i)| \right].
$$

If we assume scale separation, then $G_f(S) \approx G_c(\overline{S})$. Analysis is also performed for the cases without scale separation.

Numerical results

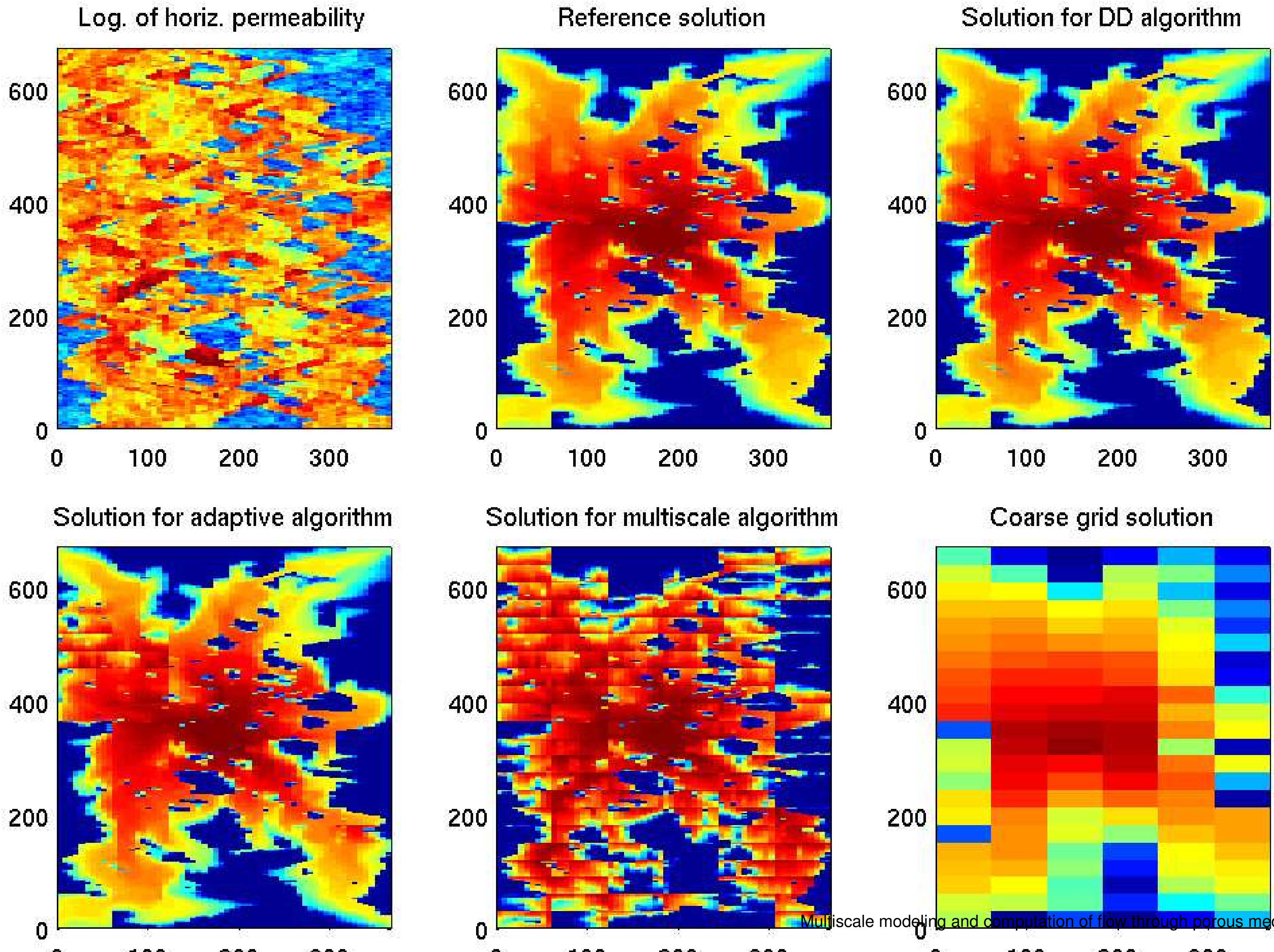

Numerical results

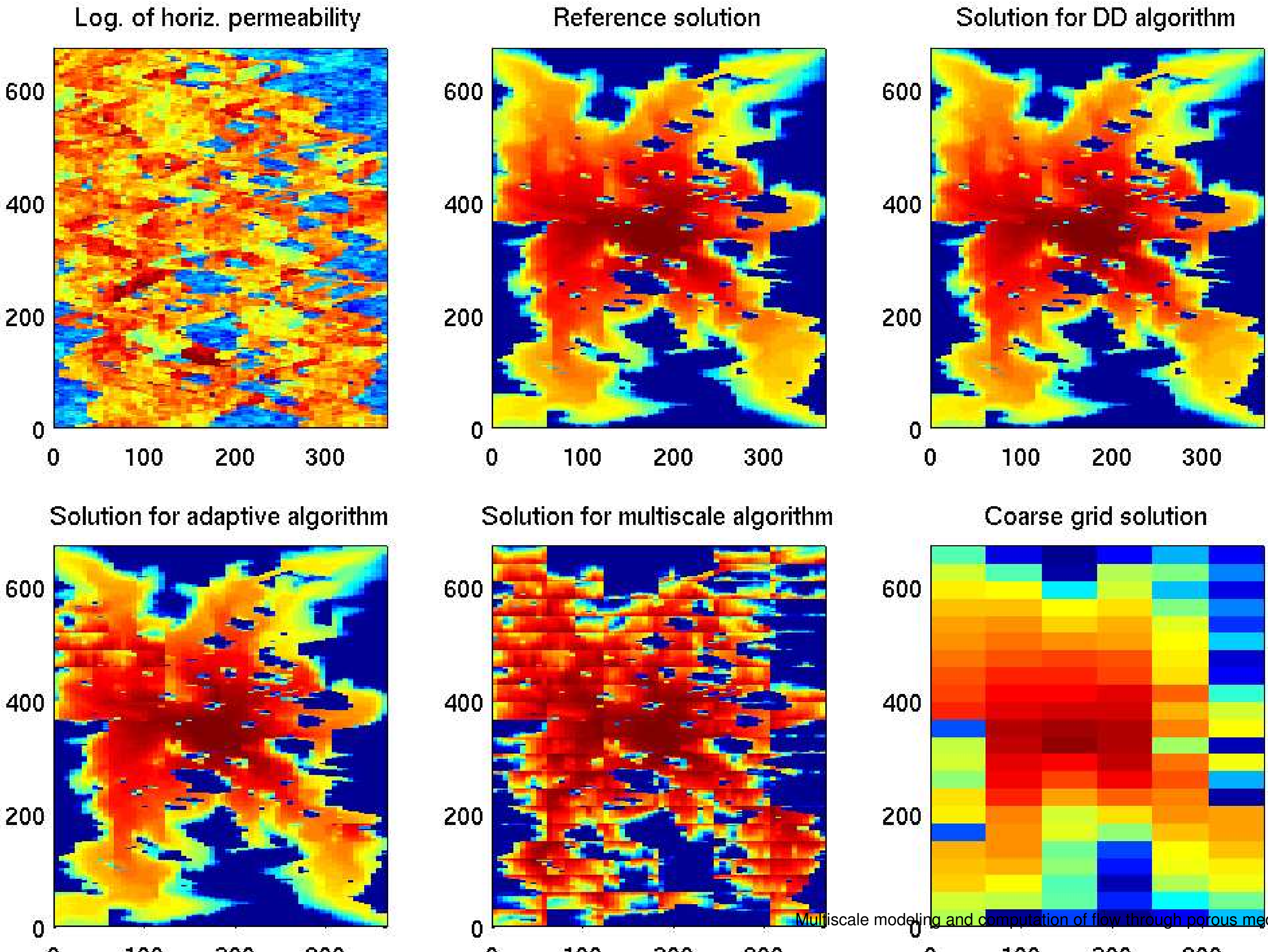

Numerical results

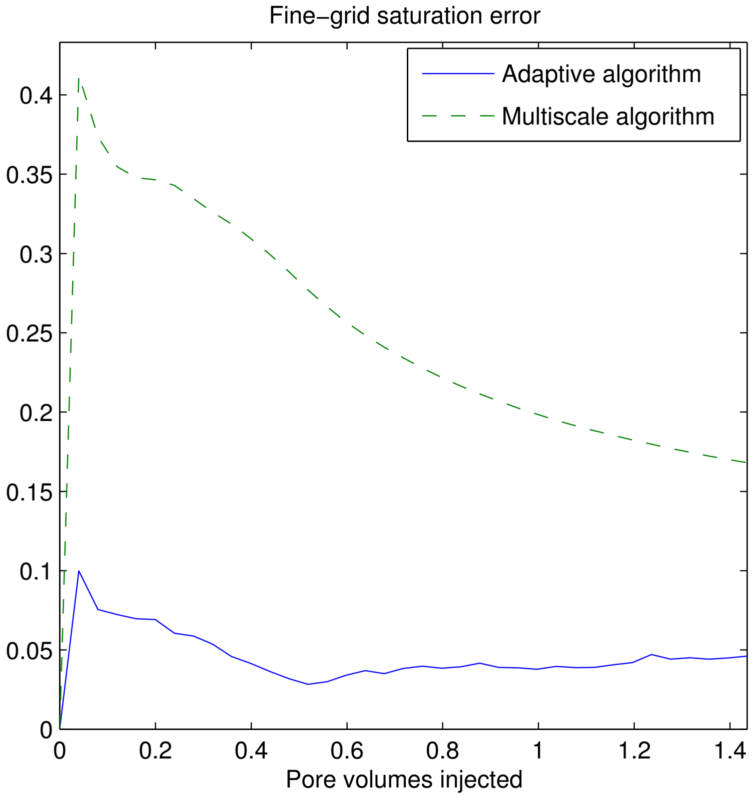

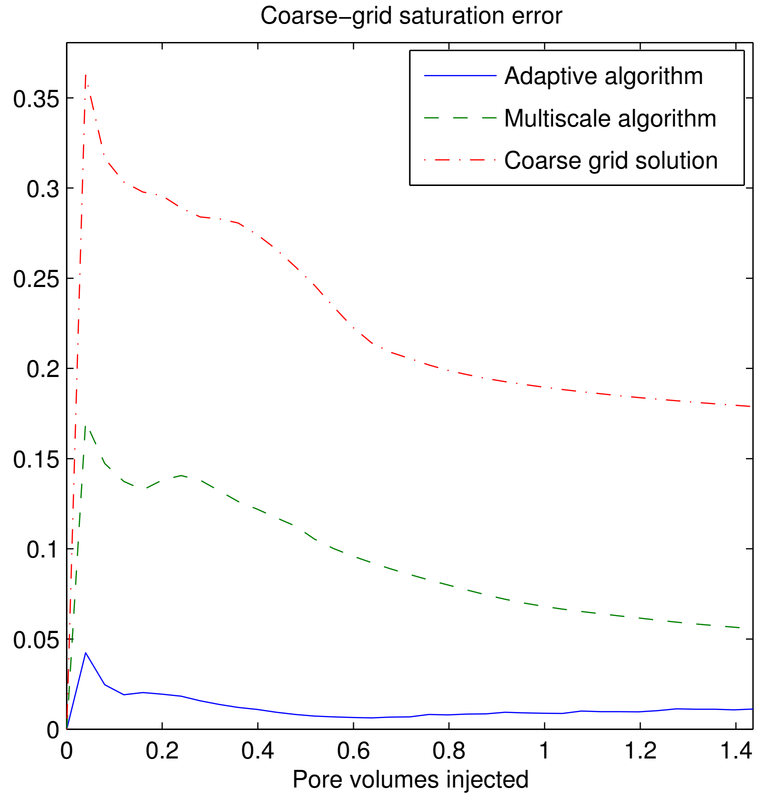

Numerical results

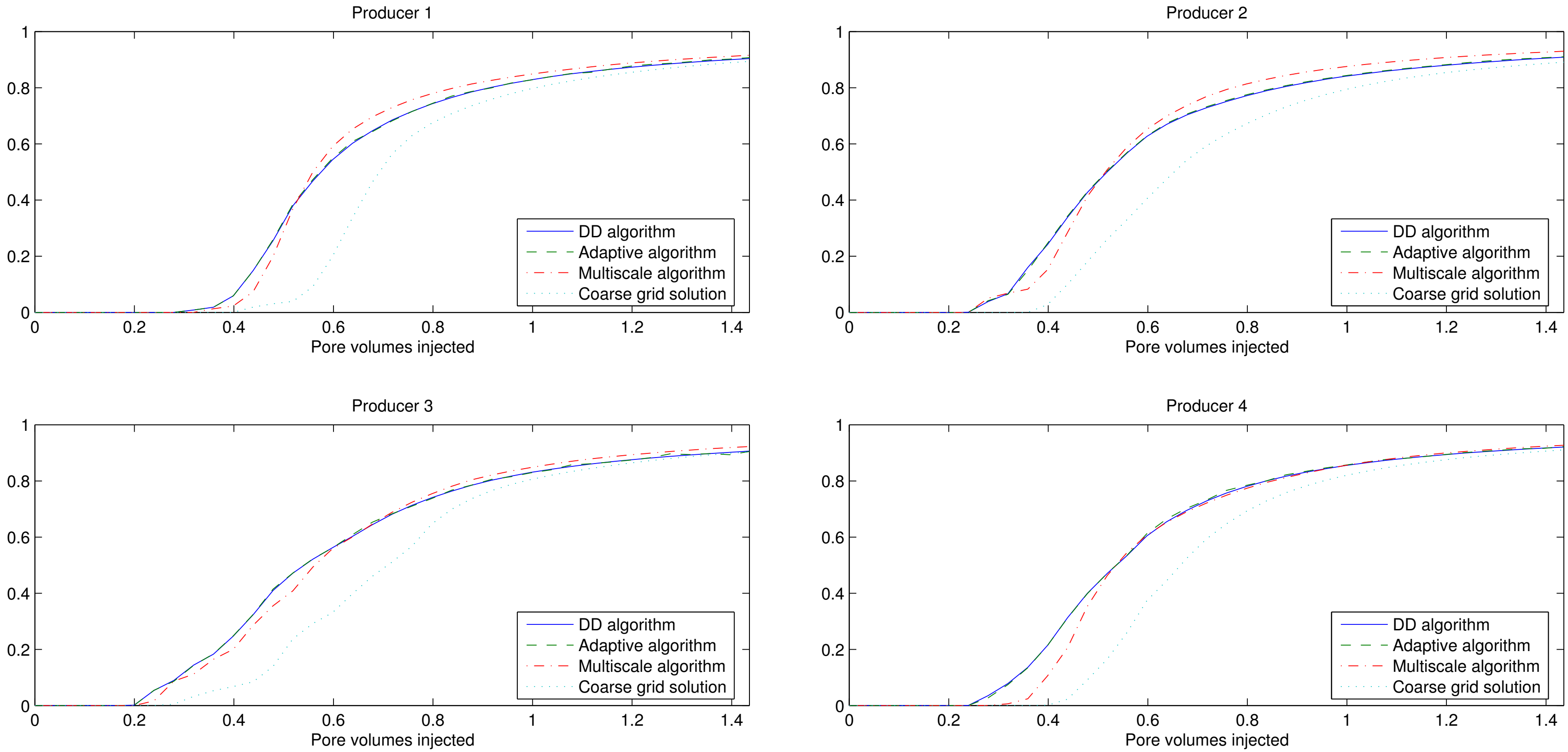

Some references

- Y. Efendiev, T. Hou and V. Ginting, Multiscale finite element methods for nonlinear partial differential equations, Comm. Math. Sci., 2(4), 2004
-Y. Efendiev and A. Pankov, Numerical homogenization and correctors for random nonlinear elliptic equations, SIAM J. Applied Math., 65 (1), pp.43-68, 2004
- Y. Efendiev and A. Pankov, Homogenization of nonlinear random parabolic operators, Advances in Differential Equations, vol. 10,Number 11, 2005, pp., 1235-1260
- Y. Efendiev and A. Pankov, "Numerical homogenization of nonlinear random parabolic operators", SIAM MMS 2(2), 2004, pp. 237–268
- Y. Efendiev, T. Hou, and T. Strinopoulos, Multiscale simulations of porous media flows in flow-based coordinate system, submitted to Comp. Geo
- J. Aarnes and Y. Efendiev, An adaptive multiscale method for simulation of fluid flow in heterogeneous porous media, submitted to SIAM MMS
- V. Ginting, R. Ewing, Y. Efendiev and R. Lazarov, Upscaled Modeling in Multiphase Flow Applications, Journal of Computational and Applied Mathematics. vol. 23, 2-3, pp.213-233, 2004
- Y. Efendiev and B. Popov, "On homogenization of nonlinear hyperbolic equations", to appear in Communications on Pure and Applied Analysis, 4(2), 2005, pp. 295-309
- Y. Efendiev, L. Durlofsky, and S. Lee, "Modeling of subgrid effects in coarse-scale simulations of transport in heterogeneous porous media", WRR 37(2000):888–910

Some references

- Y. Efendiev, V. Ginting, T. Hou and R. Ewing, "Accurate multiscale finite element methods for two-phase flow simulations", accepted to Comp. Physics